Dynamic Pile Testing Technology: Validation and Implementation

Robert Y. Liang, Ph.D., P.E.

Luo Yang, Ph.D., P.E.

for the
Ohio Department of Transportation
Office of Research and Development

and the
U.S. Department of Transportation
Federal Highway Administration

State Job Number 14794

Final Report
FHWA/OH-2007-08
May 2007

RESEARCH & DEVELOPMENT

1. Report No.	2. Government Accession No.	3. Recipient's Catalog No.
FHWA/OH-2007-08		

4. Title and subtitle	5. Report Date
Dynamic Pile Testing Technology: Validation and Implementation	**May 2007**
	6. Performing Organization Code

7. Author(s)	8. Performing Organization Report No.
Dr. Robert Liang **Luo Yang**	10. Work Unit No. (TRAIS)

9. Performing Organization Name and Address	11. Contract or Grant No.
University of Akron **Department of Civil Engineering** **Akron, OH 44325**	**147940** 13. Type of Report and Period Covered

12. Sponsoring Agency Name and Address	14. Sponsoring Agency Code
Ohio Department of Transportation **1980 West Broad Street** **Columbus, OH 43223**	

15. Supplementary Notes

16. Abstract

Driven piles are widely used as foundations to support buildings, bridges, and other structures. In 2007, AASHTO has adopted LRFD method for foundation design. The probability based LRFD approach affords the mathematical framework from which significant improvements on the design and quality control of driven piles can be achieved. In this research, reliability-based quality control criteria for driven piles are developed based on the framework of acceptance-sampling analysis for both static and dynamic test methods with the lognormal distribution characteristics. As a result, an optimum approach is suggested for the number of load tests and the required measured capacities for quality control of driven piles. Furthermore, this research has compiled a large database of pile set-up, from which the reliability-based approach of FORM is employed to develop separate resistance factors for the measured reference (initial) capacity and predicted set-up capacity. This report also provides a Bayesian theory based approach to allow for combining the information from the static pile capacity calculation and dynamic pile testing data to improve pile design process. Specifically, the results from dynamic pile tests can be utilized to reduce the uncertainties associated with static analysis methods of pile capacity by updating the corresponding resistance factors. This research has also developed one-dimensional wave equation based algorithm to interpret the High Strain Testing (HST) data for the estimation of the shaft and toe resistance of driven piles. The closed form solution is obtained for determining the Smith damping factor and the static soil resistance. Finally, a set of new wireless dynamic testing equipment (both hardware and software) is developed for more efficient dynamic pile testing.

17. Key Words	18. Distribution Statement
LRFD, Driven piles set-up, Wireless dynamic piles testing	**No restrictions. This document is available to the public through the National Technical Information Service, Springfield, Virginia 22161**

19. Security Classif. (of this report)	20. Security Classif. (of this page)	21. No. of Pages	22. Price
Unclassified	**Unclassified**		

DYNAMIC PILE TESTING TECHNOLOGY: VALIDATION AND IMPLEMENTATION

By

Robert Y. Liang
Department of Civil Engineering
The University of Akron
Akron, Ohio 44325-3905

Submitted to
The Ohio Department of Transportation
and the U.S. Department of Transportation
Federal Highway Administration

Dynamic Pile Testing Technology: Validation and Implementation

Robert Y. Liang, Ph.D., P.E.
Luo Yang, Ph.D., P.E.

431 ASEC, Civil Engineering Department
University of Akron
Akron, OH, 44325

Credit Reference: Prepared in cooperation with the Ohio Department of Transportation and the U.S. Department of Transportation, Federal Highway Administration.

May 2007

ABSTRACT

Driven piles are widely used as foundations for buildings, bridges, and other structures. Since 1994, AASHTO has been in process to change from ASD method to LRFD method for foundation design. The adoption of LRFD approach makes possible the application of reliability analysis to quantify uncertainties associated with various load and resistance components, respectively. A successful application of the probability approach will definitely result in significant improvements on the design and quality control of driven piles. Therefore, there is a need to develop the quality control criterion and to improve the LRFD design of driven piles in the framework of reliability-based analysis.

Reliability-based quality control criteria on driven piles are developed based on the framework of acceptance-sampling analysis for both static and dynamic test methods with lognormal statistical characteristics. The lognormal distribution of statistical data of various load test methods is converted to standard normal distribution for evaluating the confidence interval to assure the structure reliability. An optimum approach is suggested for the selection of the number of load tests and the required measured capacities for quality control of various load test methods of driven piles.

The databases containing a large number of pile testing data are compiled for piles driven into clay and into sand, respectively. Based on the compiled databases, the set-up effect is statistically analyzed. The reliability-based approach of FORM is employed to

develop separate resistance factors to account for different degrees of uncertainties associated with the measured reference capacity and predicted set-up capacity in the LRFD of driven piles.

Bayesian theory is employed to combine the information from the static calculation and dynamic pile testing in the reliability-based LRFD of driven piles. Specifically, the results from dynamic pile tests are incorporated to reduce the uncertainties associated with static analysis methods by updating the resistance factors.

A one-dimensional wave equation based algorithm to interpret the High Strain Testing (HST) data for estimation of the shaft and toe resistance of driven piles is proposed. Both the force and velocity time histories measured at the pile head are used as input boundary conditions in the new algorithm. The Smith damping factor and the static soil resistance can be directly determined based on the closed form solution of the one-dimensional wave equation.

A set of new wireless dynamic testing equipment is developed for dynamic pile testing. This new technology utilizes remote data acquisition and management unit to build the wireless connection between the sensors and the monitoring PC. The new wireless dynamic testing equipment is anticipated to be successfully applied in the field testing that will advance pile driving control and monitoring to a more secure environment.

TABLE OF CONTENTS

Page

LIST OF TABLES

LIST OF FIGURES

CHAPTER I

INTRODUCTION

1.1 Statement of the Problem

Deep foundations have been frequently used to support structures, such as buildings, bridges, towers, and dams, in areas where the soil conditions are unfavorable for shallow foundations. Two basic types of deep foundation are well known as drilled shafts and driven piles. Drilled shafts are usually installed by boring of the ground and filling the void with concrete. Driven piles are usually installed by using the hammer to drive the teel or concrete piles into the ground. This report is concentrated on the improvement of design and quality control of driven piles.

Traditionally, the design of pile foundations is based on static analysis methods, such as α-method, β-method, λ-method, Nordlund's method, Meyerhof's method, SPT (Standard Penetration Test) method, and CPT (Cone Penetration Test) method. However, the pile capacity estimated from static analysis based on the soil parameters obtained from the laboratory test and in-situ test may not be accurate. It can vary widely due to inherent heterogeneous nature of soil deposit, and different soil testing and evaluation methods. Consequently, some type of proof of load-carrying capacity of driven piles is needed in the field.

Static load test can serve as the ultimate verification of driven pile capacity, despite the unsettled question concerning definition of failure load. Nevertheless, the static load test is expensive and time-consuming to carry out and therefore can only be performed on a few selected driven piles, often one or two piles at most. The information obtained from static load test results cannot be easily extrapolated to other piles at the site, leaving those other piles to be unverified. Besides, the information gathered from the static load tests cannot help field engineer to decide when to stop pile driving. Estimation of pile capacity based on observation during pile driving is therefore an essential ingredient in a sound pile driving practice.

With the advent of digital computers, dynamic analysis of pile driving problem became possible. In 1960, Smith proposed the first applicable wave equation method for pile-driving analysis. Since then, the wave equation method was accepted by the engineers in the piling industry as a more accurate pile-driving analysis. With the development and acceptance of PDA (Pile Driving Analyzer), the Case method (Rausche et al. 1985), utilizing the measured force and velocity histories in approximate simple algebraic equations, has become one of the widely used methods to evaluate the pile capacities during pile driving. However, the static soil resistances determined by the Case method are very sensitive to assumed Case damping factor, and shaft and toe resistance cannot be separated by the Case method.

In an effort to overcome some of the shortcomings of the Case method, an alternative procedure, known as the CAse Pile Wave Analysis Program (CAPWAP), was developed by Rausche et al. (1972, 1985). The CAPWAP approach is based on the one-dimensional wave propagation model suggested by Smith (1960). In the CAPWAP analysis, one of the two HST data (either force or velocity) is used as input to match closely with the other by adjusting Smith model parameters. Once the acceptable match is achieved, then the pile capacities and the Smith model parameters can be determined. In addition, some other researchers such as Paikowsky et al. (1994), Hirsch et al. (1976), Liang and Zhou (1996), and Liang (2003) have proposed various approaches to interpret the measured force and velocity histories for evaluating the pile capacity. However, the capacity estimation and drivability predictions from dynamic pile tests are, sometimes, far from satisfactory. Thus, the dynamic testing technique still needs to be further improved.

Currently, dynamic pile tests are widely carried out to verify when the design pile capacity is reached during pile driving and to monitor the installation process to avoid pile damage due to hammer impact. However, there is a lack of acceptance criteria for the number of pile tests and measured capacity. Hannigan et al. (1998) suggested that a minimum of two dynamic pile tests be conducted for a small project. For large projects or small projects with anticipated installation difficulties, or significant time dependent capacity issues, a greater number of dynamic pile tests are recommended. If the test piles do not reach a prescribed design capacity, the design load for the piles must be reduced or additional number of piles or longer pile length must be installed. The recommendations of the number of dynamic pile tests are entirely based on engineering experience.

Paikowsky et al. (2004) provided recommendations for the number of piles to be dynamically tested as well as the acceptance criterion for a set of driven piles. The approach of quality assurance testing in manufacturing was employed to determine the number of dynamic tests to be performed on production piles. However, the adoption of normal distribution for dynamic test methods, which deviated from the actual cases that the probabilistic characteristics of dynamic test methods can be properly represented by the lognormal distribution, makes the recommendations very conservative. The acceptance criterion for a set of dynamic test results is subjectively chosen such that the average capacity of the tested piles is no less than 85% of the nominal ultimate capacity. In addition, the application of arithmetic mean of measured capacity is far away from the actual cases of geometric mean of measured capacity when the lognormal distribution is used to represent the probabilistic characteristics of dynamic test methods. Therefore, there is a need to develop more reasonable, reliability-based quality control criteria for driven piles.

Since 1994, AASHTO (American Association of State Highway and Transportation Officials) has been in process to change from ASD (Allowable Stress Design) method to LRFD (Load and Resistance Factor Design) method for foundation design. Whereas ASD considers all uncertainties in the applied load and ultimate geotechnical or structural capacity in a single value of factor of safety (FS), LRFD separates the variability of these design components by applying load and resistance factors to the load and material capacity, respectively. Comparing to ASD, LRFD has the following advantages:

- Accounts for variability in both resistance and load;
- Achieves relatively uniform levels of safety based on the strength of soil and rock for different limit states and foundation types;
- Provides more consistent levels of safety in the superstructure and substructure as both are designed using the same loads for predicted or target probabilities of failure.

The adoption of LRFD approach makes possible the application of reliability analysis to quantify uncertainties associated with various methods for estimating loads and resistances, respectively. In AASHTO LRFD specifications (2003), the resistance factors for various design methods are recommended with calibrations mostly based on the reliability analysis using available statistical data. The design of foundation piles is usually performed with static analytical calculations using the soil parameters from local geotechnical site investigations and accompanied laboratory test results. The uncertainties with respect to the prediction method, the errors of calculation model, and the spatial variability of soil parameters, are considered in a single resistance factor recommended for a specific design method regardless of individual site-specific situation. For each construction site, soil profiles, soil types, pile driving equipment, and hammer performance, will be unique. Thus, it is advantageous if a site-specific calibration for the resistance factors can be performed to improve design.

With the use of both static load test and dynamic pile test, the pile length estimated using static analysis methods during the design stage would be proven either adequate or

inadequate based on field pile tests during pile driving. Therefore, the uncertainties of static analysis design method could be reduced by incorporating dynamic test results. Vrouwenvelder (1992) presented an approach for incorporating either the static or dynamic test results to update the factor of safety in the ASD method of driven piles. Zhang et al. (2002) demonstrated that the results from static pile load tests could be incorporated into pile design using Bayesian theory by updating the resistance factor in LRFD. The practice in Ohio Department of Transportation nevertheless shows that more and more dynamic pile test methods have been utilized compared to static load test, due to savings in cost and time. Recognizing that dynamic pile testing is by far the much preferred pile capacity verification method, a methodology needs to be developed to update the resistance factors for static analysis method by utilizing dynamic pile test results.

The fact that axial capacity of a driven pile may change over time after initial pile installation has been reported by a number of geotechnical engineers for many years. The increase of pile capacity with time is usually referred to as set-up; conversely, the decrease of pile capacity with time is often termed as relaxation. Due to pile driving, soils around the pile are significantly disturbed and remolded, and excess pore pressures are generated. With passage of time, the excess pore pressure will dissipate and consequently pile capacity is regained. Decrease in excess pore pressure is inversely proportional to the square of the distance from the pile (Pestana et al. 2002). The time to dissipate excess pore pressure is proportional to the square of horizontal pile dimension (Holloway and Beddard 1995; Soderberg 1961), and inversely proportional to the soil's horizontal

coefficient of consolidation (Soderberg 1961). Accordingly, larger-diameter piles take longer time to set-up than small-diameter piles (Long et al. 1999; Wang and Reese 1989). As excess pore pressures dissipate, the effective stress of the affected soil increases, and set-up predominately occurs as a result of increased shear strength and increased lateral stress against the pile. Piles driven into clay tend to experience greater set-up than piles driven into sand and silt. Piles may experience relaxation when driven into dense and saturated sand and silt. Based on observations in the field, numerous geotechnical engineers developed various empirical formulas to predict the set-up behavior (e.g., Skov and Denver 1988; Svinkin et al. 1994; Huang 1988; Zhu 1988). In particular, the semi-logarithmic empirical relationship, proposed by Skov and Denver, has been widely used to predict post-installation pile capacity increase with time.

With an accumulation of more experience and knowledge on set-up phenomenon, some researchers have suggested that the set-up be formally incorporated into the prediction method to determine total pile capacity. For example, Bullock et al. (2005) proposed a conservative method for incorporating side shear set-up into the total pile capacity. The predicted set-up capacity was assumed to have the same degree of uncertainties as the measured reference capacity and a single safety factor was used to account for all uncertainties of loads and resistances. Due to different uncertainties associated with measured capacity and predicted set-up capacity, Komurka et al. (2005) proposed a method to apply separate safety factors to EOD (End of Driving) and set-up components of driven pile capacity. Furthermore, the set-up capacity was characterized as a function of pile penetration based on dynamic monitoring during both initial driving

and restrike testing. The separate safety factors recommended for EOD and set-up capacity, however, are based purely on judgment with no attendant database and statistical analysis. Therefore, the development of a reliability analysis methodology on set-up capacity will be desirable to separate the resistance factors in LRFD of driven piles.

1.2 Objectives of the Study

The objectives of this study can be enumerated as follows:

1. To develop reliability-based quality control criteria on driven piles from the framework of acceptance-sampling analysis for both static and dynamic test methods with lognormal statistical characteristics. The lognormal distribution of statistical data of various load test methods is converted to standard normal distribution for evaluating the confidence interval of the driven piles in achieving the desired capacity. An optimum approach is developed for the determination of the number of dynamic pile tests and the required measured capacities for quality control of various dynamic test methods of driven piles.
2. To present the compilation of a database containing a large number of pile testing data where piles were driven into clay and into sand, respectively. Based on the compiled databases, the set-up effect will be statistically analyzed. The compilation of the statistical database of set-up capacity makes it possible to apply a reliability-based analysis method to develop separate resistance factors to account for different degrees of uncertainties associated with the measured reference capacity and predicted set-up capacity in the LRFD framework. The reliability-based approach of FORM (First Order Reliability Method) will be used

to determine the desired separate resistance factors for various target reliability levels. The test results obtained during convenient short-time restrike can be used to predict the long-term capacity based on the proposed formula by Skov and Denver. The application of separate resistance factors in LRFD for the measured reference capacity and the predicted set-up capacity can improve the prediction of capacity of driven piles. Furthermore, by applying separate resistance factors, pile length or number of piles can be reduced and economical design of driven piles can be achieved.

3. To present a methodology for pile design by combining the information from the static calculation and dynamic pile testing. Bayesian theory is employed to combine two design methods in the framework of LRFD approach using reliability analysis. Specifically, the results from dynamic pile tests will be incorporated to reduce the uncertainties associated with static analysis methods by updating the corresponding resistance factors. The combination of two design methods could improve accuracy and confidence level on the predicted pile capacity as opposed to the case of using only one design method.
4. To develop a one-dimensional wave equation based algorithm to interpret the High Strain Testing (HST) data for estimation of the shaft and toe resistance of driven piles. Both the force and velocity time histories measured at the pile head are used as input in the new algorithm. The Smith damping factor and the static soil resistance are directly determined based on the derived closed form solution of the one-dimensional wave equation. The developed solution algorithm is computationally efficient compared to the existing numerical procedure.

Additionally, the shaft resistance and the toe resistance can be separated using the derived wave equation method.

5. To develop a set of new wireless dynamic testing device for dynamic pile testing. This new technology utilizes remote data acquisition and management unit to build the wireless connection between the sensors and the monitoring PC. The new wireless dynamic testing equipment is anticipated to be successfully applied in the field testing that will advance pile driving control and monitoring to a more secure environment.

1.3 Organization of Report

The organization of this report is as follows:

- Chapter II presents the literature review of analysis methods of driven piles.
- Chapter III presents the developed reliability-based quality control method on driven piles, particularly regarding the criteria for the number of dynamic pile tests and the acceptable measured capacity.
- Chapter IV presents a compiled database containing a large number of pile testing data in clay, from which the set-up effect is statistically analyzed. The statistical database is used in the reliability-based analysis framework to develop separate resistance factors in LRFD for the measured reference capacity in short term and the predicted set-up capacity in clay.
- Chapter V presents a database containing a large number of pile testing data in sand, from which the set-up effect is statistically analyzed. The statistical database is used in the reliability-based analysis framework to develop separate resistance

factors in LRFD for the measured short-term reference capacity and the predicted long-term set-up capacity in sand.

- Chapter VI presents the application of Bayesian theory to develop a methodology for updating the resistance factors of driven piles by combining the static analysis method and the dynamic test methods.
- Chapter VII presents a closed form solution to the one-dimensional wave equation based algorithm for estimation of shaft and toe resistance of driven piles using High Strain Testing (HST) data.
- Chapter VIII presents the developed wireless data communication device for field application in the dynamic pile testing.
- Chapter IX presents summaries and conclusions of the research work. Also, recommendations for implementations as well as future research topics are provided.

CHAPTER II

LITERATURE REVIEW

2.1 Introduction

Numerous analysis methods for the estimation of capacity of driven piles have been proposed during the past hundred years. These methods can be generally categorized into two broad groups: 1) static analysis methods based on the soil parameters obtained from the laboratory test and in-situ test; 2) direct field pile testing methods which include static load tests and dynamic pile tests. Static analysis methods are usually used prior to the installation of driven piles to determine the preliminary design of driven piles, such as pile length, pile size, pile location, and the estimation of capacity of driven piles. The dynamic and static load tests are performed during and after the installation of driven piles to verify the design capacity. Dynamic pile testing also serves as quality control of pile driving.

2.2 Quality Control on Driven Piles

The most common static analysis methods used for evaluating the static axial capacity of driven piles are as follows: α-method (Tomlinson, 1986), β-method (Esrig & Kirby, 1979), λ-method (Vijayvergiya and Focht, 1972), Nordlund's method (Nordlund, 1963), Nottingham and Schmertmann's CPT method (Nottingham and Schmertmann, 1975), and

Meyerhof's SPT method (Meyerhof, 1976). Nordlund's method, β-method, Nottingham and Schmertmann's CPT method, and Meyerhof's SPT method are generally used when calculating the design capacity of driven piles in cohesionless soils, while α-method, β-method, λ-method, and Nottingham and Schmertmann's CPT method are used to predict the pile capacity when piles are driven into cohesive soils. However, the pile capacity estimated from static analysis based on the soil parameters obtained from the laboratory test and in-situ test may not be accurate. Thus, static load test, dynamic pile test, or both, which are believed to have higher accuracy in estimation of pile capacity, have been performed to verify the design capacity calculated from static analysis method.

The static load tests have been performed to verify that the behavior of the driven piles agreed with the assumption of the design for decades. There are various definitions of pile capacity evaluated from load-movement records of a static load test. Four of them are of particular interests; namely, the Davisson Offset Limit (Davisson 1972), the DeBeer Yield Limit (DeBeer 1968), the Hansen Ultimate Load (Hansen 1963), and Decourt extrapolation (Decourt 1999). NCHRP Report 507 (Paikowsky et al. 2004) presented that Davisson's Pile failure criterion could be used to properly determine the reference pile capacity for driven piles, irrespective of the pile diameter and the static load test procedure. The static load tests have been accepted by most geotechnical engineers as the most accurate evaluation method of pile capacity. However, the cost and time needed for a static load test hindered its extensive application in field testing. Dynamic pile testing, an alternative approach of verification of pile design capacity in the

field, has become more and more attractive in geotechnical engineering due to its savings in cost and time.

Over the past one hundred years or so, many attempts have been made to predict the driving characteristics and the bearing capacity of piles through the use of dynamic energy formulas. Dynamic energy formulas are based on simple energy balance relationship in which input energy is equal to the sum of consumed energy and lost energy. In USA, most of the state highway departments still widely use the Engineering News Record (ENR) formula (Wellington, 1892) and its modified version for estimating pile capacities. However, there are some reasons that make these formulas less than satisfactory: 1) rigid pile assumption; 2) no consideration of soil-pile interaction, 3) no incorporation of damping factor. Although many efforts have been made to improve the dynamic energy formulas (Gates 1957, Liang and Husein 1993, Paikowsky et al. 1994, Liang and Zhou 1996), the accuracy of estimation from dynamic energy methods is still far from satisfactory.

As a better alternative to energy formulas for pile driving, the wave equation method was proposed by Smith (1960) for the first practical use in estimating the pile capacity. The governing one-dimensional wave equation was derived to describe the motion of pile particles by applying Newton's Second Law to a differential element of an elastic rod. In Smith model, the pile is discretized into lumped masses interconnected by pile "spring". The soil resistance to driving is provided by a series of springs that are assumed to behave in a perfectly elastic-plastic manner, and the spring stiffness is defined by the

ratio of the maximum static resistance of the soil R_s and the maximum elastic deformation or quake. Damping coefficients are introduced to account for the viscous behavior of the soil. The total soil resistance R_t is given by

$$R_t = R_s(1 + JV) \tag{2-1}$$

where R_s = the static soil resistance; J = the Smith damping coefficient; V = pile velocity.

In 1975 and 1976, the other two of the still widely used soil models were proposed. They are Case model and TTI model, by Goble at Case Western Reserve University and Hirsch at Texas Transportation Institute, respectively. These two models can be viewed as modified version of Smith model. In Case model, the soil damping force is uncoupled from the spring force and is dependent on the pile particle velocity. Case damping factor J_c was introduced to account for the soil damping effect when multiplied with pile impendence Z_p and toe velocity V. The total resistance R_t is given by

$$R_t = R_s + J_c Z_p V \tag{2-2}$$

It is worth noting that J_c is not related to soil properties, but a pure empirical value calibrated with the results of static load tests.

In TTI model, the nonlinearity of soil damping force with velocity is taken into account. The total resistance R_t during driving is given by

$$R_t = R_s(1 + JV^N) \tag{2-3}$$

where N = an exponent less than unity to reflect the nonlinearity of the damping force with velocity; 0.2 can be taken for N when lack of information.

With the development and acceptance of pile driving analyzer (PDA), Case method has become one of the widely used methods to evaluate the pile load capacity. However, its inaccuracy has also been reported (Lai and Kuo 1994; Paikowsky et al. 1994). The static soil resistances determined by the Case method are very sensitive to the assumed Case damping factor, and the shaft and the toe resistance cannot be separated by the Case method. In an effort to overcome these shortcomings, Rausche (1972, 1985) developed an alternative procedure, known as the CAse Pile Wave Analysis Program (CAPWAP). The CAPWAP approach is also based on the one-dimensional wave propagation model suggested by Smith (1960). In CAPWAP analysis, one of the two HST data on the pile head (either force or velocity) is used as input to generate output that would match closely with the other HST data by adjusting Smith model parameters. Once the acceptable match is achieved, then the pile capacities and the Smith model parameters can be determined. However, the numerical procedure in CAPWAP (lumped mass and springs) is computationally time-consuming, and the capacity estimation and drivability predictions from dynamic pile tests are, sometimes, far from satisfactory. Thus the dynamic testing technique still needs to be further improved.

Currently, dynamic pile tests are widely carried out to verify the accomplishing of design pile capacity during pile driving and to monitor the installation process for avoiding pile damage due to hammer impact. Hannigan et al. (1998) presented that the number of piles that should be dynamically tested on a project depends on the project size, variability of the subsurface conditions, the availability of static load test information,

and the reasons for performing the dynamic tests. A minimum of two dynamic pile tests is recommended to be conducted for a small project. For large projects or small projects with anticipated installation difficulties, or significant time dependent capacity issues, a larger number of dynamic pile tests are recommended. On larger projects, CAPWAP analyses are typically performed on 20 to 40% of the dynamic test data obtained from both initial driving and restrike dynamic tests. If the test piles do not reach a prescribed design capacity, the design load for the piles must be reduced or additional piles or pile lengths must be installed. The recommendations of the number of dynamic pile tests are entirely based on engineering experience.

Paikowsky et al. (2004) provided recommendations for the number of piles to be dynamically tested as well as the acceptance criterion for a driven pile project. The method of quality assurance testing in manufacturing industry is adopted to determine the number of dynamic tests to be performed on production piles. The acceptance criterion for a set of driven piles is subjectively recommended as the average capacity of the tested piles to be no less than 85% of the nominal ultimate capacity. However, the adoption of normal distribution the probabilistic characteristics of dynamic test methods deviates from the more representative lognormal distribution, thus making the recommendation very conservative. In addition, the application of arithmetic mean of measured capacity is far away from the actual cases of geometric mean of measured capacity when the lognormal distribution is used to represent the probabilistic characteristics of dynamic test methods. Therefore, there is a need to develop improved reliability-based quality control criteria on driven piles.

2.3 Reliability Analysis in LRFD

Allowable Stress Design (ASD) method has been used in civil engineering since the early 1800s. Under ASD, the design loads, which consist of the actual forces estimated to be applied to the structure (or a particular element of the structure), are compared to resistance, or strength through a factor of safety (FS):

$$Q \le Q_{all} = \frac{R_n}{FS} = \frac{Q_{ult}}{FS} \tag{2-4}$$

where Q = design load; Q_{all} = allowable design load; R_n = resistance of the element or the structure; Q_{ult} = ultimate geotechnical pile resistance.

In the 1997 version of Standard Specifications for Highway Bridges (AASHTO 1997), the traditional factors of safety are used in conjunction with different levels of control in analysis and construction. However, the recommended factors of safety do not consider the different degrees of uncertainties associated with load and resistance performance. Thus, the reasonableness and economy of design in ASD is questionable.

In reality, both load and capacity have various sources and levels of uncertainties. Since 1994, AASHTO (American Association of State Highway and Transportation Officials) has been in process to supersede ASD method with LRFD (Load and Resistance Factor Design) method for foundation design. Beginning in 2007, all federally funded projects are required to follow the new LRFD procedure. Whereas ASD considers all uncertainties in the applied load and the estimated ultimate geotechnical or structural

capacity in a single value of the factor of safety (FS), LRFD separates the variability of these design components by applying load and resistance factors to the load and material capacity, respectively. LRFD Bridge Design Specifications (AASHTO 2006) states that the ultimate resistance (R_n) multiplied by a resistance factor (Φ), which thus becomes the factored resistance, must be greater than or equal to the summation of loads (Q_i) multiplied by corresponding load factors (γ_i), and modifiers (η_i). LRFD criterion for strength limit states can be expressed as:

$$\phi R_n \geq \sum \eta_i \gamma_i Q_i \tag{2-5}$$

where

$$\eta_i = \eta_D \eta_R \eta_I > 0.95 \tag{2-6}$$

where η_D = effects of ductility; η_R = redundancy; η_I = operational importance.

McVay et al. (2000) presented the statistical parameters and the corresponding resistance factors for various dynamic methods in LRFD of driven piles based on a database of 218 pile cases in Florida. Eight dynamic methods were studied: ENR, modified ENR, FDOT, Gates driving formulas, CAPWAP, Case method for PDA, Paikowsky's energy method, and Sakai's energy method. It was demonstrated that the modern methods based on wave mechanics, such as CAPWAP, PDA, and Paikowsky's energy methods, are roughly twice as cost effective to reach the target reliability indices of 2.0 to 2.5 (probability of failure =0.62 to 2.5%) as the ENR and modified ENR driving formulas.

Paikowsky et al. (2004) compiled a large database in NCHRP Report 507 that was used for the quantitative assessment of pile capacity evaluation methods during both design and construction. The resistance factors for various design methods were calibrated according to soil types, pile types, and time of testing. Static analysis methods used in most design practices were found overall over-predicting the observed pile capacities. Most dynamic capacity evaluation methods used for quality control were found overall under-predicting the observed pile capacities. Both findings demonstrated the shortcoming of safety evaluation based on absolute values (i.e., resistance factors or factors of safety) and the need for an effective measurement index to objectively assess the performance of methods of analysis. An efficiency factor is recommended by McVay et al. (2000) and Paikowsky et al. (2004) to account for the bias of the analysis methods and to provide an objective evaluation regarding the effectiveness of the capacity prediction method.

Based on the NCHRP Report 507 (Paikowsky et al. 2004), AASHTO (2006) divided the design methods of driven piles into two major categories: static calculation and dynamic testing, and proposed an independent resistance factor for each design method. Where nominal pile axial resistance is determined during pile driving by dynamic analysis, dynamic formula, or static load test, the uncertainty in the pile axial resistance is strictly due to the reliability of the resistance determination method used in the field during pile installation. Actually, each type of design method, however, has its own merits and one method may eliminate uncertainties that otherwise may not be eliminated by the others. With the widespread uses of driven piles, the fact that the static calculation and dynamic testing play a relatively independent role in the design of driven piles has

lead to a large variability in the estimation of pile capacities and consequently high project cost.

Vrouwenvelder (1992) presented an approach for incorporating dynamic test results to update factor of safety in the ASD design of driven piles. It was stated that the rules for dynamic testing and pile driving analysis are formulated in a more strict way than those for static analysis methods. The formulation for static analysis method seems to be less restrictive. Nevertheless, the dynamic pile tests can only determine the pile capacity at the testing time and cannot predict the long-term pile capacity as a function of time after pile installation. It could be found that the various methods are not treated in a fully symmetric manner. Furthermore, it should open the possibility to combine the results of various methods. The application of reliability theory makes it possible to combine various methods.

Zhang et al. (2002) demonstrated that the results from static pile load tests could be incorporated into pile design using Bayesian theory by updating the resistance factor in LRFD. The practice in Ohio Department of Transportation nevertheless shows that more and more dynamic pile test methods have been utilized compared to static load test, due to savings in cost and time. Recognizing that dynamic pile testing is by far the much preferred pile capacity verification method, there will be a need to update the resistance factors for static analysis method by utilizing dynamic pile test results.

2.4 Set-up Effect

Set-up (time-dependent increase in pile capacity) has long been recognized as a well-known phenomenon, and can contribute significantly to long-term pile capacity. Economical design of driven piles would not be achieved without the recognition of set-up effect. When a pile is driven into the ground, the soils surrounding the pile are significantly disturbed and excess pore pressure is generated. After pile driving, the pile regains its capacity with time primarily due to the dissipation of excess pore pressure. Set-up behaviors have been reported for various types of soil and pile during the past decades. Numerous researchers have also developed various formulas to predict the development of set-up capacity after the installation of driven piles.

Skov and Denver (1988) investigated the set-up effects by arranging restrike on piles of different age. It was found that, after a certain period of time, depending on soil conditions, the time-dependent increase in capacity can be considered approximately linear with the logarithm of time. Skov and Denver also presented an empirical equation for set-up based on a logarithmic increase of pile capacity with time as follows

$$Q_t = Q_0 (1 + A \log \frac{t}{t_0}) \tag{2-7}$$

where

Q_t = axial capacity at time t after driving,

Q_0 = axial capacity at time t_0,

A = a factor that is a function of soil type and can be determined as the slope of the linear portion of the normalized capacity (Q_t/Q_0) versus log(t) plot.

t = time since installation, and

t_0 = time after installation at which point the capacity gain becomes linear on a log(t) plot.

They also recommended numerical values for A and t_0 as 0.6 and 1 day in clay and 0.2 and 1 day in sand, respectively.

Zhu (1988) presented an empirical expression for the set-up coefficient in terms of sensitivity of cohesive soil for the determination of regain of capacity by performing pile tests in the coastal area of East China. According to collected information, the maximum adhesion at soil-pile interface, when reinforced concrete piles are driven into clay, is approximately equal to cohesion of undisturbed soil. The bearing capacity of the pile, as a function of time, is related to the reconsolidation of soil and can be expressed in terms of sensitivity as Eq. (2-8). The more sensitive the soil, the more obvious the regain of bearing capacity after pile installation.

$$Q_{14} = Q_{EOD}(1 + 0.375S_t) \tag{2-8}$$

where

Q_{14} = pile capacity 14 days after pile installation;

Q_{EOD} = pile capacity at end of driving;

S_t = sensitivity of soil.

Svinkin (1994) studied a number of piles driven into mostly sandy soil and presented the upper and lower boundaries to predict the development of set-up of driven piles in sandy soil. Pile capacity at end of initial driving is the important value in sandy soil and

can be taken as the lower limit of pile capacity. It was found that the tendency of soil set-up for all five investigated piles was generally the same, but the set-up coefficient ranged between upper boundary which can be expressed as

$$Q_t = 1.4 Q_{EOD} t^{0.1} \tag{2-9}$$

and lower boundary which can be expressed as

$$Q_t = 1.025 Q_{EOD} t^{0.1} \tag{2-10}$$

where

Q_t = pile capacity at the time t after pile driving;

Q_{EOD} = pile capacity at end of driving;

t = time after pile driving (days).

Svinkin also concluded that the set-up effect in sandy soils to a certain degree depends on the level of ground water table.

The effects of time on pile capacity are believed affected by the type of soil into which the pile is driven. Set-up is recognized as occurring in organic and inorganic saturated clay, and loose to medium dense silt, silty sand, and fine sand (Astedt and Holm, 1992; Attwooll et al., 1999; Hannigan et al., 1998). Holloway and Beddard (1995) observed little or no set-up in very silty low-plasticity cohesive materials. Walton and Borg (1998) indicated that set-up in sand and gravel may not be a significant factor in long-term pile capacity. Percentage-wise, piles driven into soft clay tend to experience greater set-up than piles driven into stiff clay. Piles driven into loose sands and silts generally experience a smaller magnitude of set-up than those in soft clays. Piles driven

into saturated, dense sands and silts or into shales may experience relaxation (Long et al., 1999; Svinkin, 1994, 2002; Titi and Wathugala, 1999).

Set-up is not only affected by soil type, but also related to the pile type. Set-up rate decreases as pile size increases (Camp and Parmar, 1999). Long et al. (1999) offered that there is no clear evidence of difference in set-up between small- and large-displacement piles. A study by Finno et al. (1989) reported that a pipe pile generated higher excess porewater pressures during installation than did an H-pile, but that unit shaft resistance for the two piles were approximately equal after 43 weeks. Wood piles tend to set-up faster than steel or concrete piles, and more permeable wood piles set-up faster than less-permeable wood piles (Bjerrum, et al., 1958; Yang, 1956). For piles installed in organic silt, Yang (1956) observed greater set-up for wood piles than for steel piles. Pre-stressed concrete piles generally exhibit more set-up than steel piles. This phenomenon has been attributed to a higher soil/pile interface coefficient of friction (Priem et al. 1989).

Long et al. (1999) used a database of pile load tests (both static and dynamic) collected from the literature to quantify time effects on pile capacity. The database is divided into three groups according to the primary subsurface soil profile: clay, sand, and mixed soil. Set-up in clay and mixed profiles varied from one to more than six times the axial capacity estimated immediately after driving. The gain in axial pile capacity with time is explained only partially by the dissipation of excess pore pressures. Aging can also contribute to the increase in capacity with time.

Camp and Parmar (1999) observed that the piles driven into the Cooper Marl, a stiff and overconsolidated cohesive calcareous soil, experienced significant set-up. The data available from 14 sites involving 114 tests were analyzed to evaluate whether the Skov and Denver formulas would apply. They proposed the use of 2 days as the time for the onset of the linear set-up on the semi-logarithm plot. With this assumption, the back-calculated A values generally follow the expected trends. The average A value decreases as the pile size increases. This means that the smaller piles gain capacity at a faster rate than the larger piles, which is in agreement with Soderberg's work (1961).

With an accumulation of more experience and knowledge on set-up phenomenon, some researchers have suggested that the set-up be formally incorporated into the prediction method to determine total pile capacity. For example, Bullock et al. (2005) proposed a conservative method for incorporating side shear set-up into the total pile capacity by analyzing the results of a driven pile side shear set-up (SSS) test program performed at the University of Florida. It was observed that all pile segments showed SSS, with similar magnitude in both cohesionless and cohesive soils, and irrespective of depth. Pile load tests and standard penetration tests with torque measurement (SPT-T) confirmed the approximate semilog-linear time versus SSS behavior and usefulness of the set-up factor A. They believed that engineers can include SSS in routine design using a minimum set-up factor A=0.1 for soils. The predicted set-up capacity was assumed to have the same degree of uncertainties as the measured reference capacity and a single safety factor was used to account for all uncertainties of loads and resistances.

Due to different uncertainties associated with measured capacity and predicted set-up capacity, Komurka et al. (2005) proposed a method to apply separate safety factors to EOD (End of Driving) and set-up components of driven pile capacity. CAPWAP results were used to estimate unit shaft resistance distribution (unit shaft resistance as a function of depth) at EOD and at BOR (Beginning of Restrike). Furthermore, the set-up capacity was characterized as a function of pile penetration based on dynamic monitoring during both initial driving and restrike testing. The separate safety factors recommended for EOD and set-up capacity, however, are based purely on judgment with no attendant database and statistical analysis.

2.5 Current Wireless Applications in Dynamic Pile Testing

Dynamic pile testing has evolved from the traditional energy method to the more accurate wave equation method since the first applicable one-dimensional wave propagation model was suggested by Smith (1960). The work done by Smith opened new horizons for subsequent researchers to follow and to improve on. In 1976, two widely used computer programs, TTI and WEAP (Wave Equation Analysis of Pile), were developed by Hirsch at Texas Transportation Institute and Goble et al. at Case Western Reserve University, respectively.

Aiming at solving the actual input hammer energy to piles and providing a better understanding of soil-pile interaction during pile driving, PDA (Pile Driving Analyzer) was developed in the 1970's as a method to directly measure dynamic pile response during driving. As the name implies, it was developed to analyze pile driving and

evaluate pile driveability, including the range of stresses imparted to the pile, hammer efficiency, etc. During dynamic pile testing, the strain gages and accelerometers are usually attached near the pile head to record the waveforms. The sensors are typically connected to the monitoring computer with 100-ft cables hanging down from pile top. The measured strains are converted into axial forces and the measured accelerations are integrated over time to velocity, both as a function of real time. With the development and acceptance of PDA (Pile Driving Analyzer), the Case method (Rausche et al. 1985), utilizing the measured force and velocity time histories in approximate simple algebraic equations, has become one of the widely used methods to evaluate the pile capacities during pile driving. Rausche et al. (1972, 1985) also developed a numerical program known as CAPWAP in which one of the two HST data (either force or velocity) from PDA is used as input in a numerical simulation to match closely with the other HST data by adjusting Smith model parameters. Once the acceptable match is achieved, then the distribution of side and toe resistances and the Smith model parameters can be determined.

The current dynamic testing hardware and analysis software are rather expensive. The operation of the PDA and attendant CAPWAP analysis requires highly trained personnel to carry out. Furthermore, the typically 100-ft long sensor cables are difficult to handle and often time can lead to safety hazards to engineers and operators attempting to install the gages to the piles. These cables can be damaged by the construction and pile driving equipments, resulting in considerable delays. Therefore, there is a need to develop an

alternative, robust, easy to handle wireless communication capability between the sensors and a data acquisition unit from a distance.

McVay et al. (2002) developed a technology consisting of non-recoverable (cast into the pile) wireless transmitter and instrumentation package at the University of Florida for pile monitoring. The new testing system can be divided into two modules – Non-Recoverable Unit and Receiver and Data Processing Unit. The Non-Recoverable Unit embedded into concrete piles consists of two strain gages, two accelerometers, a signal conditioning and sending unit, and antenna. The Non-Recoverable Unit is capable of broadcasting the stress wave information to the Receiver and Data Processing Unit during pile driving. The Receiver and Data Processing Unit receives the information from the Non-Recoverable Unit to calculate force traces, velocity traces and pile capacities. The Receiver and Data Processing Unit is made of receiver antenna, receiver and conditioning unit, data acquisition card, laptop computer, and data acquisition and processing software.

Since the Non-Recoverable Unit is pre-installed directly into the concrete piles, no installation set-up is required at the time of pile driving. The wireless operation of proposed technology minimizes the accident potential and construction delays (e.g., engineers attempting to install the gages to the piles and connection cables being damaged). The Non-Recoverable Unit can be installed into both pile top and bottom so that the force-time and velocity-time histories at the pile top and bottom can be obtained, thus resulting in a more accurate analysis on the distributions of pile stresses and pile capacities. Additional benefits include that the wireless system sleeps and is capable of

waking itself up during an extreme event (e.g., earthquake, collision); therefore, it can report the magnitude of the event and the resulting structural damage.

Laboratory and full-scale field tests have been performed by the University of Florida for calibrating and validating equipment responses. The output signals from wireless analysis package (WAP) system were very strong with less noise and can be achieved within the distance of 60 m. The WAP output signals show a very satisfactory comparison with the PDA outputs. An acquisition and data processing software was developed by LABVIEW to process the testing data for pile capacity determination, as well as pile stress monitoring during driving. The program is called Pile-Monitoring. vi including three theoretical methods of capacity assessment: Case Method, Paikowsky energy approach, and UF method.

Although the favorable field testing results could be obtained, many problems arose in the development of the equipment, the installation of the Non-Recoverable Unit, and the wireless transmission. The sensors, cables, and conditioners in Non-Recoverable Unit are easily broken and misaligned due to the concrete pouring. Due to the embedment of the Non-Recoverable Unit into the piles, it is not easily checked if errors happened during the pile driving. The wireless analysis package (WAP) system was not able to wake up from the low hammer strike accelerations.

The cost is a major limitation for the application of the developed WAP system. The approximate cost of $300 is needed for Non-Recoverable Unit (transmitters, conditioners,

and instruments: accelerometers, strain gages, etc.). The cost is about $6,400 for acquiring the Receiver and Data Processing Unit (receiver, PCMCA card, laptop computer, and LABVIEW software). The requirement of the experienced engineers on the installation and operation of WAP system may potentially hinder its extensive application.

2.6 Summary

From the review presented in this chapter, it can be seen that, over the last ten or fifteen years, several researchers have made major advances in applying reliability analysis to driven pile problems. Although the geotechnical engineers long ago learned practical ways to deal with uncertainties, they have been reluctant to embrace the more formal and rational approaches of reliability theory while other fields of civil engineering have made major commitments to probabilistic approaches. However, it is undeniable that reliability analyses provide insight into the relative contributions of different factors to the uncertainty of the prediction results and thus giving guidance for where further investigations are more fruitful. The reliability-based methodology could be used to further improve the quality control on pile driving and refine the LRFD of driven piles.

The purpose of this study is to develop a reliability-based quality control method on pile driving, to develop an updating methodology for improving resistance factors in LRFD by combining static analysis methods with dynamic test methods, and finally to incorporate set-up into reliability-based design of driven piles in clay and in sand. In addition to enhancing reliability based approach outlined above, this study also provides

new wave equation simulation technique for pile driving, which can minimize the need for CAPWAP trial-and-error procedure in achieving best matches. Finally, the research has resulted in a development of a new generation wireless communication technology with the necessary hardware and software to support its operation in dynamic pile testing applications.

CHAPTER III

QUALITY CONTROL METHOD FOR PILE DRIVING

3.1 Introduction

Static load tests have been used to verify the load-carrying capacity of driven piles. Additionally, dynamic pile tests have also been used as a quality control measure during pile driving to ensure adequacy of pile capacity. It has been suggested that the number of static load tests required to support the use of the resistance factor in the LRFD (Load and Resistance Factor Design) should be established based on site subsurface conditions characterized by field exploration and laboratory testing program. One or more static load tests should be performed per site to justify using the specified resistance factors for piles installed within a site (AASHTO 2006). Although dynamic pile tests have been widely used for quality control of driven piles, there is a lack of acceptance criteria for linking the number of dynamic pile tests and the required measured pile capacity.

Hannigan et al. (1998) suggested that a minimum of two dynamic pile tests be conducted for a small project. For large projects or small projects with anticipated installation difficulties, or significant time dependent capacity issues, a greater number of dynamic pile tests is recommended. If the test piles do not reach a prescribed design capacity, the design load for the piles is reduced or additional piles or pile lengths are

installed. Paikowsky et al. (2004) provided recommendations for the number of piles to be dynamically tested as well as the corresponding acceptance criterion for driven pile project. The quality assurance testing used approach in the manufacturing industry was employed to determine the number of dynamic tests to be performed on production piles. However, the use of normal distribution to characterize the statistics of dynamic test methods is very conservative, since the lognormal distribution has been known to better represent the probabilistic distribution characteristics of dynamic pile test results. The acceptance criterion for a set of piles was subjectively chosen so that the average capacity of the tested piles was no less than 85% of the nominal ultimate capacity. The use of arithmetic mean of the measured capacities is far different from the geometric mean of the measured capacities when the lognormal distribution is used to represent the probabilistic characteristics of dynamic pile tests.

In this chapter, quality control criteria for driven piles are developed from the framework of acceptance-sampling analysis for both static and dynamic pile test methods, adopting a more realistic lognormal distribution function to characterize the probabilistic properties of results of various prediction methods. The lognormal distribution of statistical data of various load test methods is converted into a standard normal distribution for evaluating the confidence interval to assure that the population mean of pile capacities be no less than the factored design loads. The number of load tests and the required measured capacities are interrelated, since reducing one of them invariably increases the other. An optimum approach is recommended for the selection of the

number of load tests and the required measured capacities for different quality control methods in driven piles.

3.2 Distribution Function of Static and Dynamic Pile Test Results

A database of 16 static pile load tests at a site in southern Italy, reported by Evangelista et al. (1977), showed that the lognormal distribution could represent the range of the pile capacities. Static pile load tests directly measure driven pile capacity; therefore, the mean of bias factor, λ_1, is 1.0. The coefficient of variation, COV_1, reflects the effects of the spatial variation from one pile location to another, the soil disturbance caused by pile driving, and set-up or relaxation after pile installation. Empirical data of sufficient quality to estimate within-site variability is not available. The site spatial variation, in general, could be categorized as low, medium, or high variability with the corresponding COV of 0.15, 0.25, and 0.35, respectively (Phoon and Kulhawy 1996, 1999a, and 1999b). A study by Zhang and Tang (2002) has shown that the COV of the capacity of driven piles from static pile load tests at eight sites ranged from 0.12 to 0.28, thus providing support for the suggested classification by Phoon and Kulhawy.

The pile capacities measured by dynamic load tests, R_d, can be related to the pile capacities from static pile load tests, R_s, by the bias factor, λ_2, as follows

$$R_s = \lambda_2 R_d \tag{3-1}$$

Other than the uncertainty of static pile load tests, the dynamic pile test itself also introduces variability due to model and systematic errors. For example, the dynamic formulas, such as ENR and Gates formulas, suffer a great deal of uncertainties in

determining input energy. Although the wave equation methods, such as CAPWAP (CAse Pile Wave Analysis Program) and Case methods using the PDA (Pile Driving Analyzer), may partially eliminate the uncertainties associated with the energy methods, these methods nevertheless introduce other uncertainties, such as the error of signal recording of the transducers as well as simplification of damping factors in the soil-pile interaction model. The set-up or relaxation after pile installation, especially in clayey soil, could not be properly accounted for in these dynamic pile testing methods. The variability of hammer performance and pile material properties could also introduce the errors to the dynamic pile testing method. The statistical characteristics for the bias factor for various dynamic test methods are needed for formulating the reliability-based pile acceptance criteria. Recently, McVay et al. (2000) and Paikowsky et al. (2004) have presented these statistical characteristics and they are summarized in Table 3-1. It has been found that the lognormal function could properly represent the distribution of the bias factor, λ_2.

3.3 Determination of Number of Load Tests and Corresponding Acceptance Criterion

The reliability-based acceptance-sampling analysis could provide a theoretical framework from which to estimate the mean of pile population. In the acceptance-sampling analysis, confidence intervals offer a means of establishing a range of values in which a true value is expected to lie, thus providing a probability statement about the likelihood of correctness (Ayyub and McCuen 2003). A test statistics Z can be used to compute the confidence interval for the case of normal distribution where the standard

deviation, σ, is known. The lower one-sided confidence intervals on the population mean, μ, are given by:

$$\overline{X} - Z_{\alpha}(\frac{\sigma}{\sqrt{n}}) \leq \mu \leq \infty \tag{3-2}$$

where $\overline{X}$ is the sample mean; n is the sample size; Z_{α} is reliability index corresponding to the value of random variables having the standard distribution and cutting off α percent in the tail of the distribution; and α is the level of significance and equal to 1-γ where γ is the level of confidence.

For quality control purpose of pile driving, field engineers usually select a certain number of test piles to determine the population mean of the pile capacity and to make sure that the population mean is no less than the factored design load at a certain level of reliability. It can be stated as:

$$L \leq \overline{R} - Z_{\alpha}(\frac{\sigma_R}{\sqrt{n}}) \leq \infty \tag{3-3}$$

where L = factored design load; $\overline{R}$ = the mean of equivalent static resistance that is computed as the product of the mean of bias factor and the dynamically measured capacity; σ_R = the standard deviation of equivalent static resistance; n = the number of dynamic pile tests. The reliability index Z_{α} is derived from the hypotheses test based on a test statistics Z. The reliability index in this chapter relates to the probability that a set of pile is incorrectly accepted as good, where the population mean is less than the factored design load. Therefore, the reliability index in this chapter carries different significance

from that commonly accepted in the LRFD design outlined by Withiam et al. (2001). Assuming

$$Y = \lambda t \tag{3-4}$$

where Y = ratio of equivalent static capacity to the factored design load; λ = bias factor for a type of dynamic pile test method; t = ratio of static or dynamic measured capacity to the factored design load. The variable λ is a random variable that accounts for the variability of the predicted capacity from various load test methods. The variable t is treated as a deterministic variable obtained as the ratio of actual static or dynamic measured capacity to the factored design load. Although there is a limitation in ignoring the uncertainties in design load herein, for simplification, the variability associated with design load is taken into account by the load factors because the uncertainties associated with load components are much smaller than those associated with resistance components. Therefore, the following expressions can be obtained for the ratio Y:

$$\mu_Y = \mu_\lambda t \tag{3-5}$$

$$\sigma_Y = \sigma_\lambda t \tag{3-6}$$

where μ_λ and σ_λ are mean value and standard deviation of bias factor, λ, respectively. The lognormal distribution can be employed to express the variable Y as $Y \sim LN(\psi_Y, \zeta_Y)$ where $\psi_Y = \ln\mu_Y - \frac{1}{2}\zeta_Y^{\,2}$, and $\zeta_Y^{\,2} = \zeta_\lambda^{\,2} = \ln(1 + \frac{\sigma_\lambda^{\,2}}{\mu_\lambda^{\,2}})$. Therefore, by utilizing the transformation relationship between the lognormal distribution $Y \sim LN(\psi_Y, \zeta_Y)$ and the standard normal distribution $Z \sim N(0,1)$, and the integration results for the standard normal, the cumulative distribution function for the lognormal distribution can be evaluated using the following transformation:

$$Z = \frac{\ln Y - \psi_Y}{\zeta_Y} \tag{3-7}$$

Fig. 3-1 shows the tail areas of the normal and lognormal distributions in which $\mu = 1$ and $\sigma = 0.3$. It can be seen that the difference between the corresponding deviations from mean is very large for the normal and lognormal distribution when the required levels of significance (i.e., value of tail area) is very small. For example, if the mean of a normal distribution lies two standard deviations above a single lower specification limit, the levels of confidence accepting the set of piles is 97.7% for the population with the normal distribution and 99.8% for the population with the lognormal distribution, respectively. It is obvious that when requiring high level of confidence, the use of sampling characteristics must be extremely careful (Phoon and Kulhawy 2005).

Now, considering ln(y) as a sample value, Eq. (3-2) can be expressed as:

$$\overline{\ln y} - Z_\alpha(\frac{\zeta_Y}{\sqrt{n}}) \le \psi_Y \le \infty \tag{3-8}$$

Noting that $\psi_Y = \ln \mu_Y - \frac{1}{2}\zeta_Y^2$, $y = \lambda t$, and $\zeta_Y = \zeta_\lambda$, Eq. (3-8) becomes:

$$\overline{\ln \lambda t} + \frac{1}{2}\zeta_\lambda^2 - Z_\alpha(\frac{\zeta_\lambda}{\sqrt{n}}) \le \ln \mu_Y \le \infty \tag{3-9}$$

In order to assure that μ_Y is no less than 1 (i.e. $\ln \mu_Y \ge 0$), the following expression can be obtained:

$$0 \le \overline{\ln t} + \psi_\lambda + \frac{1}{2}\zeta_\lambda^2 - Z_\alpha \frac{\zeta_\lambda}{\sqrt{n}} \le \infty \tag{3-10}$$

where $\psi_\lambda = \overline{\ln \lambda} = \ln \mu_\lambda - \frac{1}{2}\zeta_\lambda^2$. By requiring that the mean capacity of population piles be no less than the factored design load, the relationship of the required ratio, t, and the number of load tests can be derived for a particular dynamic pile test method and the chosen level of reliability.

3.4 Target Reliability Index vs. $\bar{t}$

The test statistics Z is applied to determine the lower one-sided confidence interval, from which the relationship between target reliability index, β, and level of significance, α, can be expressed as:

$$\beta = Z_\alpha = \Phi^{-1}(1-\alpha) \tag{3-11}$$

where Φ^{-1} is the inverse of the cumulative distribution function of the standard normal distribution. The target reliability index increases approximately proportionally with an exponential decrease in level of significance.

The lognormal distribution has been demonstrated to represent the statistics of static and dynamic pile test results, thus the mean of $\bar{t}$ can be expressed as:

$$\bar{t} = \sqrt[n]{t_1 t_2 \cdots t_n} \tag{3-12}$$

where t_n is the ratio of n^{th} measured capacity of pile test to the factored design load. When the test method and the number of test piles are pre-set, the relationship between reliability indexes β and the geometric mean of $\bar{t}$ could be obtained from Eq. (3-10)

based on the statistics of the test method. Fig. 3-2 shows the relationship between reliability indexes β and the geometric mean of $\bar{t}$ for the static load test method with the high site variability. It can be seen that the required $\bar{t}$ increases with an increase in the desired reliability index. The observation is consistent with experience-based quality control approach, where the higher target reliability index demands the higher measured mean capacity of load test for a given number of pile load tests. Furthermore, the required $\bar{t}$ is very sensitive to the selected target reliability index when the number of load tests is small. With an increase in the number of load tests, the sensitivity of $\bar{t}$ to the reliability index is lessened. At a certain target reliability level, an increase in the number of load tests provides higher confidence on the estimation of the mean capacity of pile population, thus allowing for the adoption of lower required $\bar{t}$.

3.5 Number of Load Tests vs. $\bar{t}$

As suggested in NCHRP Report 507 (Paikowsky et al. 2004), the target reliability index of β = 2.33 corresponding to the level of significance α = 1% is recommended for redundant piles defined as 5 or more piles per pile cap; the target reliability index of β = 3.00 corresponding to the level of significance α = 0.1% is recommended for nonredundant piles defined as 4 or fewer piles per pile cap. Figs. 3-3 and 3-4 present the relationship between the number of pile load tests and $\bar{t}$ for different dynamic pile test methods for reliability index β = 2.33 and 3.00, respectively. It can be seen that the required $\bar{t}$ decreases with an increase in the number of load test for all dynamic pile test methods. The first several load tests exert more pronounced effects on the reduction of the required $\bar{t}$, compared to the rest of load tests. The required $\bar{t}$ is not only dependent

on the number of load tests, but also related to the statistical distribution of load test capacity. For static load test with lowest COV, the required $\bar{t}$ exhibits the least sensitivity to the number of load tests. On the other hand, for the CAPWAP EOD method with the largest COV, the required $\bar{t}$ exhibits the highest sensitivity to the number of load tests. Figs. 3-3 and 3-4 can be adopted as an efficient and economical basis to determine the number of load tests and the corresponding required acceptance criterion for various pile test methods at the selected target reliability indices.

3.6 Correction Factor for Finite Population

When the number of tested sample n is comparable to the total number of population N, that is, the sampling fraction, f = n/N, is greater than about 10%, the effect of finite population comes into play. Ayyub and McCuen (2003) have proposed a finite population correction factor, (N-n)/(N-1), to account for the effect of finite population. Thus, the variance of the sample mean, $\overline{X}$, can be calculated with the known standard deviation, σ, as follows:

$$Var(\overline{X}) \cong \frac{(N-n)}{(N-1)} \frac{\sigma^2}{n} \tag{3-13}$$

The application of correction factor for finite population reduces the sampling variance, because the assumption of sampling without replacement in entire population is no longer reasonable. For most piling projects, the effect of finite population must be considered in determining the number of pile load tests and the corresponding acceptance criterion.

Fig. 3-5 illustrates the effect of finite population on the required number of pile load tests and the corresponding acceptance criterion for static load tests at high site variability for $\beta = 3.00$. It can be seen that an increase of sampling fraction corresponds to a decrease of the variance of the sample mean, thus resulting in a decrease of the required $\bar{t}$ for a given number of pile load tests. For the cases where the number of population piles is low, the relationship between the number of load tests and the required $\bar{t}$ exhibits a drastic change from the case where the number of population piles is infinitely large. It should be noted that the required $\bar{t}$ is 1.0 for the case of 10 test piles when the total number of piles is 10. It means that there is no variance in the sample average since all the production piles have been accounted for. It is consistent with engineering experience that the mean of the measured capacity of test piles is required to be no less than the factored design load when all the production piles are tested.

3.7 Quality Control Criteria

When the correction factor on finite population is considered and a target reliability index is preset, the relationship between the number of pile load tests and the required $\bar{t}$ can be obtained for different load test methods from Eq. (3-10). Tables 3-2 and 3-3 provide the number of pile load tests and the corresponding acceptance criteria for the quality control of driven piles using various load test methods for the target reliability indices $\beta = 2.33$ and 3.00, respectively. The number of piles that should be tested at a given construction site depends on the project size, the variability of the subsurface conditions, the adopted load test method, the target reliability index, and the relationship between the measured capacity of load test and the factored design load. In general, an

increase in the number of load tests gives engineers more confidence on the prediction of the overall behavior of population piles.

For all dynamic testing methods with signal measurements, the selection of the number of load tests and the corresponding acceptance criterion is suggested as the point at which the required $\bar{t}$ decreases about 10 percent when an additional load test is performed. It means, at that point, increasing the number of pile load tests can no longer effectively reduce the required $\bar{t}$. The number of pile load tests and the required $\bar{t}$ at this point are recommended as an optimum point for selection of quality control criterion. In Tables 3-2 and 3-3, the difference between statistical characteristics for various dynamic test methods results in the different required $\bar{t}$. However, it can be found that the ratios of equivalent static capacity to factored design load, $\overline{Y} = \lambda\bar{t}$, are about 1.87, 1.85, 1.81, 1.76, 1.79, and 1.73 for dynamic test methods of CAPWAP EOD, CAPWAP BOR, PDA EOD, PDA BOR, EA EOD, and EA BOR, respectively. It means that various dynamic test methods demand almost the same required design capacities to verify the structure reliability, based on the above approach of determining the required $\bar{t}$ and the number of load tests. On the other hand, it is noted that the dynamic test methods with relatively small COV, such as CAPWAP BOR, demand a less number of load tests. In other words, in order to obtain the same level of reliability, the more accurate dynamic test methods require a less number of test piles for a given construction site.

For static load tests, the total number of production piles has small effect on determining the quality control criteria due to the method's high accuracy. Due to high

cost and time-consuming nature of static load tests, it is not economical to increase the number of load tests to reduce the required $\bar{t}$. For a project, if the site has similar subsurface soil conditions, the overall project piles can be considered as the entire population. Otherwise, the criteria should be independently applied to each part of the project site where similar subsurface soil conditions exist. If the measured pile capacity cannot satisfy the required criteria, the alternative solution is to install additional piles or to drive piles deeper. It should be noted that, when pile relaxation occurs at a project site, the quality control criteria should be carefully used for dynamic pile tests at EOD, since higher degree of confidence could be obtained from static load test or dynamic pile tests at BOR.

3.8 Conclusions

In this chapter, acceptance-sampling analysis has been employed to develop quality control criteria for driven piles. The more representative lognormal distribution of statistical data of various load test methods is used to evaluate the confidence interval for assuring that the population mean of pile capacities be no less than the factored design loads. The required measured capacity decreases with an increase in the number of load test in achieving the same level of reliability. Theoretically, an increase of both the required measured capacity and the number of load tests enhances the reliability level of population pile capacity. However, there is an optimum point where the number of load test and the required measured capacity are economically associated to yield reasonable quality control criteria based on acceptance-sampling analysis techniques. The correction factor of finite population has been incorporated in interpreting the cases of limited pile

population that represent most of geotechnical projects. The number of load tests associated with the criteria of the measured capacities for driven piles has been recommended in Tables 3-2 and 3-3 for different load test methods with different levels of reliability.

Table 3-1 Distribution Parameters of Various Dynamic Test Methods for Driven Piles

Load test method	Number of cases	Mean of bias factor, λ_2	Standard deviation	Coefficient of variation, COV	References
CAPWAP EOD	125	1.626	0.797	0.490	Paikowsky et al. (2004)
CAPWAP BOR	162	1.158	0.393	0.339	Paikowsky et al. (2004)
PDA EOD	48	1.344	0.443	0.329	McVay et al. (2000)
PDA BOR	42	1.036	0.322	0.311	McVay et al. (2000)
EA EOD	128	1.084	0.431	0.398	Paikowsky et al. (2004)
EA BOR	153	0.785	0.290	0.369	Paikowsky et al. (2004)

CAPWAP = Case Pile Wave Analysis Program; PDA = Case Method Using the Pile Driving Analyzer; EA = Paikowsky's Energy Approach; EOD = End of Driving; BOR = Beginning of Restrike.

Table 3-2 Recommended Number of Load Tests to Be Conducted for Quality Control of Driven Piles (Reliability β=2.33)

		Site Variability																				
		Low							Medium								High					
Test methods		SLT	CAPWAP		PDA		EA		SLT	CAPWAP		PDA		EA			SLT	CAPWAP		PDA		EA	
Time of test			EOD	BOR	EOD	BOR	EOD	BOR		EOD	BOR	EOD	BOR	EOD	BOR			EOD	BOR	EOD	BOR	EOD	BOR
Required ratio $\bar{t}$		1.45	1.15	1.60	1.35	1.70	1.65	2.20	1.75	1.15	1.60	1.35	1.70	1.65	2.20		1.75	1.15	1.60	1.35	1.70	1.65	2.20
No. of pile population	<=10	1	3	2	2	2	3	3	1	3	3	3	3	3	3		2	4	3	3	3	4	4
	11~20	1	3	2	2	2	3	3	1	4	3	3	3	3	3		2	4	3	3	4	4	4
	21-50	1	4	2	2	2	3	3	1	4	3	3	3	4	4		2	4	3	4	4	4	4
	51-100	1	4	2	2	2	3	3	1	4	3	3	3	4	4		2	5	3	4	4	4	5
	>=100	1	4	2	2	2	3	3	1	4	3	3	3	4	4		2	5	3	4	4	4	5

SLT = Static Load Test; CAPWAP = Case Pile Wave Analysis Program; PDA = Case Method Using the Pile Driving Analyzer; EA = Paikowsky's Energy Approach; EOD = End of Driving; BOR = Beginning of Restrike.

$\bar{t} = \sqrt[n]{t_1 t_2 \cdots t_n}$, where t_n is the ratio of n^{th} measured capacity of pile test to the factored design load.

Table 3-3 Recommended Number of Load Tests to Be Conducted for Quality Control of Driven Piles (Reliability β=3.00)

		Site Variability																				
		Low							Medium							High						
Test methods		SLT	CAPWAP		PDA		EA		SLT	CAPWAP		PDA		EA		SLT	CAPWAP		PDA		EA	
Time of test			EOD	BOR	EOD	BOR	EOD	BOR		EOD	BOR	EOD	BOR	EOD	BOR		EOD	BOR	EOD	BOR	EOD	BOR
Required ratio $\bar{t}$		1.60	1.15	1.60	1.35	1.70	1.65	2.20	2.10	1.15	1.60	1.35	1.70	1.65	2.20	2.10	1.15	1.60	1.35	1.70	1.65	2.20
No. of pile population	<=10	1	4	3	3	3	4	4	1	5	4	4	4	4	4	2	5	4	4	4	5	5
	11~20	1	5	3	3	3	4	4	1	5	4	4	4	4	5	2	6	5	5	5	6	6
	21-50	1	5	3	3	4	5	5	1	6	4	4	4	5	6	2	6	5	5	5	6	7
	51-100	1	6	3	4	4	5	5	1	6	4	4	4	5	6	2	7	5	6	6	7	7
	>=100	1	6	4	4	4	5	5	1	6	4	4	5	6	6	2	7	5	6	6	7	7

SLT = Static Load Test; CAPWAP = Case Pile Wave Analysis Program; PDA = Case Method Using the Pile Driving Analyzer; EA = Paikowsky's Energy Approach; EOD = End of Driving; BOR = Beginning of Restrike.

$\bar{t} = \sqrt[n]{t_1 t_2 \cdots t_n}$, where t_n is the ratio of n^{th} measured capacity of pile test to the factored design load.

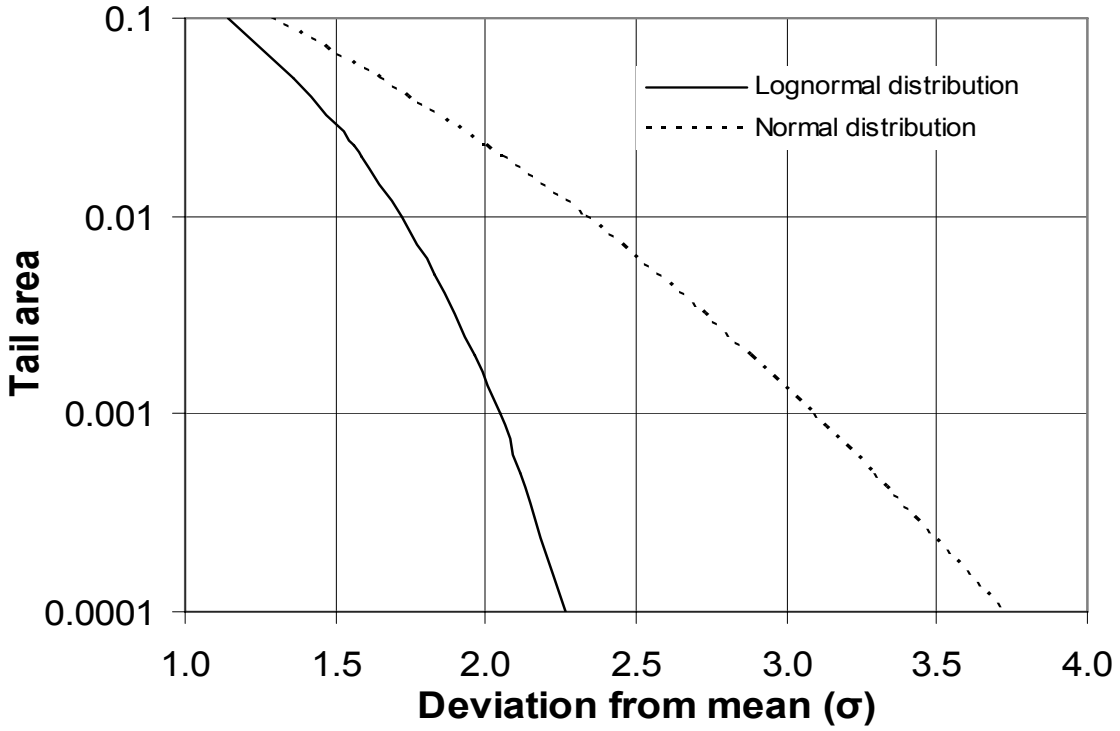

Figure 3-1 Tail Area of the Normal and Lognormal Distributions

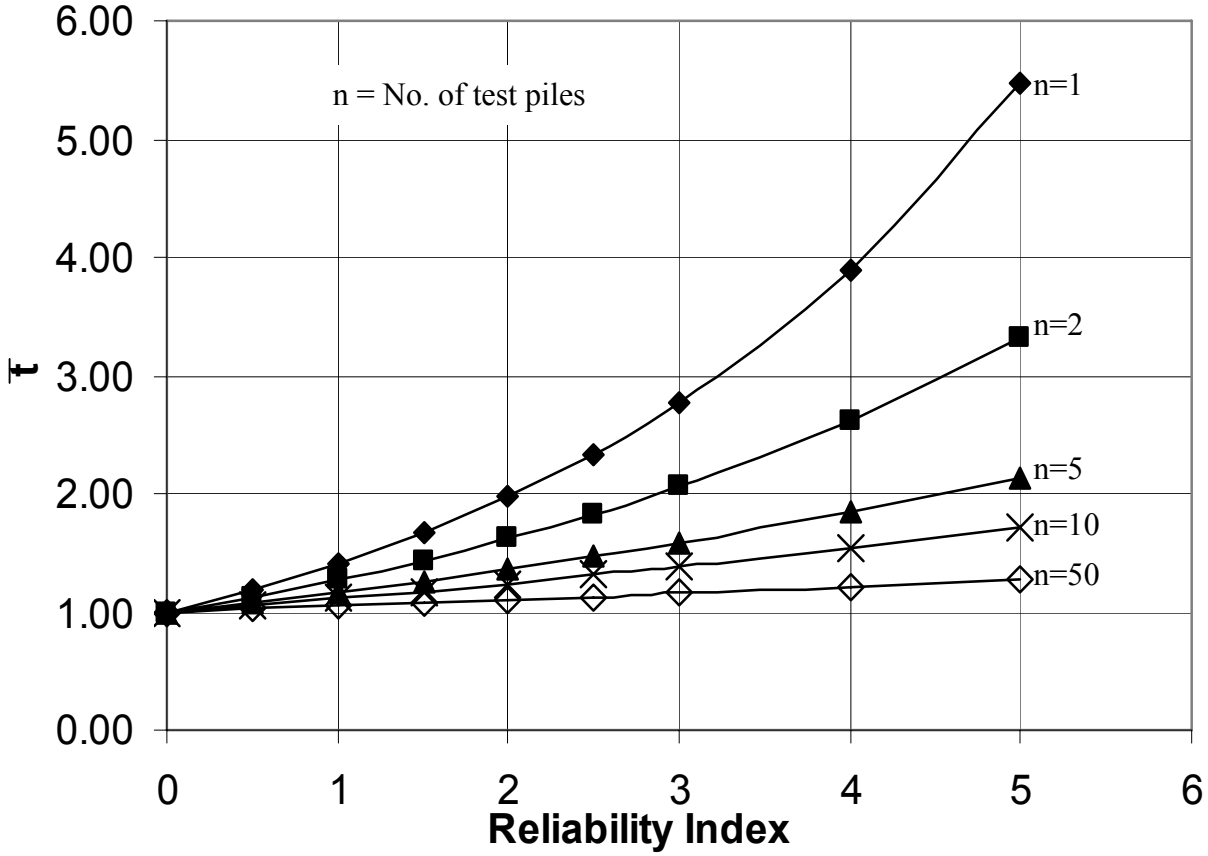

Figure 3-2 Reliability Index and $\bar{t}$ with Different n

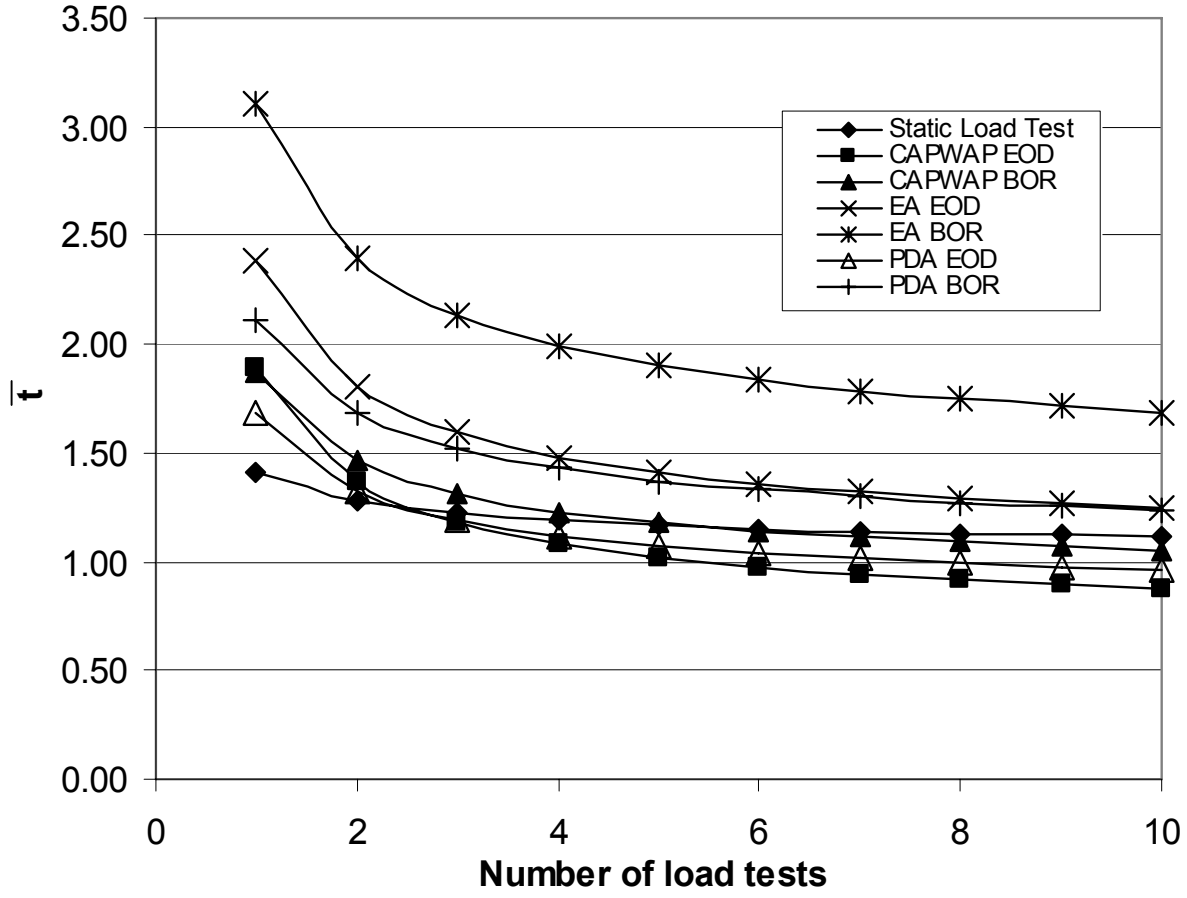

Figure 3-3 Relationship between $\bar{t}$ and Number of Load Tests at Target Reliability Index β =2.33

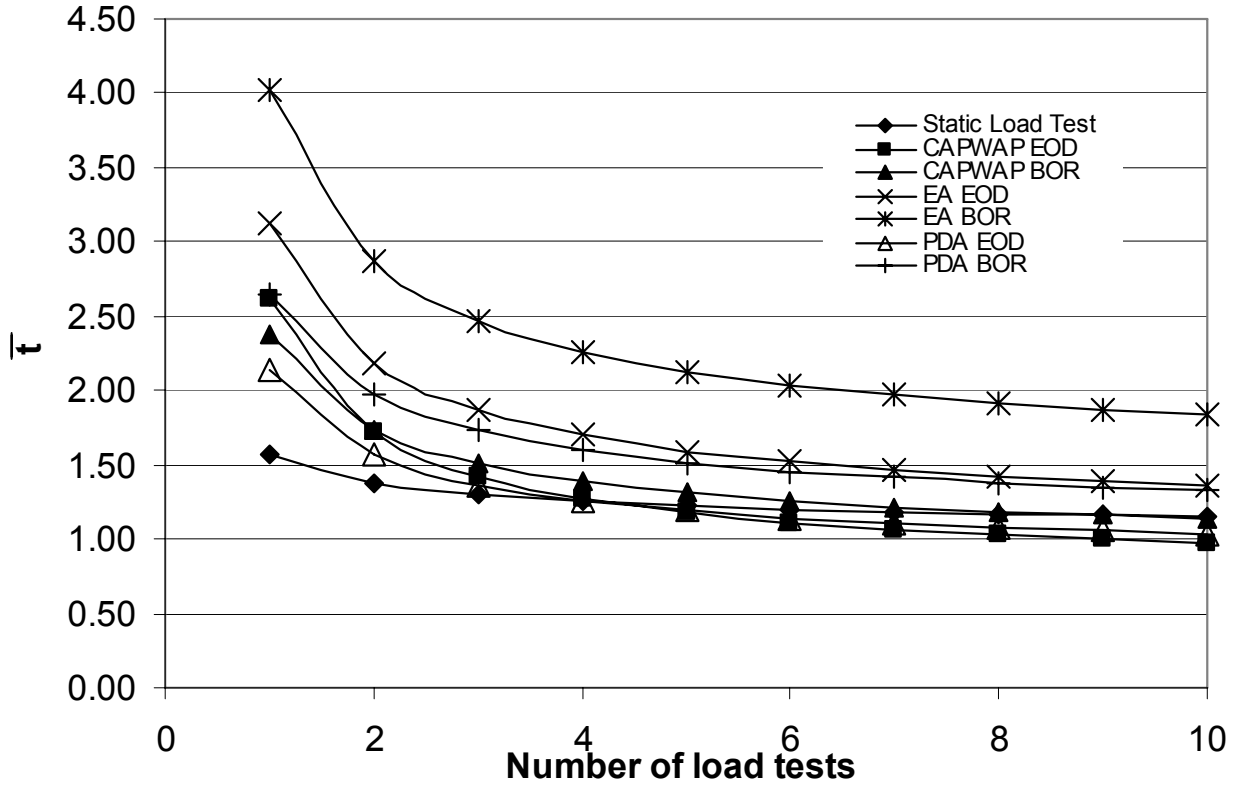

Figure 3-4 Relationship between $\bar{t}$ and Number of Load Tests at Target Reliability Index β =3.00

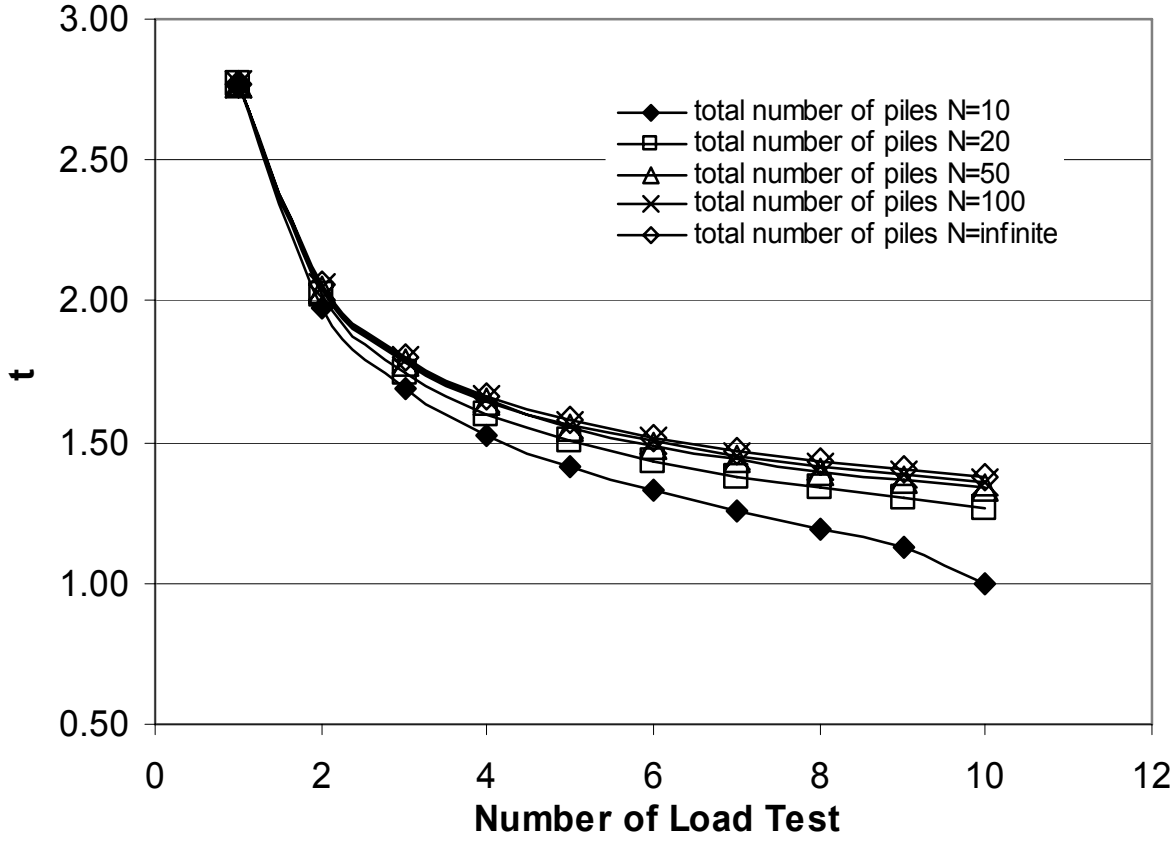

Figure 3-5 Effect of Finite Population on Different Total Numbers of Load Tests

CHAPTER IV

INCORPORATING SET-UP INTO RELIABILITY-BASED DESIGN OF DRIVEN PILES IN CLAY

4.1 Introduction

The fact that axial capacity of a driven pile may change over time after initial pile installation has been reported by a number of geotechnical engineers for many years. The significance of time effects on pile capacity, however, is dependent upon the type of soil which piles are driven into. The increase of pile capacity with time is usually referred to as set-up, while the decrease of pile capacity with time is often termed as relaxation. Due to pile driving, soils around the pile are significantly disturbed and remolded, and excess pore pressures are generated in saturated cohesive soils. With passage of time, the excess pore pressure will dissipate and consequently pile capacity is regained. Decrease in excess pore pressure is inversely proportional to the square of the distance from the pile (Pestana et al. 2002). The time to dissipate excess pore pressure is proportional to the square of the horizontal pile dimension (Holloway and Beddard 1995; Soderberg 1961), and inversely proportional to the soil's horizontal coefficient of consolidation (Soderberg 1961). Accordingly, Larger-diameter piles take longer to set-up than smaller-diameter piles (Long et al. 1999; Wang and Reese 1989). On a percentage-basis, piles driven into clay generally tend to experience greater set-up

than piles driven into sand and silt. Piles may experience relaxation when driven into dense and saturated sand and silt (Long et al. 1999). Numerous geotechnical engineers developed various empirical formulas to predict the set-up behavior (e.g., Skov and Denver 1988; Svinkin et al. 1994; Huang 1988). In particular, the semi-logarithmic empirical relationship, proposed by Skov and Denver, has been widely used to predict post-installation pile capacity increase with time.

With an accumulation of more experience and knowledge on set-up phenomenon, some researchers have suggested that the set-up be formally incorporated into the prediction method to determine total pile capacity. For example, Bullock et al. (2005) proposed a conservative method for incorporating side shear set-up into the total pile capacity. The predicted set-up capacity was assumed to have the same degree of uncertainties as the measured reference capacity and a single safety factor was used to account for all uncertainties of loads and resistances. Due to different uncertainties associated with measured capacity and predicted set-up capacity, Komurka et al. (2005) proposed a method to apply separate safety factors to EOD (End of Driving) and set-up components of driven pile capacity. Furthermore, the set-up capacity was characterized as a function of pile penetration based on dynamic monitoring during both initial driving and restrike testing.

This chapter presents a database containing a large number of pile testing data in clay, from which the set-up effect is statistically analyzed. The compilation of the statistical database of set-up capacity makes it possible to apply reliability-based

analysis techniques to develop separate resistance factors to account for different degrees of uncertainties associated with the measured reference capacity and the predicted set-up capacity in the LRFD (Load and Resistance Factor Design) of driven piles. The First-Order Reliability Method (FORM) is used to determine the separate resistance factors for various target reliability levels. The test results obtained during a convenient short-time restrike (usually 1 day after initial pile driving) can be used to predict the long-term capacity based on the proposed formula by Skov and Denver (1988). The application of separate resistance factors in LRFD for the measured reference capacity and the predicted set-up capacity can remarkably improve the prediction of driven pile capacity. Furthermore, by incorporating pile set-up capacity, pile length or number of piles can be reduced and economical design of driven piles can be achieved.

4.2 Statistical Study of Pile Set-up

Pile set-up has been widely observed in piles driven into saturated clays. Due to pile driving, soils around the pile are significantly disturbed and remolded, and excess pore pressures are generated. With passage of time, the excess pore pressure dissipates and consequently pile capacity is increased. Based on observations in the field, some researchers have developed predictive equations for the time-dependent increase in pile capacity. Skov and Denver (1988) presented an empirical equation for set-up based on a logarithmic increase of pile capacity with time as follows

$$Q_t = Q_0 (1 + A \log \frac{t}{t_0}) \tag{4-1}$$

where

Q_t = axial capacity at time t after driving,

Q_0 = axial capacity at time t_0,

A = a factor that is a function of soil type and can be determined as the slope of the linear portion of the normalized capacity Q_t/Q_0 versus log(t) plot,

t = time since pile installation, and

t_0 = time after installation at which point the capacity gain becomes linear on a log(t) plot.

Based on Eq. (4-1), the set-up capacity can be expressed as

$$Q_{set-up} = Q_0 A \log \frac{t}{t_0} \tag{4-2}$$

Skov and Denver also recommended numerical values for A and t_0 as 0.6 and 1 day in clay and 0.2 and 0.5 days in sand, respectively. Reasearchers, such as Svinkin et al. (1994), Camp and Parmar (1999), and Bullock et al. (2005), have also provided a range of numerical values for these two parameters.

Because of the highly disturbed state of the soil, there is a brief period following installation during which the initial rate of capacity gain with time is different from the later rate. During this period, the affected soil experiences an increase in effective and horizontal stress, consolidates, and gains strength in a manner which is not well-understood and is difficult to model and predict. After the time t_0, the affected soil experiences an increase in effective vertical and horizontal stress, consolidates, and

gains shear strength according to conventional consolidation theory. The time t_0 is a function of soil type, permeability, and sensitivity and pile type, permeability, and size. The less permeable the soil and pile and the greater volume of soil displaced by pile driving, the longer the time t_0. The A parameter is a function of soil type, pile material, type, size, and capacity to account for the degree of the capacity gain with the elapse of time (Camp and Parmar 1999; Svinkin et al. 1994; Svinkin and Skov 2000). Although there should be physical meanings behind these parameters, both the parameters t_0 and A are back-calculated from field data, or gleaned from empirical relationships in the literatures (Skov and Denver 1988; Svinkin et al. 1994; Chow 1998; Axelsson 1998; Bullock 1999; Camp and Parmar 1999; Bullock et al. 2005). It should be noted that determination of A is a function of the value used for t_0, and visa-versa; these two variables are not independent (Bullock 1999). On a percentage-basis, piles driven into clay generally tend to experience greater set-up than piles driven into sand and silt (Long et al. 1999); therefore, the focus of this chapter is on piles driven into clay.

A database containing both dynamic pile and static load tests is compiled in Table 4-1. The table includes information about the test piles and source of references. For each pile in the table, at least two load tests at different time after pile installation (whether dynamic or static methods) are performed so that the development of set-up capacity can be quantified. The database is statistically analyzed to compare with the time-capacity relationship proposed by Skov and Denver (1988).

Based on the compiled database, most of pile testing data show that the pile capacity gain becomes approximately linear with the logarithm of time 1 day after pile installation. Researchers, such as Svinkin et al. (1994), Alexsson (1998), McVay (1999), and Bullock et al. (2005), have proposed the use of $t_0 = 1$ day. Using $t_0 = 1$ day, the normalized axial pile capacity (i.e., Q_t/Q_0) versus the logarithm of time is plotted in Fig. 4-1 for all cases in the database. The time corresponding to the pile capacity measured at EOD is taken as 0.01 day in the plot. The dashed line defines an approximate range of A from 0.1 to 1.0. The mean value of A for all 37 testing piles is close to the value of 0.5. Chow (1998) reported the values of A ranging from 0.25 to 0.75. Studies by Axelsson (1998) yielded the values of A ranging from 0.2 to 0.8. The observations from this compiled database seem to conform with the previous experiences. Therefore, the reference time $t_0 = 1$ day and A = 0.5 are used for the subsequent statistical analyses in this chapter. When further data becomes available, the values of t_0 and A could be modified. It is interesting to note that, in some cases, the axial capacity after installation reaches 8 times the axial capacity at EOD. A couple of cases show that pile capacity increases linearly with the logarithm of time until 100 days after driving. After time elapse of 100 days, the increase of pile capacity with time becomes less pronounced compared to those during the first 100 days after driving. The compiled database supports the general notion that 100 days after EOD can be taken as the time after which the set-up effect would be minimal.

The accuracy of the Skov and Denver Equation is analyzed by examining the ratio of the measured set-up capacities to the predicted using $t_0 = 1$ day and A = 0.5. The

frequency distribution for all 127 cases of 37 piles is shown in Fig. 4-2. It can be seen that a normal distribution seems to approximately represent the distribution. The mean value μ, standard deviation σ, and Coefficient of Variation, COV, of the fitted normal distribution are 1.141, 0.543 and 0.475, respectively. To verify the assumed theoretical distributions, the Kolmogorov-Smirnov test (Ang and Tang 1975) was carried out. The maximum differences in cumulative frequency between the observed data and the theoretical distributions are $D_n = 0.058$ that is smaller than the critical value $D_n^{\alpha} = 0.121$ at the 5% significance level. Therefore, the assumed normal distribution for the predicted set-up capacity is valid. However, the current use of a normal distribution to describe the statistical characteristics of the predicted set-up capacity does involve limitations. For a normal random variable with mean = 1.141 and standard deviation = 0.543, the probability of realizing negative values is about 2%. The database shown in this chapter, on the other hand, fails to detect any negative value. Therefore, it is expected that, with the accumulation of additional pile test data, the fitted probability model and the relevant statistical parameters may require further modifications if a larger dataset still fails to detect negative value.

4.3 Correlation between Reference Capacity Q_0 and Set-up Capacity $Q_{set\text{-}up}$

A statistical analysis result on CAPWAP EOD and BOR (Beginning of Restrike) methods by Paikowsky et al. (2004) is summarized in Table 4-2. It was found that the time of testing (EOD vs. BOR) significantly affected the accuracy of CAPWAP prediction, regardless of soil type (Paikowsky and Stenerson 2000; Paikowsky et al. 2004). The BOR statistics included only the last blow of BOR for all the case histories,

and the time of the dynamic test is generally close to the time of static load tests. Therefore, CAPWAP BOR results were used to evaluate the accuracy of CAPWAP approach. Comparing the statistical parameters, COV of CAPWAP EOD and CAPWAP BOR, one can see that CAPWAP BOR provides better accuracy than CAPWAP EOD. The statistical database in Fig. 4-1 shows that the pile capacity at BOR is significantly larger than that at EOD for piles in clay. Therefore, the factored capacity from EOD test result is much less than that from BOR test result for the same pile driven into clay. The unreasonableness of different factored capacity for the same pile can be attributed to higher COV value for EOD, caused primarily by more varied set-up effects during the time period from EOD to the static load test. The database of pile set-up in clay supports the notion that predicting pile set-up effect involves higher uncertainties than the measured CAPWAP results. Therefore, it is necessary to separate the resistance factors to account for the different degrees of uncertainties associated with the measured capacity and the predicted set-up capacity.

The relationship between the measured reference capacity Q_0 and the predicted pile set-up capacity $Q_{set\text{-}up}$ is not at all clear. However, since the uncertainties of pile set-up prediction are contributed by empirical relationship of Skov and Denver, it may be reasonable to assume that the measured CAPWAP results and the prediction of set-up capacity are independent of each other. To verify this assumption, a total of 16 piles in the database (each has 2 or more CAPWAP dynamic testing results and 1 static load test result) is used to investigate the correlation between the measured CAPWAP results and

the predicted set-up capacity. The correlation coefficient ρ, based on Eq. (4-3), is calculated as -0.243.

$$\rho = \frac{Cov(X,Y)}{\sigma_X \sigma_Y} = \frac{E[(X-\mu_X)(Y-\mu_Y)]}{\sigma_X \sigma_Y} \tag{4-3}$$

where μ_X and μ_Y = means of the random variables X and Y, respectively; σ_X and σ_Y = standard deviation of X and Y, respectively. In this case, X = the measured reference capacity from CAPWAP method; Y = the predicted set-up capacity from Eq. (4-2). It can be seen that the correlation coefficient between Q_0 and $Q_{set\text{-}up}$ is very small, thus supporting the notion that Q_0 and $Q_{set\text{-}up}$ can be assumed to be independent of each other. In this chapter, the uncertainties associated with dead and live loads as well as the measured reference capacity Q_0 and the predicted set-up capacity $Q_{set\text{-}up}$ are systemically accounted for in a framework of First-Order Reliability Method (FORM). Separate resistance factors are derived for Q_0 and $Q_{set\text{-}up}$ for adoption in the Load and Resistance Factor Design (LRFD) of driven piles.

4.4 First-Order Reliability Method (FORM)

Load and Resistance Factor Design (LRFD) method for foundations has evolved beyond First-Order Second Moment (FOSM), which is being used in the existing AASHTO specifications to calibrate the resistance factors, to the more invariant FORM approach. Phoon et al. (2003a and 2003b), Paikowsky et al. (2004), and Allen et al. (2005) have proposed the application of FORM approach to calibrate resistance factors for deep foundation. Ang and Tang (1984) provide detailed descriptions about the procedure of using FORM to calibrate LRFD partial safety factors. FORM can be used

to assess the reliability of a pile with respect to specified limit states as well as to calculate partial safety factors ϕ_i and γ_i for resistances and loads, respectively, for a chosen target reliability index β. In design practice, the limit state can be represented by a performance function of the form,

$$g(X) = g(X_1, X_2, ..., X_n) \tag{4-4}$$

in which $X=(X_1, X_2,\ldots,X_n)$ is a vector of basic random variables of strengths and loads. The limit is defined as $g(X)=0$, implying failure when $g(X)<0$. When performing FORM analysis, it can be stated that a measure of safety in the form of the reliability index β is defined as the shortest distance from the origin to the failure surface (limit state) in the reduced coordinates (Ayyub and McCuen 2003). The reliability index according to this definition is shown in Fig. 4-3 for a nonlinear performance function g. The point on the failure surface that corresponds to the shortest distance is called the design (or failure) point at which the load and resistance factors can be respectively determined for the components of load and resistance in the reliability-based design.

Iterative steps for determining β using FORM (Ang and Tang 1984) are outlined herein:

1. Assume an initial value for the design point. It is common to start with the mean values of the basic random variables. The design point in the reduced coordinates should then be computed as

$$x_i'^{*} = \frac{x_i^{*} - \mu_{X_i}}{\sigma_{X_i}} \tag{4-5}$$

where μ_{X_i} = mean value of the basic random variable X_i, σ_{X_i} = standard deviation of the basic random variable X_i, the notations x^* and x'^* are used to denote the design point in the regular coordinates and in the reduced coordinate system, respectively.

2. If the distribution of basic random variables is non-normal, approximate this distribution with an equivalent normal distribution at the design point, having the same tail area and ordinate of the density function with equivalent mean,

$$\mu_X^N = x^* - \Phi^{-1}(F_X(x^*))\sigma_X^N \tag{4-6}$$

and equivalent standard deviation

$$\sigma_X^N = \frac{\phi(\Phi^{-1}(F_X(x^*)))}{f_X(x^*)} \tag{4-7}$$

where μ_X^N = mean value of the equivalent normal distribution, σ_X^N = standard deviation of the equivalent normal distribution, $F_X(x^*)$ = original cumulative distribution function (CDF) of X_i evaluated at the design point, $f_X(x^*)$ = original PDF of X_i evaluated at the design point, $\Phi(\bullet)$ =CDF of the standard normal distribution, and $\phi(\bullet)$ = PDF of the standard normal distribution.

3. Set $x_i'^* = \alpha_i^* \beta$, in which the α_i^* are direction cosines. Compute the directional cosines (α_i^*, i = 1, 2,…, n) using,

$$\alpha_i^* = \frac{(\frac{\partial g}{\partial x_i'})_*}{\sqrt{\sum_{i=1}^{n}(\frac{\partial g}{\partial x_i'})_*^2}} \text{ for I =1,2,…,n} \tag{4-8}$$

where

$$(\frac{\partial g}{\partial x_i^{'}})_* = (\frac{\partial g}{\partial x_i})_* \sigma_{X_i}^N \tag{4-9}$$

4. With α_i^*, $\mu_{X_i}^N$, $\sigma_{X_i}^N$ now known, the following equation is solved for β:

$$g[(\mu_{X_1}^N - \alpha_{X_1}^* \sigma_{X_1}^N \beta),...,(\mu_{Xn}^N - \alpha_{Xn}^* \sigma_{Xn}^N \beta)] = 0 \tag{4-10}$$

5. Use the β obtained from step 4, a new design point is obtained from

$$x_i^* = \mu_{X_i}^N - \alpha_{X_i}^* \sigma_{X_i}^N \beta \tag{4-11}$$

6 Repeat steps1 to 5 until convergence of β is achieved.

4.5 Calibrate Partial Load and Resistance Factors Based on FORM

The database shows that driven piles in clay experience set-up. The magnitude of set-up is so significant that economical design of driven piles is not possible without recognition of the anticipated capacity gain with time. Within the last decade, dynamic pile testing during restrikes for capacity determination has been adopted in practice to account for the set-up. However, the set-up may continue 100 days after driving. Thus, the restrike capacity measured at 7 days or less after initial pile installation is likely to underpredict the actual capacity. Therefore, it would be advantageous to develop a method to enable predication of long-term capacity based on the test data obtained during short-term restrike.

When the set-up capacity is incorporated into the driven pile design, the strength limit state at the failure point can be expressed as

$$g = R^* - L^* = Q_0^* + Q_{set-up}^* - L_D^* - L_L^* = 0 \tag{4-12}$$

where R^* = total resistance, L^* = total load, Q_0^* = measured pile axial capacity at reference time t_0, Q_{set-up}^* = predicted pile set-up capacity after time t_0, L_D^* = dead loads, and L_L^* = live loads. The probabilistic characteristics of the random variables L_D and L_L are well documented in AASHTO (Nowak 1999). The probabilistic characteristics of the random variables Q_0 is taken as that of CAPWAP BOR presented by Paikowsky et al. (2004). The probabilistic characteristics of the random variables Q_{set-up} is assumed as a normal distribution:

$$f(z) = \frac{1}{\sqrt{2\pi}\sigma} \exp[-\frac{1}{2}(\frac{x-\mu}{\sigma})^2] \tag{4-13}$$

where $\mu = 1.141$ and $\sigma = 0.543$ in Fig. 4-2, based on Eq. (4-2) ($A = 0.5$ and $t_0 = 1$ day). Table 4-3 summarizes the statistical parameters and distribution function for each random variable. With the known load and resistance statistical characteristics, the iterative solution of FORM approach can be applied to determine the load and resistance factors for the chosen target reliability index (Ang and Tang 1984; Phoon et al. 2003a and 2003b; Ayyub and McCuen 2003; Paikowsky et al. 2004).

Based on AASHTO LRFD Highway Bridges Design Specifications (2003), the ratio of dead to live load is a function of a bridge's span length. The following values of L_D/L_L are recommended as: 0.52, 1.06, 1.58, 2.12, 2.64, 3.00, and 3.53 for span lengths of 9, 18, 27, 36, 45, 50, and 60 m, respectively. The relationship between the partial safety factor (i.e., load and resistance factors) and the target reliability index is shown in Fig. 4-4, where the ratio of dead load to live load is selected as 1.58:1 to represent a bridge span length of 27m, and the ratio of Q_0 to Q_{set-up} is 1:1 based on the Skov and

Denver equation with A = 0.5 and t =100 days. The partial safety factors for all loads and resistances vary approximately linearly with the target reliability index. The resistance factors for Q_0 are higher than those for $Q_{set\text{-}up}$ at a given reliability level because uncertainties for Q_0 are less than those for $Q_{set\text{-}up}$. The fact that COV of two loads are much smaller than those of two resistances has resulted in smaller variation of load factors with the target reliability index for the live and dead load in Fig. 4-4. The variance of target reliability index imposes the largest effect on the resistance factor for the set-up capacity with the highest uncertainty (the highest COV value). Fig. 4-4 shows that the percentage of the capacity component with the higher uncertainty (i.e., $Q_{set\text{-}up}$), which can be utilized in design to resist the load, decreases with an increase of the desired target reliability index. The negative value for the resistance factor of $Q_{set\text{-}up}$ in Fig. 4-4 does not mean that the consideration of set-up effect will reduce the total factored design capacity. It can be interpreted as the most possible failure point at which the combination of Q_0 and $Q_{set\text{-}up}$ is optimized to resist the given load effects. The same statistics of load and resistance components can be used to determine the relationship between partial safety factors and reliability index in Fig. 4-5, where the resistance components only include Q_0 without considering the set-up effects. Compared to the approximately invariant load factors with the change of target reliability index for the case of considering set-up effect, the load factors for the case of not considering set-up effects vary more pronouncedly. This may be attributed to the fact that the resistance component (i.e., Q_0) possesses the relatively similar COV values with the load components. When the ratio of dead load to live load is considered as 1.58:1 and the nominal live load is assumed as 1.0, Fig. 4-6 shows that the required resistances Q_0 to

satisfy the predefined structural reliability for the cases with and without considering the set-up effects, respectively. It can be seen that although the resistance factor of Q_{set-up} is negative for the target reliability index β=2.35 in Fig. 4-4, the required Q_0 with considering the set-up effect is still smaller than that without considering the set-up effect until the target reliability index β=3.00 is chosen as shown in Fig. 4-6. It means that, when the target reliability index is low (β<3.00), the incorporation of set-up effect into the design of driven piles can advantageously enhance the prediction of design capacity so that shorter pile length or less number of piles can be chosen to achieve economical design. When the reliability index is greater than 3.00, the incorporation of set-up effect can no longer improve the prediction of design capacity of driven piles due to higher uncertainties associated with the prediction of set-up capacity.

4.6 Practical Load and Resistance Factors for Piles Driven into Clay

For a given reliability index β and probability distribution for resistance and load effects, the partial safety factor determined by the FORM approach may differ for different failure modes. For this reason, calibration of load and resistance factors is important in order to maintain the same values of load factors for all loads at different failure modes. In order to be consistent with the existing experience in LRFD, the calibrations of resistance factor for set-up is performed for a set of load factors already specified in the structural code. The resistance factors of Q_0 for CAPWAP approach are taken as the same as those recommended in NCHRP Report 507. When incorporating the set-up effect into the design of driven pile, the LRFD criterion can be expressed as

$$\phi_0 Q_0 + \phi_{set-up} Q_{set-up} \geq \gamma_L L_L + \gamma_D L_D \tag{4-14}$$

where ϕ_0 and $\phi_{set\text{-}up}$ = resistance factors for reference resistance at t_0 and set-up resistance, respectively; γ_L and γ_D = load factors for live and dead loads, respectively.

The relationship between the reliability index and the probability of failure can be expressed as

$$\beta = \Phi^{-1}(1 - P_f) \tag{4-15}$$

where Φ^{-1} is the inverse of the cumulative distribution function of the standard normal distribution and P_f is probability of failure. The target reliability index increases approximately exponentially with a decrease of probability of failure. As suggested in NCHRP Report 507 (Paikowsky et al. 2004), the target reliability index of β=2.33 corresponding to the probability of failure P_f= 1% is recommended for redundant piles defined as 5 or more piles per pile cap; the target reliability index of β=3.00 corresponding to the probability of failure P_f= 0.1% is recommended for nonredundant piles defined as 4 or fewer piles per pile cap. The resistance factors are ϕ_0 = 0.65 and ϕ_0 = 0.50 for CAPWAP approach at β=2.33 and β=3.00, respectively. As specified by AASHTO (Novak 1999), the load factors γ_L=1.75 and γ_D=1.25 are used for live and dead loads, respectively. The above load and resistance factors can be used to determine the resistance factor $\phi_{set\text{-}up}$ for predicted set-up capacity in the following algorithm based on the FORM approach.

$$\phi_{set-up} = \frac{\frac{\gamma_L \mu_{L_L}}{\lambda_{L_l}} + \frac{\gamma_D \mu_{L_D}}{\lambda_{L_D}} - \frac{\phi_0 \mu_{Q_0}}{\lambda_{Q_0}}}{\frac{\mu_{Q_{set-up}}}{\lambda_{Q_{set-up}}}} \tag{4-16}$$

where μ_{L_L}, μ_{L_D}, μ_{Q_0}, and $\mu_{Q_{set-up}}$ are the mean values of random variables L_L, L_D, Q_0, and $Q_{set\text{-}up}$, respectively, calculated from FORM approach; λ_{L_l}, λ_{L_D}, λ_{Q_0}, and $\lambda_{Q_{set-up}}$ are the bias factors of random variables L_L, L_D, Q_0, and $Q_{set\text{-}up}$, respectively.

Fig. 4-7 shows the effect of the variation of the ratio of dead to live load on the calculated resistance factors for set-up capacity at the reliability level β=2.33 and β=3.00, respectively. The load factors for dead and live load and the resistance factor for Q_0 are fixed as mentioned earlier when calculating the resistance factor for $Q_{set\text{-}up}$. It can be seen that the calculated resistance factor for $Q_{set\text{-}up}$ decreases slightly with an increase in the ratio of dead to live load. In general, however, the calculated resistance factor for $Q_{set\text{-}up}$ is not very sensitive to the ratio of dead to live load. The calculated resistance factor for $Q_{set\text{-}up}$ is approximately equal to 0 at the target reliability index β=3.00. It is because that, at higher reliability level, the higher uncertainty associated with the set-up effect results in its lower contribution to the total pile capacity. It means that the set-up effect could be ignored in driven pile design at target reliability index β=3.00 when the predefined resistance factor for Q_0, dead load factor, and live load factor are 0.50, 1.25, and 1.75, respectively. The resistance factor for $Q_{set\text{-}up}$ can be conservatively taken as 0.3 for the span length less than 60 m at target reliability index β=2.33, when the predefined resistance factor for Q_0, dead load factor, and live load factor are 0.65, 1.25, and 1.75, respectively. The recommended partial safety factors are tabulated in Table 4-4 for different reliability levels. It should be noted that the recommended resistance factors for $Q_{set\text{-}up}$ in Table 4-4 are calibrated based on the compiled database presented in this chapter. If additional pile test data could be

obtained to supplement the current database, the recommended resistance factors for $Q_{set\text{-}up}$ should be modified according to the potential change of the probability model and the relevant statistical parameters for the updated database.

The corresponding F.S (Factor of Safety) in ASD (Allowable Stress Design) can be calculated as follows:

$$F.S. = \frac{\dfrac{\gamma_D L_D / L_L + \gamma_L}{L_D / L_L + 1}}{\dfrac{\phi_0 Q_0 / Q_{set-up} + \phi_{set-up}}{Q_0 / Q_{set-up} + 1}} \tag{4-17}$$

Fig. 4-8 shows the relationship between the corresponding F.S. in ASD and the ratio of dead to live load. The corresponding F.S. decreases slightly with an increase of the ratio of dead to live load. The corresponding F.S. is about 3.00 and 5.80 for the recommended load and resistance factors at target reliability index β=2.33 and β=3.00, respectively.

4.7 Proposed Procedure to Incorporate Set-up into LRFD of Driven Piles in Clay

The incorporation of set-up effect at the lower target reliability level can efficiently improve the estimation of capacity of driven piles so that pile length or numbers of piles can be economically reduced. The proposed design procedure for incorporating set-up into LRFD of driven piles in clay is illustrated as follows:

1. Assign a pile size, length, and type for preliminary design using available site information and a static analytical design method.

2. Perform CAPWAP dynamic testing 1 day after pile installation and record the measured capacity as Q_0.
3. Estimate the set-up capacity based on the proposed semi-logarithmic empirical relationship: $Q_{set-up} = Q_0 A \log \frac{t}{t_0}$ (where A = 0.5, t = 100 days, and t_0 = 1 day).
4. Use the recommended resistance and load factors in Table 4-4 and the following formula, $\phi_0 Q_0 + \phi_{set-up} Q_{set-up} \geq \gamma_L L_L + \gamma_D L_D$, to evaluate the reasonableness of the preliminary design.
5. Based on the result from step 4, change the pile length or number as desired to optimize the design.

4.8 Conclusions

A database of pile set-up capacity has been compiled and presented in this chapter. The compiled database showed that the logarithmic empirical relationship proposed by Skov and Denver (1988) could be used to predict pile set-up. The reference time t_0 = 1 day and mean value A = 0.5 were found to be optimum for the prediction equation. The pile set-up database indicated that the time duration of 100 days after EOD may be considered as the point after which the set-up effect would be diminished. The normal distribution was shown to adequately represent the probabilistic characteristics of the predicted pile set-up capacity. The mean value μ, standard deviation σ, and COV of the fitted normal distribution are 1.141, 0.543 and 0.475, respectively. The calculated correlation coefficient between the measured reference pile capacity, Q_0, and the

predicted set-up capacity, $Q_{set\text{-}up}$, suggested that these two pile capacity components could be treated as if they were statistically independent.

The statistical parameters of the pile set-up capacity derived from the compiled database, together with previous statistical analysis of CAPWAP approach (Paikowsky et al. 2004), were systematically incorporated within the framework of FORM to develop separate resistance factors using the load conditions specified in AASHTO (Novak 1999). The incorporation of set-up effect into the prediction of total pile capacity gives advantageous contribution to the estimated total pile capacity at a low target reliability index ($\beta<3.00$). However, due to higher uncertainty associated with the predicted pile set-up capacity, the incorporation of the set-up capacity into the pile design yields more conservative prediction on the total pile capacity at higher reliability index ($\beta\geq3.00$). To be consistent with the existing experience about the load and the resistance effects, the load factors and resistance factors for Q_0 are pre-set in the present chapter when performing FORM analysis to determine the resistance factors for the pile set-up capacity. The set-up effect could be ignored in driven pile design if a target reliability index $\beta=3.00$ is chosen and the pre-set resistance factor for Q_0, dead load factor, and live load factor are 0.50, 1.25, and 1.75, respectively. The resistance factor for $Q_{set\text{-}up}$ can be conservatively taken as 0.3 for a bridge span length less than 60 m if a target reliability index $\beta=2.33$ is chosen and the pre-set resistance factor for Q_0, dead load factor, and live load factor are 0.65, 1.25, and 1.75, respectively. The corresponding F.S. in ASD is about 3.00 and 5.80 for the recommended load and

resistance factors in LRFD at the target reliability index β=2.33 and β=3.00, respectively.

Table 4-1 Summary of Load Test Database for Driven Piles in Clay

Pile series #	Source of references	Paper pile #	Pile type
1	Paikowsky et al. (2004)	FN1	HP 10x42
2	Paikowsky et al. (2004)	FL3	PSC24”sq
3	Paikowsky et al. (2004)	CHA1	CEP 12.75”
4	Paikowsky et al. (2004)	CHB2	HP 12x63
5	Paikowsky et al. (2004)	CHB3	HP 12x63
6	Paikowsky et al. (2004)	CH39	CEP9.63”
7	Paikowsky et al. (2004)	LB3	PSC24”sq
8	Paikowsky et al. (2004)	LB4	PSC30”sq
9	Paikowsky et al. (2004)	LB5	PSC30”sq
10	Paikowsky et al. (2004)	LB6	PSC36”cyl
11	Paikowsky et al. (2004)	LB7	PSC36”cyl
12	Paikowsky et al. (2004)	NBTP2	HP 12x74
13	Paikowsky et al. (2004)	NBTP3	HP 12x74
14	Paikowsky et al. (2004)	UMLNB2	CEP 324mm
15	Paikowsky et al. (2004)	UMLNB3	PSC 356mm sq
16	Skov and Denver (1988)	Case1 P9	Concrete 25x25 cm^2
17	Skov and Denver (1988)	Case1 P3	Concrete 25x25 cm^2
18	Skov and Denver (1988)	Case1 P5	Concrete 25x25 cm^2
19	Skov and Denver (1988)	Case1 P6	Concrete 25x25 cm^2
20	Long et al. (1999)	Pile 70	Close-end pipe
21	Long et al. (1999)	Pile 71	Close-end pipe
22	Long et al. (1999)	Pile 72	Wood
23	Long et al. (1999)	Pile 101	Timber
24	Long et al. (1999)	Pile 102	Timber
25	Long et al. (1999)	Pile 103	Reinf Concrete
26	Long et al. (1999)	Pile 104	Reinf Concrete
27	Long et al. (1999)	Pile 105	Reinf Concrete
28	Long et al. (1999)	Pile 106	NP30 Steel Grdr
29	Long et al. (1999)	Pile 107	Timber, Box
30	Long et al. (1999)	Pile 108	Timber, Box
31	Long et al. (1999)	Pile 109	Reinf Concrete
32	Long et al. (1999)	Pile 110	Reinf Concrete
33	Long et al. (1999)	Pile 111	Capped Pie-pile
34	Long et al. (1999)	Pile 112	Capped Pie-pile
35	Long et al. (1999)	Pile 113	Capped Pie-pile
36	Long et al. (1999)	Pile 114	Capped Pie-pile
37	Long et al. (1999)	Pile 115	Monotube

Table 4-2 Statistical Details and Resistance Factors of CAPWAP EOD and BOR

Method	No. of cases	Bias factor λ	COV	Φ (β=2.33)	Φ (β=3.00)
CAPWAP EOD	125	1.626	0.490	0.64	0.46
CAPWAP EOD AR<350 & Bl. Ct. <16 BP10cm	37	2.589	0.921	0.41	0.23
CAPWAP BOR	162	1.158	0.339	0.65	0.51

EOD = end of driving; BOR = beginning of restrike; AR= ratio of surface area in contact with soil to area of pile tip; Bl. Ct. = blow count; BP10cm =blows per 10cm

Table 4-3 Probabilistic Characteristics of Random Variables of Loads and Resistances for Piles Driven into Clay

Random variables	Bias factor λ	Standard deviation σ	Coefficient of variation COV	Distribution type
Q_0	1.158	0.393	0.339	Lognormal
$Q_{set\text{-}up}$	1.141	0.543	0.475	Normal
L_L	1.150	0.230	0.200	Lognormal
L_D	1.050	0.105	0.100	Lognormal

Table 4-4 Recommended LRFD Partial Safety Factors for Driven Piles in Clay

Random variables	**Bias factor λ**	**Coefficient of variation COV**	**Partial safety factor (β=2.33)**	Partial safety factor (β=3.00)
Q_0	**1.158**	**0.339**	**0.65**	0.50
$Q_{set\text{-}up}$	**1.242**	**0.474**	**0.30**	0.00
L_L	**1.150**	**0.200**	**1.75**	1.75
L_D	1.050	0.100	1.25	1.25

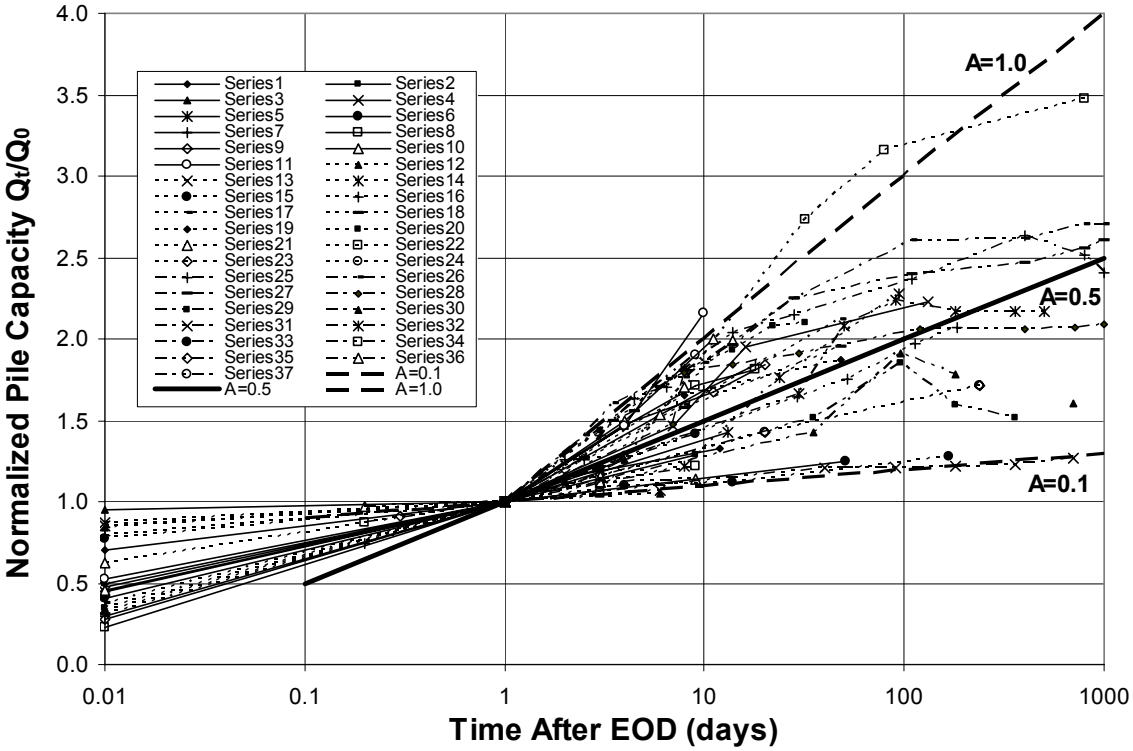

Figure 4-1 Variation of Normalized Capacity with Time for Driven Piles in Clay

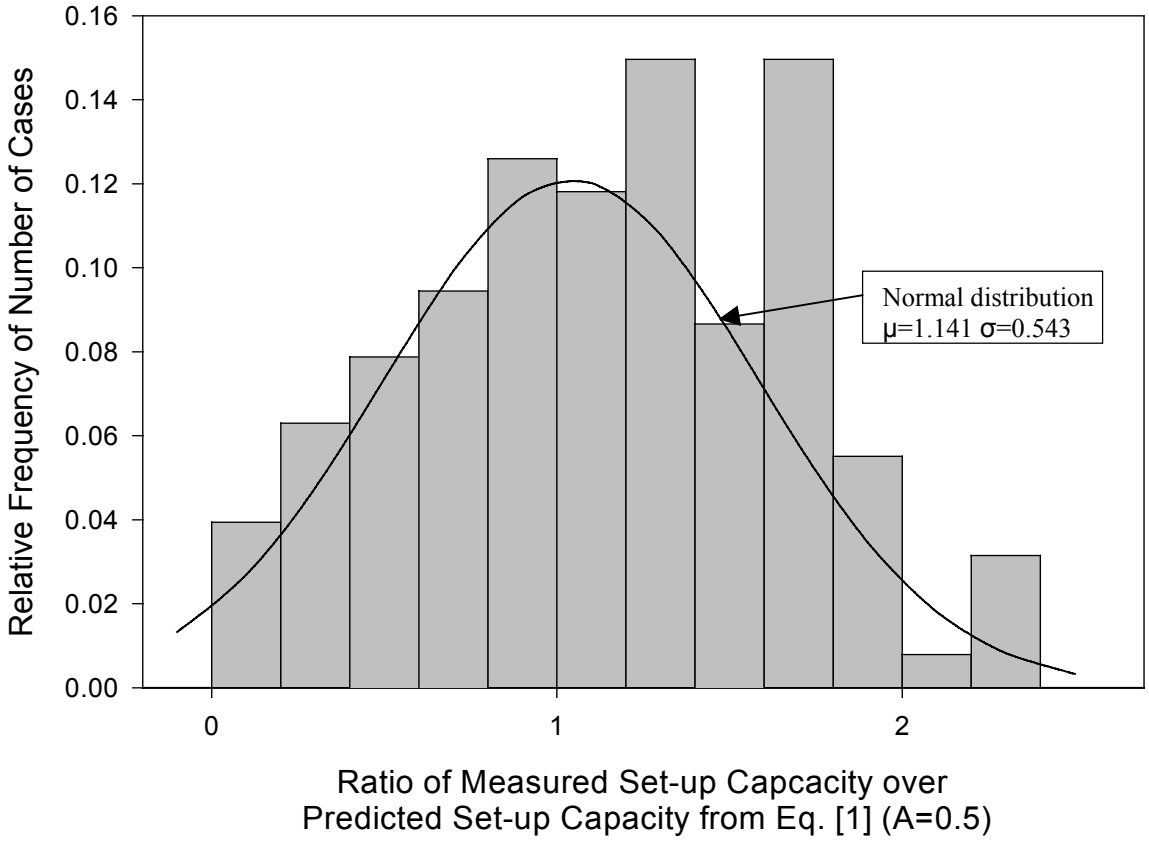

Figure 4-2 Frequency Distribution of the Ratio of Measured Set-up Capacities to the Predicted

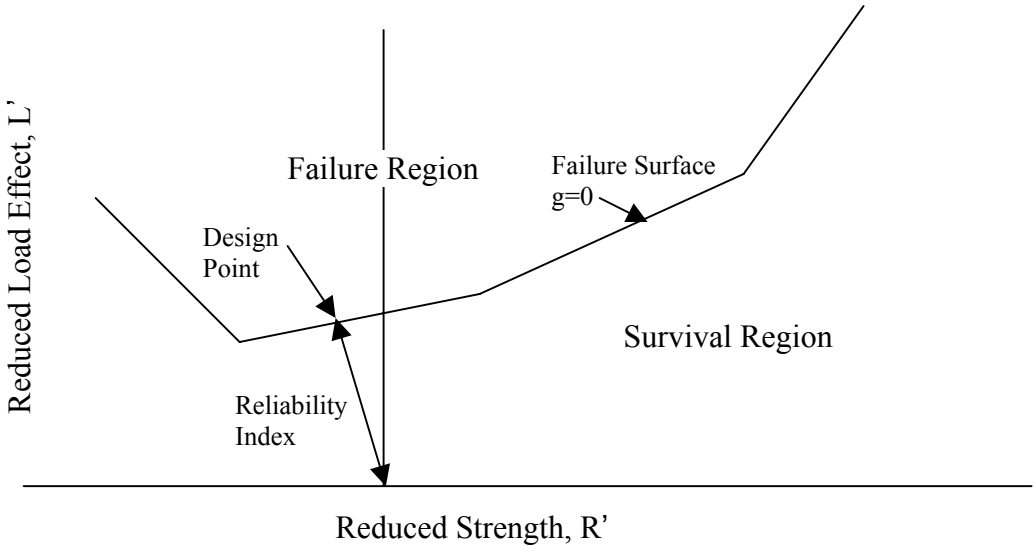

Figure 4-3 Performance Space in Reduced Coordinates

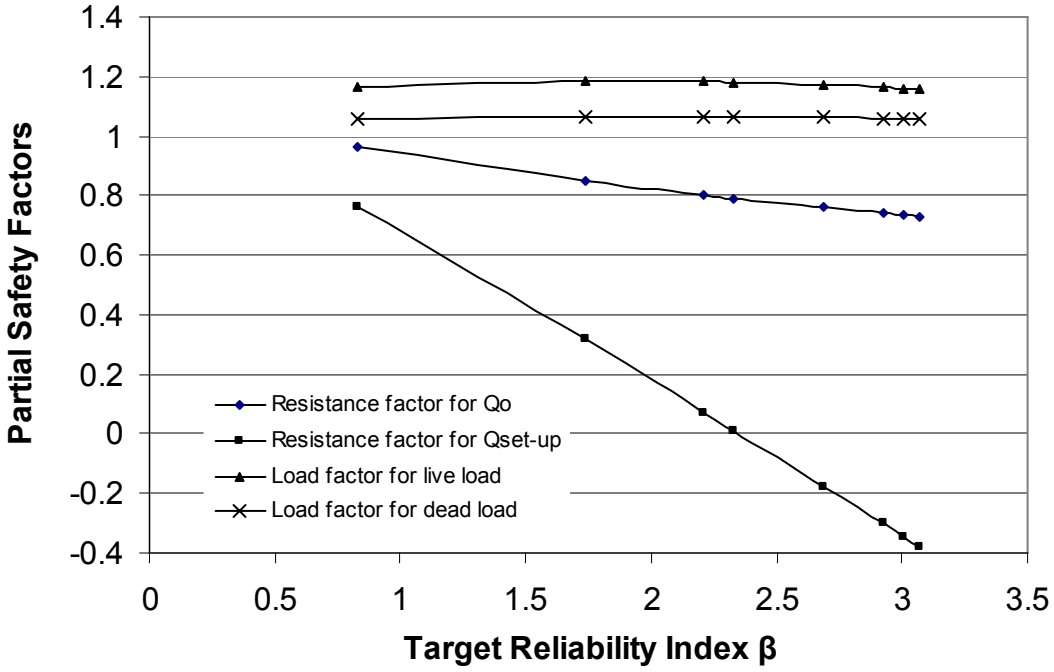

Figure 4-4 Relationship between Partial Safety Factor and Target Reliability Index When Incorporating Set-up into the Design of Driven Piles

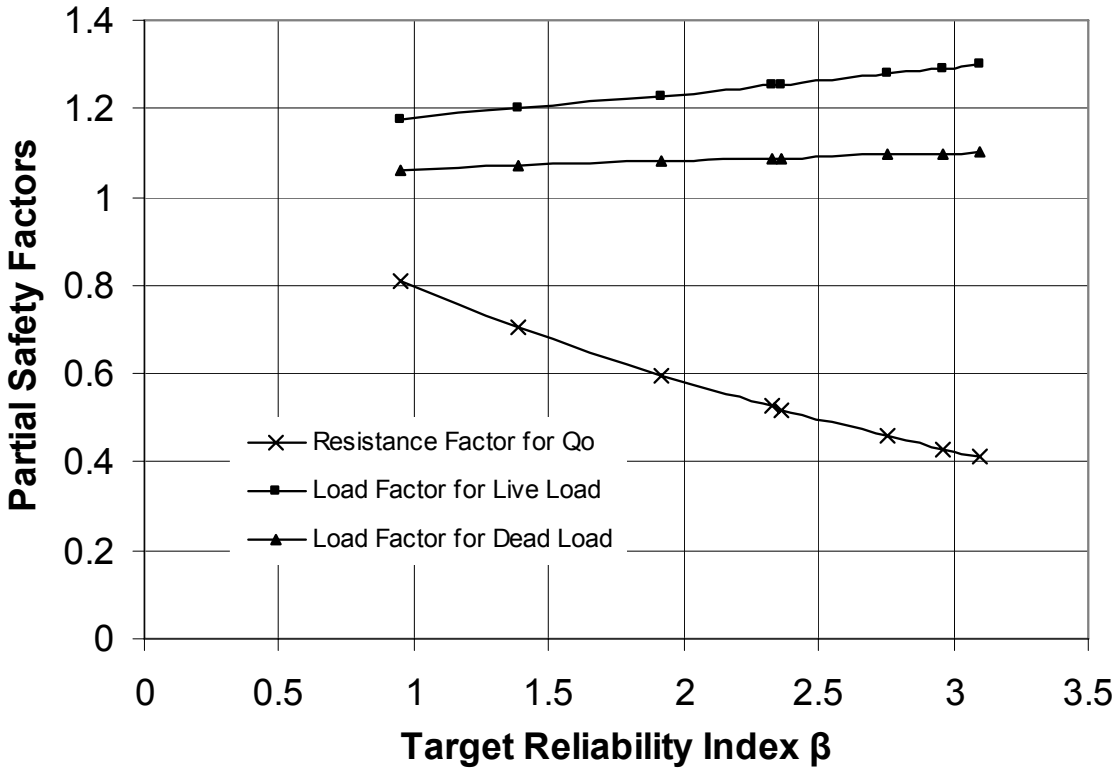

Figure 4-5 Relationship between Partial Safety Factor and Target Reliability Index without Considering Set-up in the Design of Driven Piles

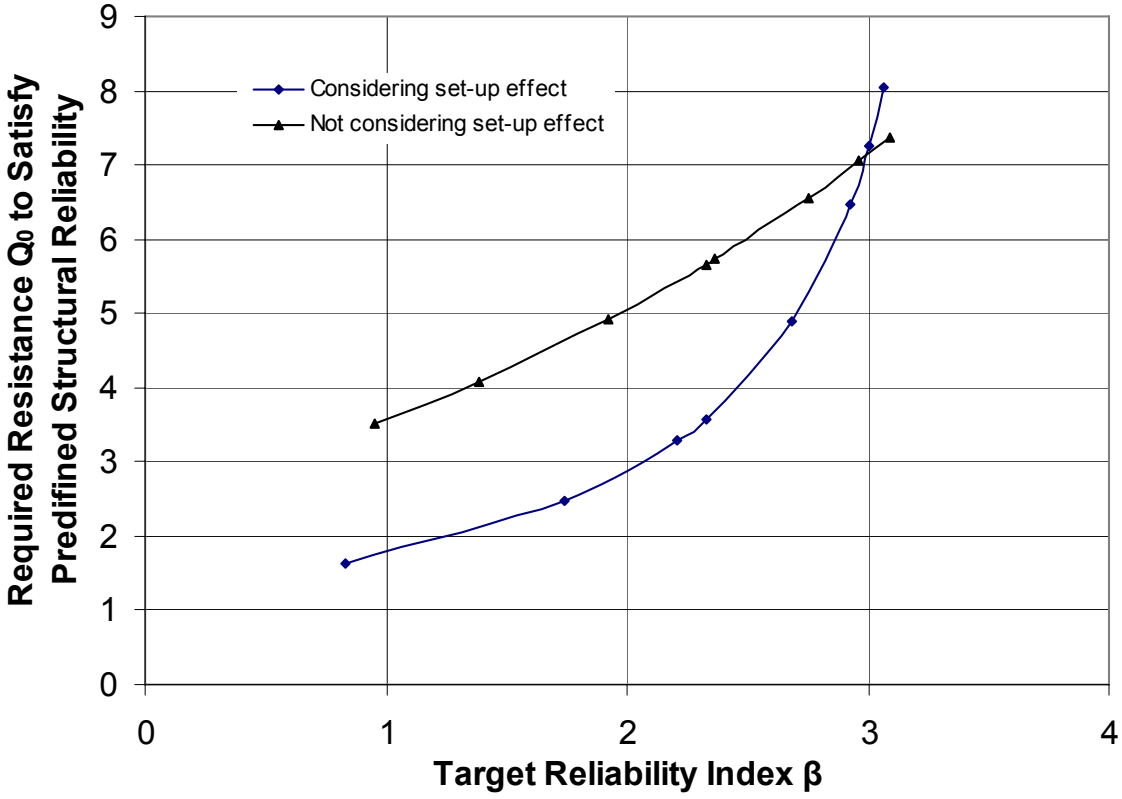

Figure 4-6 Comparison between Considering and Not Considering Set-up Effect

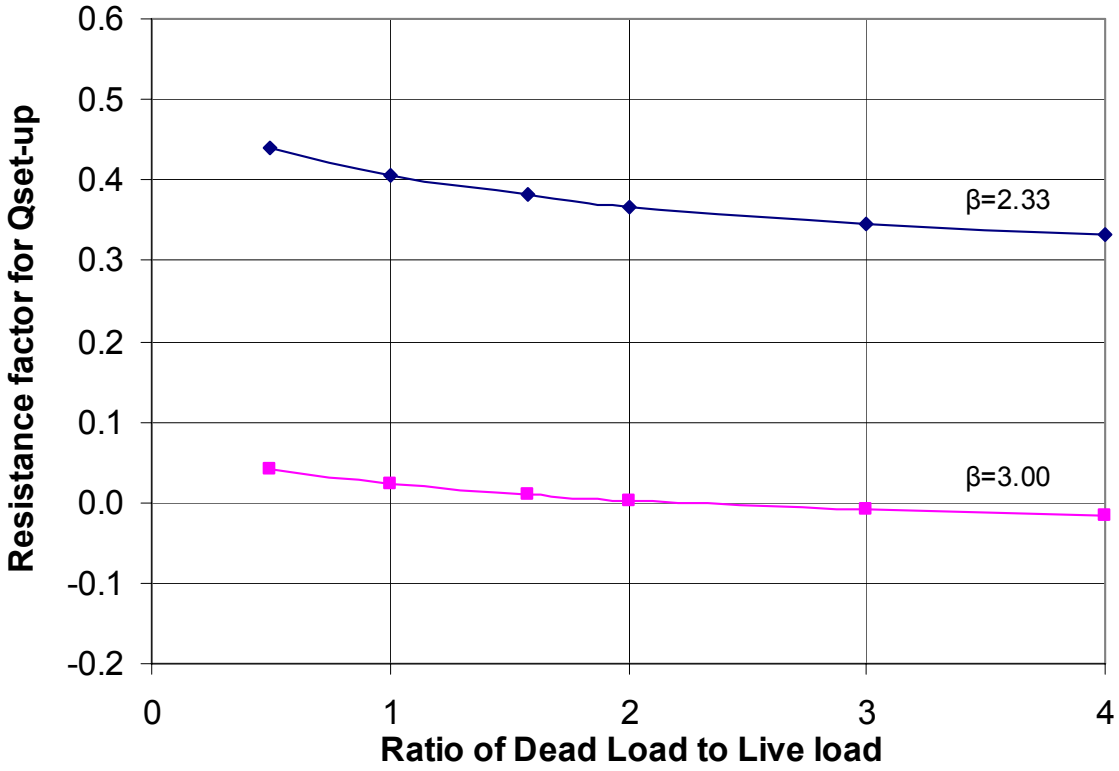

Figure 4-7 Variation of Resistance Factor for $Q_{set\text{-}up}$ in Clay versus the Ratio of Dead Load to Live Load

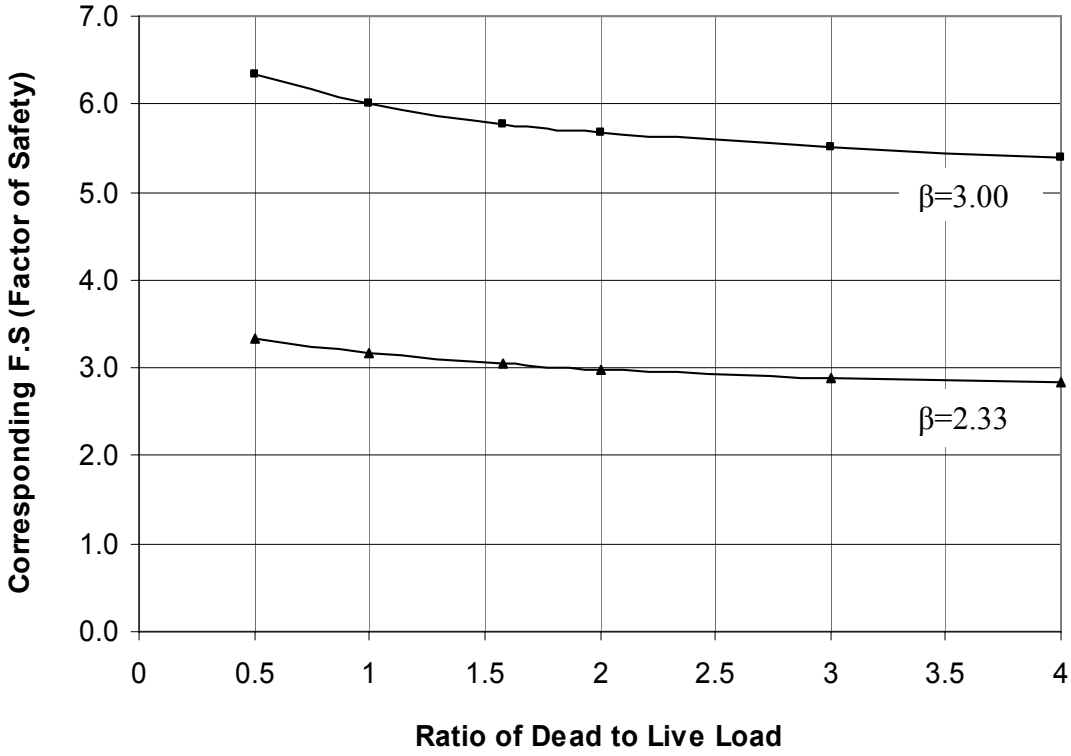

Figure 4-8 Variation of the F.S versus the Ratio of Dead Load to Live Load for Piles Driven into Clay

CHAPTER V

INCORPORATING SET-UP INTO RELIABILITY-BASED DESIGN OF DRIVEN PILES IN SAND

5.1 Introduction

Set-up is defined as an increase in bearing capacity with time that takes place after pile installation. It is believed that excess pore pressures induced during driving dissipates very quickly in sand, usually within a few hours. Tavenas and Audy (1972) first reported the well-documented cases of pile long-term set-up in sand, which was not attributable to pore pressure changes. During the last decade, the phenomenon of long-term set-up of piles driven in sand has been highlighted in many studies. Long-term set-up in sand can roughly be divided into two vital but substantially different causes, based on Chow et al. (1997, 1998) and Axelsson (1998, 2002). The first is stress relaxation in the soil arching generated during pile driving, which leads to an increase in horizontal effective stress on the pile shaft. The second is the soil aging caused mainly by rearrangement and interlocking of soil particles, which results in an increase in stiffness and dilatancy of the soil. Numerous geotechnical engineers have developed various empirical formulas to predict the set-up behavior in sand (e.g., Skov and Denver 1988, Svinkin et al. 1994, and Long et al. 1999). However, the beneficial effect of long-term set-up of driven piles in sand has very seldom been utilized to any

significant extent in piling projects for a long time, due to high uncertainties of predicting the development of set-up.

With the AASHTO (American Association of State Highway and Transportation Officials) migration from ASD (Allowable Stress Design) method to LRFD (Load and Resistance Factor Design) method for foundation design, there is a need to develop separate resistance factors for initial capacity and set-up capacity, respectively. This chapter presents a database containing a large number of pile testing data in sand, from which the set-up effect is statistically analyzed. Follow the procedure proposed in Chapter IV, the separate resistance factors are obtained to account for different degrees of uncertainties associated with measured short-term capacity and predicted set-up capacity in sand at various reliability levels.

5.2 A Compiled Database of Case Histories of Driven Piles in Sand

Pile set-up in sand was first reported by Tavenas and Audy (1972) and Samson and Authier (1986). Subsequently, a number of other case histories have been reported in the literature. Chow et al. (1998) summarized the results from 11 case histories with long-term set-up effects for driven pile in sand, indicating that most of pile capacities increase by around 50% (±25%) per log cycle of time from 1 day after pile driving. Long et al. (1999) also compiled a database of set-up cases, and categorized the soil into three main groups: clayey soil, mixed soil, and sand. The sand group contained 6 case histories; many of them are the same as in Chow et al. (1998). Axial pile capacity was found to increase from 30% to more than 100% of the pile capacity at the end of

driving (EOD). Axelsson (2002) presented a database showing the set-up rate ranging from 15% to 65% per log cycle of time. Komurka et al. (2003) provided an extensive bibliography related to the topic of pile set-up. In general, the increase in the capacity of driven piles in sand is believed to be due to the aging effect and the increase of horizontal effective stress (Chow 1997 and 1998, Axelsson 1998 and 2002).

A database containing both static and dynamic load tests was collected and listed in Table 5-1 based on the previous studies of the driven piles in sand. The database consists of 190 loading tests in total, performed on 73 piles where at least two separate tests at different times are performed for each pile to determine the set-up. Table 5-1 provides information about the test pile, soil conditions of the site, and the sources of references. However, it should be noted that the database suffers from the following shortcomings:

- There exists a difference in the definition of the reference capacity Q_{re}. Tavenas and Audy (1972) and Bullock et al. (2005a, 2005b) assessed Q_{re} from tests conducted about 0.5 days after driving. In the remaining cases, Q_{re} was defined as the measured capacity at EOD.
- The capacity was determined either by static or dynamic testing, but both dynamic and static load test results could have been used in the same test series without distinguishing them. Furthermore, the different static loading failure criteria have been used in the references.
- It is generally believed that the set-up mainly takes place along the pile shaft. However, the total capacity was used in this database, since it was not possible

to separate the toe and shaft capacities with sufficient accuracy in many cases in the database. The testing results from Bullock et al. (2005a, 2005b) are for changes in shaft capacity only.

Pile axial capacities are shown to increase with time after driving in Fig. 5-1. It is noted that, in some cases, the long-term axial capacity after the installation reaches 3-4 times the axial capacity at EOD. Most of piles experience 20%~100% set-up after the installation. No cases of relaxation in sand were found in the compiled database. Parsons (1966) reported the relaxation of driven piles in New York area based on the reduction of pile penetration resistance in granular soils from EOD to BOR (beginning of restrike), but provided no alternative explanations for the observations. Yang (1970) also reported the relaxation of piles in sand, but did not provide the actual load test results. York et al. (1994) argued that the relaxation could be initiated in pile group when driving pile into saturated sand. Pile-driving vibrations densify the surrounding soils. Subsequently, driving additional piles may cause the sand to dilate rather than compress, resulting in the conditions for potential relaxation. However, York et al. (1994) also proposed that set-up can occur following cessation of relaxation and result in a net increase of pile capacity.

5.3 Empirical Relationships

Empirical relationships have been proposed for quantifying the set-up by many researchers. Skov and Denver (1988) presented an empirical equation for the set-up based on a logarithmic increase of pile capacity with time. Svinkin et al. (1994)

developed a formula predicting the set-up based on load test data on five concrete piles in dense silty sand. Long et al. (1999) proposed an equation predicting the rate at which the pile capacity increases with time. The equation proposed by Long et al. is very similar to Svinkin et al.'s where the pile capacity after installation is proportional to the time with an exponential efficiency. An alternative method of using a hyperbolic function to predict the set-up was proposed by Bogard and Matlock (1990) and Tan et al. (2004). Zhu (1988) presented an equation for the set-up in soft clay based on the soil sensitivity. Huang (1988) also presented a formula predicting the development of pile capacity in the soft soil of Shanghai, China. These empirical formulas are listed in Table 5-2.

Among those proposed formulas, Skov and Denver's and Svinkin et al.'s equations are most commonly used for the prediction of the set-up in sand, since they require only a short-term capacity to be measured as the reference capacity. Based on Skov and Denver's equation, the predicted set-up capacity can be expressed as

$$Q_{set-up} = Q_0 A \log \frac{t}{t_0} \tag{5-1}$$

where

Q_{set-up} = predicted set-up capacity at time t after driving,

Q_0 = measured axial capacity at time t_0,

A = a factor that is a function of soil type and can be determined as the slope of the linear portion of the normalized capacity Q_{set-up}/Q_0 versus log(t) plot,

t = time since pile installation, and

t_0 = time after installation at which the capacity gain becomes linear on a log(t) plot.

Skov and Denver also recommended numerical values for A and t_0 as 0.6 and 1 day in clay and 0.2 and 0.5 day in sand, respectively. Researchers such as Svinkin et al. (1994), Camp and Parmar (1999), and Bullock et al. (2005b), also provided a range of numerical values for these two parameters.

Based on Skov and Denver's equation, the normalized axial pile capacity (i.e., Q_t/Q_0) versus the logarithm of time is plotted in Fig. 5-2 for the 47 pile cases where at least two separate load tests are performed after EOD. The reference capacity Q_0 was measured between 0.5 days to 2 days after EOD. The capacity Q_t was measured days, weeks, and months after EOD. The dashed lines define an approximate range of A from 0.1 to 0.9. The mean value of A for all 47 testing piles is close to the value of 0.4.

Based on Svinkin et al.'s equation, the predicted set-up capacity can be expressed as:

$$Q_{set-up} = BQ_{EOD}(t^{0.1} - 1) \tag{5-2}$$

where

Q_{EOD} = measured pile capacity at EOD,

t = time since pile installation (>1 day),

B = 1.025 and 1.4 as lower and upper bound, respectively.

The normalized axial pile capacity (i.e., Q_t/Q_{EOD}) versus the time is plotted in Fig. 5-3. The dash lines define the lower and upper boundaries as proposed by Svinkin et al. (1994). The mean value of B is close to the value of 1.25 for all 42 test piles where the measured capacities at EOD are available.

Comparing Fig. 5-2 to Fig. 5-3, it can be seen that the set-up capacity predicted by Svinkin et al.'s equation shows the larger scatter than that predicted by Skov and Denver's equation. The calculated mean value μ, standard deviation σ, and Coefficient of Variation (COV) of the ratio of measured to predicted capacity are 1.023, 0.593, and 0.580, respectively, when Skov and Denver's equation is used (A = 0.4, t_0 = 1 days). However, The calculated mean value μ, standard deviation σ, and Coefficient of Variation (COV) of the ratio of measured to predicted capacity are 1.211, 0.911, and 0.752, respectively, when Svinkin et al's equation is used (B = 1.25). The comparison of the COV values demonstrates that Skov and Denver's equation provides the higher accuracy on predicting the set-up than Svinkin et al.'s equation. The higher uncertainties associated with Svinkin et al.'s equation may be primarily due to the selection of the reference capacity. Because of the highly disturbed state of the soil, there is a brief period following installation during which the initial rate of capacity gain with time is different from the later rate. During this period, the affected soil experiences an increase in effective and horizontal stress, consolidates, and gains strength in a manner which is not well-understood and is difficult to model and predict (Komurka et al. 2003). The use of Q_{EOD} as the reference capacity inevitably needs to account for the high variability of the changes of pile capacity in this period. Therefore,

Skov and Denver's equation is used to predict the set-up in the following statistical study.

5.4 Statistical Study of Pile Set-up

Based on the compiled database, most of pile testing data show that the pile capacity gain becomes approximately linear with the logarithm of time 1 day after pile installation. Researchers, such as Svinkin et al. (1994), Axelsson (1998, 2002), McVay (1999), and Bullock et al. (2005a, 2005b), have proposed the use of $t_0 = 1$ day in Skov and Denver's equation.

Chow (1998) reported the values of A around 0.5 (±0.25). Studies by Axelsson (2002) yielded the average value of 0.4 for A, with a range from 0.15 to 0.65. The observations from the compiled database in Fig. 5-2 seem to conform with the previous experiences. Therefore, the reference time t_0 = 1 day and A = 0.4 are used for the subsequent statistical analyses in this chapter. When further data becomes available, the values of t_0 and A could be modified. Most of pile tests are performed in 30 days after EOD in the compiled database. It can be seen that pile capacity increases approximately linearly with the logarithm of time within 30 days after EOD. Tevenas and Audy (1972) concluded that the ultimate pile capacity increase during the first 15 to 20 days after EOD could be 70% higher than that observed at 0.5 day. Studies by York et al. (1994) showed that set-up could have approached a maximum value within 15 to 25 days. Although some piles in the compiled database exhibit set-up after months or years, the increase of pile capacity with time after 30 days becomes less pronounced compared to

those during the first 30 days after driving. Therefore, 30 days after EOD can be conservatively taken as the time after which the set-up effect in sand would be minimal.

The accuracy of Skov and Denver's equation is analyzed by examining the ratio of the measured set-up capacities to the predicted using t_0 = 1 day and A = 0.4. The frequency distribution for 47 piles is shown in Fig. 5-4. It can be seen that a lognormal distribution seems to approximately represent the distribution. The mean value μ_{lnx} and standard deviation σ_{lnx} of the fitted lognormal distribution are -0.122 and 0.538, respectively. To verify the assumed theoretical lognormal distributions, the Kolmogorov-Smirnov test (Ang and Tang 1975) was carried out. Fig. 5-5 shows the empirical cumulative frequency and the theoretical cumulative distribution of the ratio of the measured to the predicted set-up capacity. The maximum differences in cumulative frequency between the observed data and the theoretical distributions are D_n = 0.096 that is smaller than the critical value D_n^{α} = 0.200 at the 5% significance level. Therefore, the assumed lognormal distribution for the predicted set-up capacity is valid.

CAPWAP approach (Rausche et al. 1972, 1985) has been widely used for quality control and capacity determination of driven piles. Also, most of pile testing data in the compiled database are from CAPWAP results. Therefore, CAPWAP approach is recommended for determining the measured short-term capacity Q_0. The statistical analysis results of the CAPWAP BOR measured capacity by Paikowsky et al. (2004) and the predicted set-up capacity by the Skov and Denver's equation are summarized in Table 5-3. Comparing the COV values, it is found that predicting pile set-up effect

involves significantly higher uncertainties than measuring capacity Q_0 by CAPWAP. Therefore, it is necessary to separate the resistance factors to account for the different degrees of uncertainties associated with the measured capacity and the predicted set-up capacity. The relationship between the measured reference capacity Q_0 and the predicted pile set-up capacity $Q_{set\text{-}up}$ is not at all clear. As discussed in Chapter 4, it may be reasonable to assume that the measured Q_0 by CAPWAP and the predicted $Q_{set\text{-}up}$ are independent of each other. In this chapter, the uncertainties associated with dead and live loads as well as the measured reference capacity Q_0 and the predicted set-up capacity $Q_{set\text{-}up}$ are systemically accounted for in a framework of FORM. Separate resistance factors are derived for Q_0 and $Q_{set\text{-}up}$ for adoption in the LRFD of driven piles.

5.5 Calibrate Partial Load and Resistance Factors Based on FORM

The database shows that driven piles in sand experience the set-up. The magnitude of the set-up is so significant that economical design of driven piles is not possible without recognition of the anticipated capacity gain with time. When the set-up capacity in sand is incorporated into the driven pile design, the strength limit state at the failure point can be expressed as

$$g = R^* - L^* = Q_0^* + Q_{set-up}^* - L_D^* - L_L^* = 0 \tag{5-3}$$

where R^* = total resistance, L^* = total load, Q_0^* = measured pile axial capacity at reference time t_0, Q_{set-up}^* = predicted pile set-up capacity after time t_0, L_D^* = dead loads, and L_L^* = live loads.

The probabilistic characteristics of the random variables L_D and L_L are well documented in AASHTO (Nowak 1999). The probabilistic characteristics of the random variables Q_0 is taken as that of CAPWAP BOR presented by Paikowsky et al. (2004). The probabilistic characteristics of the random variables $Q_{set\text{-}up}$ is taken as a lognormal distribution with mean value μ_{lnx} of -0.122 and standard deviation σ_{lnx} of 0.538 in Fig. 5-4, based on Eq. (5-1) (A = 0.4 and t_0 = 1 day). Table 5-3 summarizes the statistical parameters and distribution function for each random variable. With the known load and resistance statistical characteristics, the iterative solution of FORM approach (See Section 4.4 in Chapter IV) can be applied to determine the load and resistance factors for the chosen target reliability index (Ang and Tang 1984; Phoon et al. 2003a and 2003b; Ayyub and McCuen 2003; Paikowsky et al. 2004).

Based on AASHTO LRFD Highway Bridges Design Specifications (2006), the ratio of dead to live load is a function of a bridge's span length. The following values of L_D/L_L are recommended as: 0.52, 1.06, 1.58, 2.12, 2.64, 3.00, and 3.53 for span lengths of 9, 18, 27, 36, 45, 50, and 60 m, respectively. The relationship between the partial safety factors (i.e., load and resistance factors) and the target reliability index is shown in Fig. 5-6, where the ratio of dead load to live load is selected as 1.58:1 to represent a bridge span length of 27 m, and the ratio of Q_0 to $Q_{set\text{-}up}$ is 1:0.59 based on the Skov and Denver's equation with A = 0.4, t_0 = 1 day, and t = 30 days. The partial safety factors for all loads and resistances vary approximately linearly with the target reliability index. The resistance factors for Q_0 are higher than those for $Q_{set\text{-}up}$ at a given reliability level because uncertainties for Q_0 are less than those for $Q_{set\text{-}up}$. The fact that COV values of

two load components are much smaller than those of two resistances has resulted in smaller variation of load factors with the target reliability index in Fig. 5-6.

5.6 Practical Load and Resistance Factors for Piles Driven into Sand

For a given reliability index β and probability distributions for resistance and load effects, the partial safety factors determined by the FORM approach may differ for different failure modes. For this reason, calibration of load and resistance factors is important in order to maintain the same values of load factors for all loads at different failure modes. In order to be consistent with the current experience in LRFD, the calibrations of resistance factor for the set-up is performed for a set of load factors already specified in the AASHTO code (Novak, 1999). The resistance factors of Q_0 for CAPWAP approach are taken as the same as those recommended in NCHRP Report 507 (Paikowsky et al. 2004). When incorporating the set-up effect into the design of driven pile, the LRFD criterion can be expressed as

$$\phi_0 Q_0 + \phi_{set-up} Q_{set-up} \geq \gamma_L L_L + \gamma_D L_D \tag{5-4}$$

where ϕ_0 and $\phi_{set\text{-}up}$ = resistance factors for reference resistance at t_0 and set-up resistance, respectively; γ_L and γ_D = load factors for live and dead loads, respectively.

The target reliability index increases approximately exponentially with a decrease of probability of failure. As suggested in NCHRP Report 507, the target reliability index of β=2.33 corresponding to the probability of failure P_f = 1% is recommended for redundant piles defined as 5 or more piles per pile cap; the target reliability index of β=3.00 corresponding to the probability of failure P_f = 0.1% is recommended for

nonredundant piles defined as 4 or fewer piles per pile cap. The resistance factors are $\phi_0 = 0.65$ and $\phi_0 = 0.50$ for CAPWAP approach at $\beta=2.33$ and $\beta=3.00$, respectively. As specified by AASHTO (Novak 1999), the load factors $\gamma_L=1.75$ and $\gamma_D=1.25$ are used for live and dead loads, respectively. The above load and resistance factors can be used to determine the resistance factor $\phi_{set\text{-}up}$ for the predicted set-up capacity in the following algorithm based on the FORM approach.

$$\phi_{set-up} = \frac{\frac{\gamma_L \mu_{L_L}}{\lambda_{L_l}} + \frac{\gamma_D \mu_{L_D}}{\lambda_{L_D}} - \frac{\phi_0 \mu_{Q_0}}{\lambda_{Q_0}}}{\frac{\mu_{Q_{set-up}}}{\lambda_{Q_{set-up}}}} \tag{5-5}$$

where μ_{L_L}, μ_{L_D}, μ_{Q_0}, and $\mu_{Q_{set-up}}$ are the mean values of random variables L_L, L_D, Q_0, and $Q_{set\text{-}up}$, respectively, calculated from FORM approach; λ_{L_l}, λ_{L_D}, λ_{Q_0}, and $\lambda_{Q_{set-up}}$ are the bias factors of random variables L_L, L_D, Q_0, and $Q_{set\text{-}up}$, respectively.

Fig. 5-7 shows the effect of the variation of the ratio of dead to live load on the calculated resistance factors for set-up capacity at the reliability level $\beta=2.33$ and $\beta=3.00$, respectively. The load factors for dead and live loads and the resistance factor for Q_0 are fixed as mentioned earlier when calculating the resistance factor for $Q_{set\text{-}up}$. It can be seen that the calculated resistance factor for $Q_{set\text{-}up}$ decreases slightly with an increase in the ratio of dead to live load. In general, however, the calculated resistance factor for $Q_{set\text{-}up}$ is not very sensitive to the ratio of dead to live load. The calculated resistance factor for $Q_{set\text{-}up}$ can be conservatively taken as 0.4 for the span length less than 60 m at the target reliability index $\beta=3.00$, when the predefined resistance factor

for Q_0, dead load factor, and live load factor are 0.50, 1.25, and 1.75, respectively. The resistance factor for $Q_{set\text{-}up}$ can be conservatively taken as 0.5 for the span length less than 60 m at target reliability index β=2.33, when the predefined resistance factor for Q_0, dead load factor, and live load factor are 0.65, 1.25, and 1.75, respectively.

The recommended load and resistance factors are tabulated in Table 5-4 for different reliability levels. The corresponding F.S. (Factor of Safety) in ASD (Allowable Stress Design) can be calculated as follows:

$$F.S. = \frac{\dfrac{\gamma_D L_D / L_L + \gamma_L}{L_D / L_L + 1}}{\dfrac{\phi_0 Q_0 / Q_{set-up} + \phi_{set-up}}{Q_0 / Q_{set-up} + 1}} \tag{5-6}$$

Fig. 5-8 shows the relationship between the corresponding F.S. in ASD and the ratio of dead to live load. The corresponding F.S. decreases with an increase in the ratio of dead to live load. The corresponding F.S. are about 2.40 and 3.00 for the recommended load and resistance factors at target reliability index β=2.33 and β=3.00, respectively.

5.7 Proposed Procedure to Incorporate Set-up into LRFD of Driven Piles in Sand

The incorporation of set-up effect can efficiently improve the estimation of total capacity of driven piles so that pile length or numbers of piles can be economically reduced. The proposed design procedure for incorporating set-up into LRFD of driven piles in sand is illustrated as follows:

1. Assign a pile size, length, and type for preliminary design using available site information and a static analytical design method.
2. Perform CAPWAP dynamic testing 1 day after pile installation and record the measured capacity as Q_0.
3. Estimate the set-up capacity based on the proposed semi-logarithmic empirical relationship: $Q_{set-up} = Q_0 A \log \frac{t}{t_0}$ (where A = 0.4, t = 30 days, and t_0 = 1 day).
4. Use the recommended resistance and load factors in Table 5-4 and the following formula, $\phi_0 Q_0 + \phi_{set-up} Q_{set-up} \geq \gamma_L L_L + \gamma_D L_D$, to evaluate the reasonableness of the preliminary design.
5. Based on the result from step 4, change the pile length or number as desired to optimize the design.

The engineering judgment is very important in a given project site when using the proposed procedure to consider the set-up capacity, because the database in this chapter is collected based on a wide range of site variability. The site-specific experience on set-up capacity is more desirable when the pile test results are available to estimate the development of long-term set-up at the given site. It is recommended that additional pile testing data be obtained to supplement the current database, thus allowing for more comprehensive statistical analysis of the pile set-up.

5.8 Conclusions

A database of pile set-up capacity in sand has been compiled and presented in this chapter. The compiled database showed that the logarithmic empirical relationship proposed by Skov and Denver (1988) could be used to predict pile set-up. The reference time t_0 = 1 day and mean value A = 0.4 were suggested for Skov and Denver's equation. The pile set-up database indicated that the time duration of 30 days after EOD may be considered as the point after which the set-up effect would be minimal. Based on the Kolmogorov-Smirnov test, the lognormal distribution was shown to adequately represent the probabilistic characteristics of the predicted pile set-up capacity. The mean value μ_{lnx} and standard deviation σ_{lnx} of the fitted lognormal distribution are -0.122 and 0.538, respectively.

The statistical parameters of the pile set-up capacity derived from the compiled database, together with previous statistical analysis of CAPWAP approach (Paikowsky et al. 2004), were systematically incorporated within the framework of FORM to develop separate resistance factors using the load conditions specified in AASHTO (Novak 1999). The incorporation of set-up effect into the prediction of total pile capacity gives advantageous contribution to the estimated total pile capacity. To be consistent with the existing experience about the load and the resistance effects, the load factors and resistance factors for Q_0 are pre-set in the present chapter when performing FORM analysis to determine the resistance factors for the pile set-up capacity. For piles driven into sand, the resistance factor for $Q_{set\text{-}up}$ can be taken as 0.4 for a bridge span length less than 60 m if a target reliability index β=3.00 is chosen and

the pre-set resistance factor for Q_0, dead load factor, and live load factor are 0.50, 1.25, and 1.75, respectively. The resistance factor for $Q_{set\text{-}up}$ can be taken as 0.5 for a bridge span length less than 60 m if a target reliability index β=2.33 is chosen and the pre-set resistance factor for Q_0, dead load factor, and live load factor are 0.65, 1.25, and 1.75, respectively. The corresponding F.S. in ASD are about 2.40 and 3.00 for the recommended load and resistance factors in LRFD at the target reliability index β=2.33 and β=3.00, respectively.

Table 5-1 Summary of Load Test Database for Driven Piles in Sand

References	Site locations	Number of piles	Main soil type	Pile type	Depth (m)	Testing type
Tevenas and Audy (1972)	Canada	27	Uniform medium sand, SPT N≈23	D=305mm Concrete hex.	8.5~13	Static
Samson and Authier (1986)	Canada	1	Medium sand, gravel	HP 12*63	22	Stat. & Dyn.
Seidel et al. (1988)	Australia	1	Loose to dense sand	450*450mm prestressed concrete	10.5	Stat. & Dyn.
Skov and Denver (1988)	Germany	2	Medium to coarse sand	350*350mm concrete, and D=762mm pipe	21, 33.7	Stat. & Dyn.
Zai (1988)	China	5	Fine sand	D=610mm pipe	40~45	Stat. & Dyn.
Preim et al. (1989)	USA	2	Loose to medium fine sand	355*355mm concrete, and D=323mm closed-end pipe	27, 25	Stat. & Dyn.
Svinkin et al. (1994)	USA	6	Silty sand	457~915mm square concrete	19.5~22.9	Stat. & Dyn.
York et al. (1994)	USA	15	Medium dense sand	D=355mm monotube	10.7~21.6	Stat. & Dyn.
Chow et al. (1998)	France	2	medium to very dense sand, Dr ≈ 75%	D=324mm open-end pipe	11, 22	Stat. & Dyn.
Axelsson (1998)	Sweden	3	Loose to medium dense glacial sand	235*235mm concrete	19	Dynamic
Attwooll et al. (1999)	USA	1	Unsaturated, dense sand	D=324mm pipe	10.1	Stat. & Dyn.
Tan et al. (2004)	USA	5	Loose to medium dense sand	356mm H-pile, D=610mm closed-end pipe	34~37	Dynamic
Bullock et al. (2005)	USA	3	Dense fine sand	457*457mm prestressed concrete	9~25	O-Cell

Table 5-2 Empirical Formulas for Predicting Pile Capacity with Time

References	Equation		Comments
Skov and Denver (1988)	$Q_t = Q_0(1 + A\log\frac{t}{t_0})$	(5-7)	where t_0=0.5 and A=0.2 in sand t_0=1.0 and A=0.6 in clay
Svinkin et al. (1994)	$Q_t = BQ_{EOD}t^{0.1}$	(5-8)	B = 1.4 upper bound B = 1.025 lower bound
Long et al. (1999)	$Q_t = 1.1Q_{EOD}t^{\alpha}$	(5-9)	values of α: average = 0.13, lower bound = 0.05, upper bound = 0.18,
Bogard and Matlock (1990)	$Q_t = Q_u[0.2 + 0.8(\frac{t/T_{50}}{1+t/T_{50}})]$	(5-10)	Q_u = ultimate capacity with 100% of setup realized T_{50} = time required to realize 50% of pile set-up
Zhu (1998)	$Q_{14} = (0.375S_t + 1)Q_{EOD}$	(5-11)	Q_{14} = pile capacity at 14 day after EOD S_t = sensitivity of soil
Huang (1998)	$Q_t = Q_{EOD} + 0.236[1 + (Q_{\max} - Q_{EOD})\log t]$	(5-12)	Q_{max} = maximum pile capacity with 100% of setup realized

Table 5-3 Probabilistic Characteristics of Random Variables of Loads and Resistances for Piles Driven into Sand

Random variables	Bias factor λ	Standard deviation σ	Coefficient of variation, COV	Distribution type	References
Q_0	1.158	0.393	0.339	Lognormal	Paikowsky et al.(2004)
$Q_{set\text{-}up}$	1.023	0.593	0.580	Lognormal	Current Study
L_L	1.150	0.230	0.200	Lognormal	AASHTO (Nowak 1999)
L_D	1.050	0.105	0.100	Lognormal	AASHTO (Nowak 1999)

Table 5-4 Recommended Partial Safety Factors (i.e. load and resistance factors) for Driven Piles in Sand

Random variables	**Bias factor λ**	**Coefficient of variation COV**	**Partial safety factor (β=2.33)**	**Partial safety factor (β=3.00)**	References
Q_0	**1.158**	**0.339**	**0.65**	**0.50**	Paikowsky et al.(2004)
$Q_{set\text{-}up}$	**1.023**	**0.580**	**0.50**	**0.40**	Current Study
L_L	**1.150**	**0.200**	**1.75**	**1.75**	AASHTO (Nowak 1999)
L_D	1.050	0.100	1.25	1.25	AASHTO (Nowak 1999)

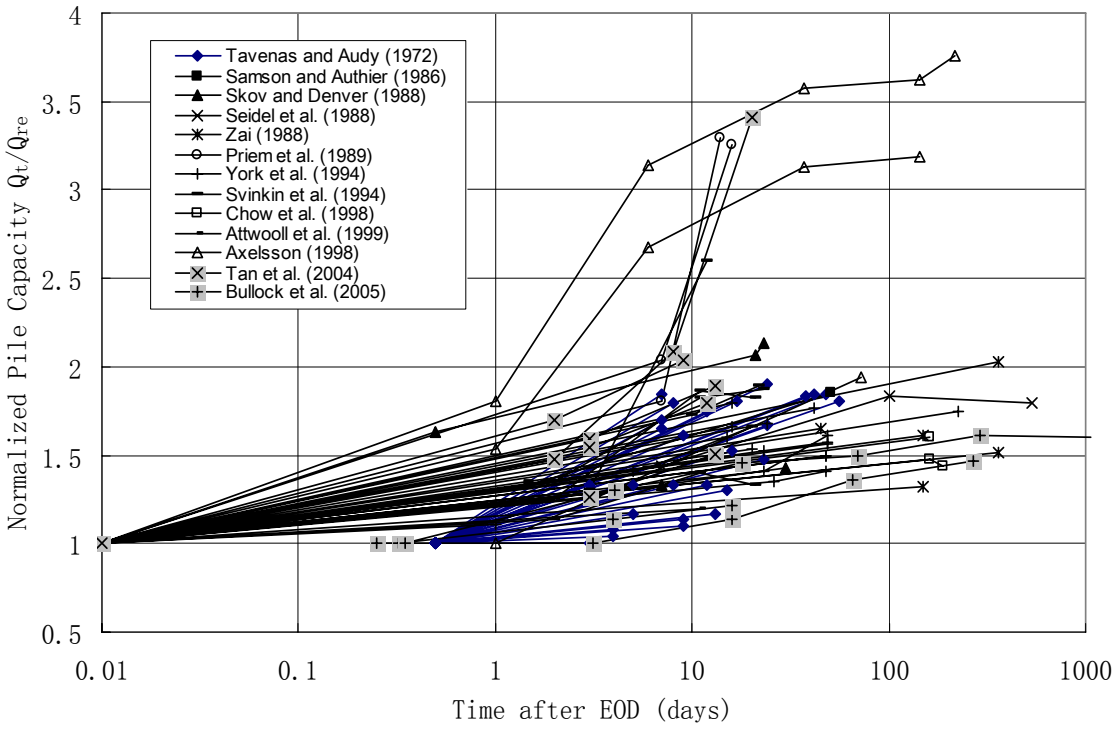

Figure 5-1 Case Histories of Pile Set-up in the Compiled Database

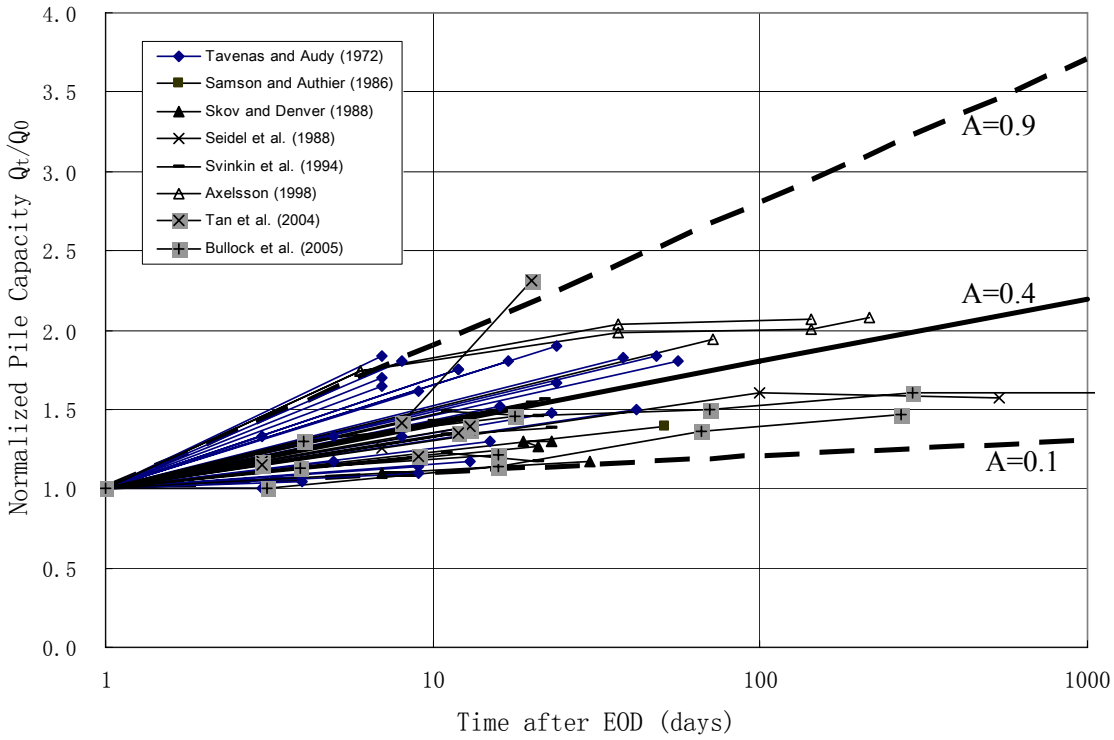

Figure 5-2 Variation of Normalized Capacity with Time Based on Skov and Denver's Equation

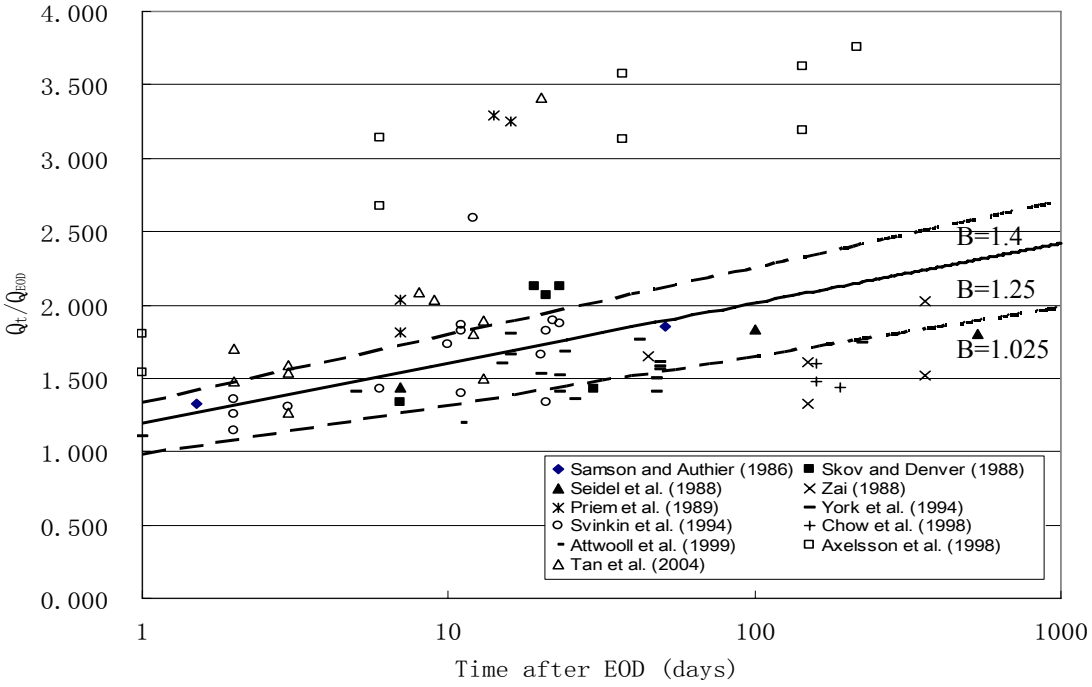

Figure 5-3 Variation of Normalized Capacity with Time Based on Svinkin et al.'s Equation

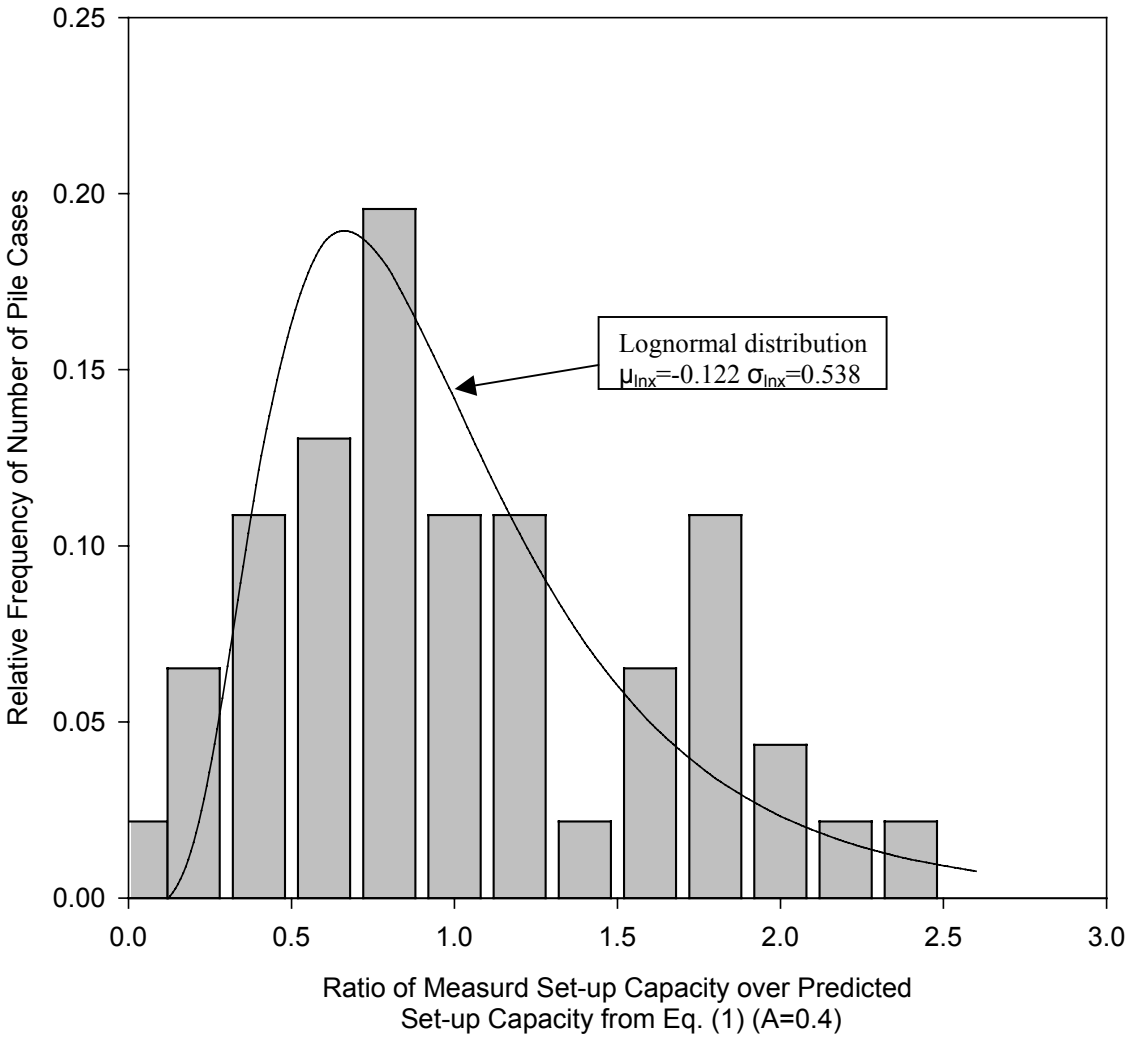

Figure 5-4 Frequency Distribution of the Ratio of Measured Set-up Capacities to the Predicted, Based on Skov and Denver's Equation

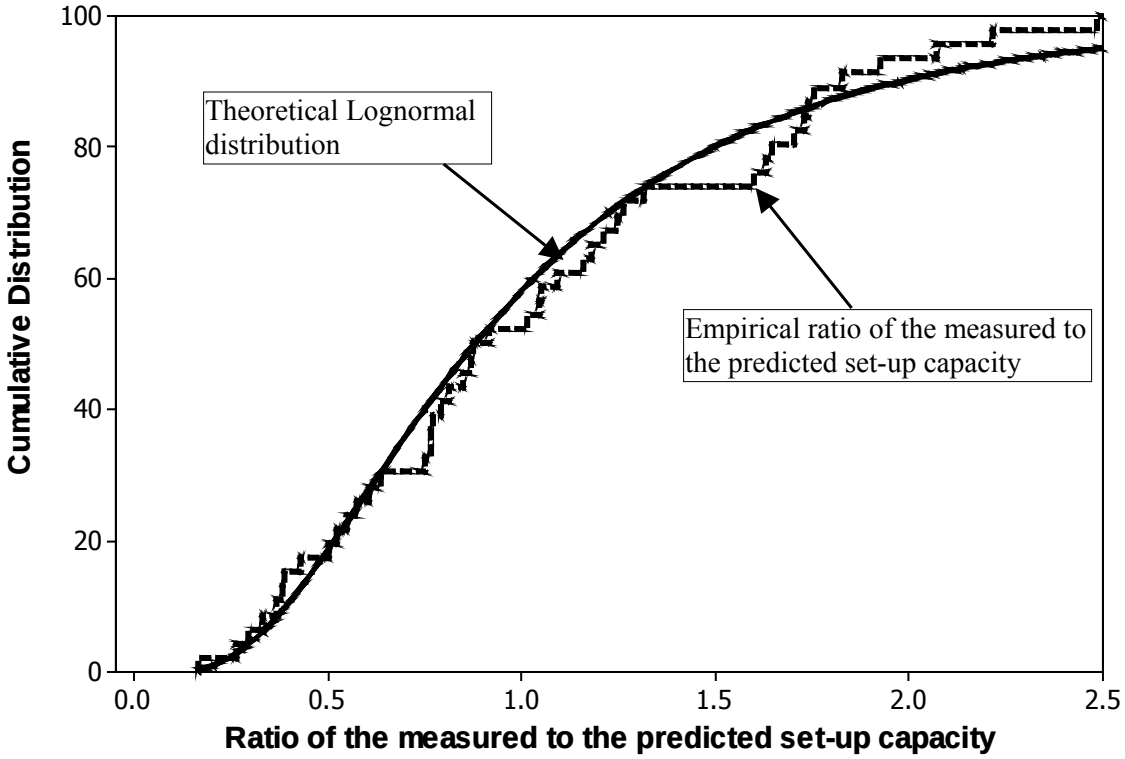

Figure 5-5 Kolmogorov-Smirnov Test for Assumed Lognormal Distribution of the Ratio of the Measured to the Predicted Set-up Capacity

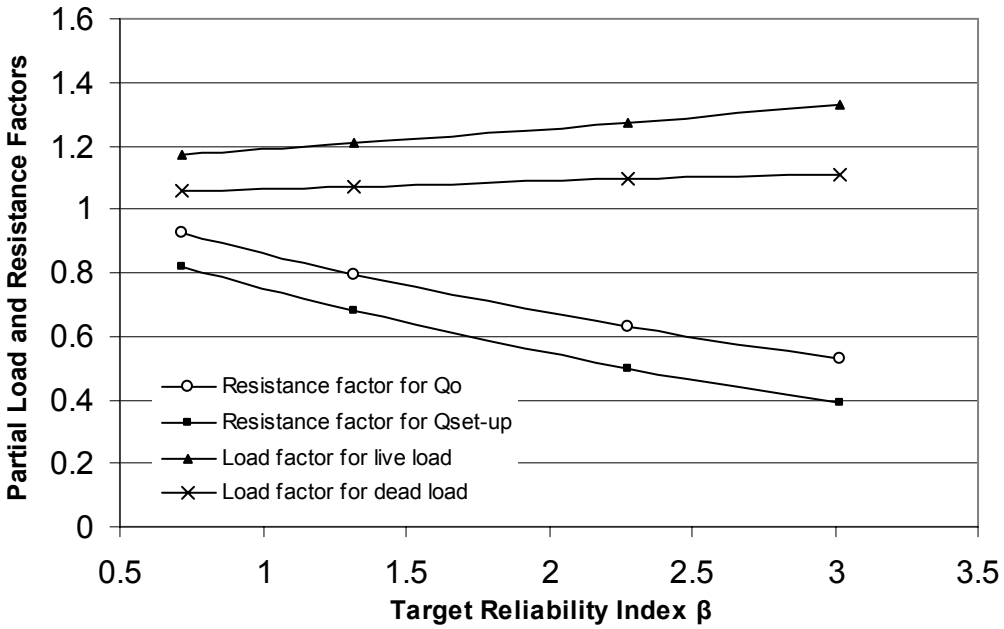

Figure 5-6 Relationship between Partial Safety Factor and Target Reliability Index

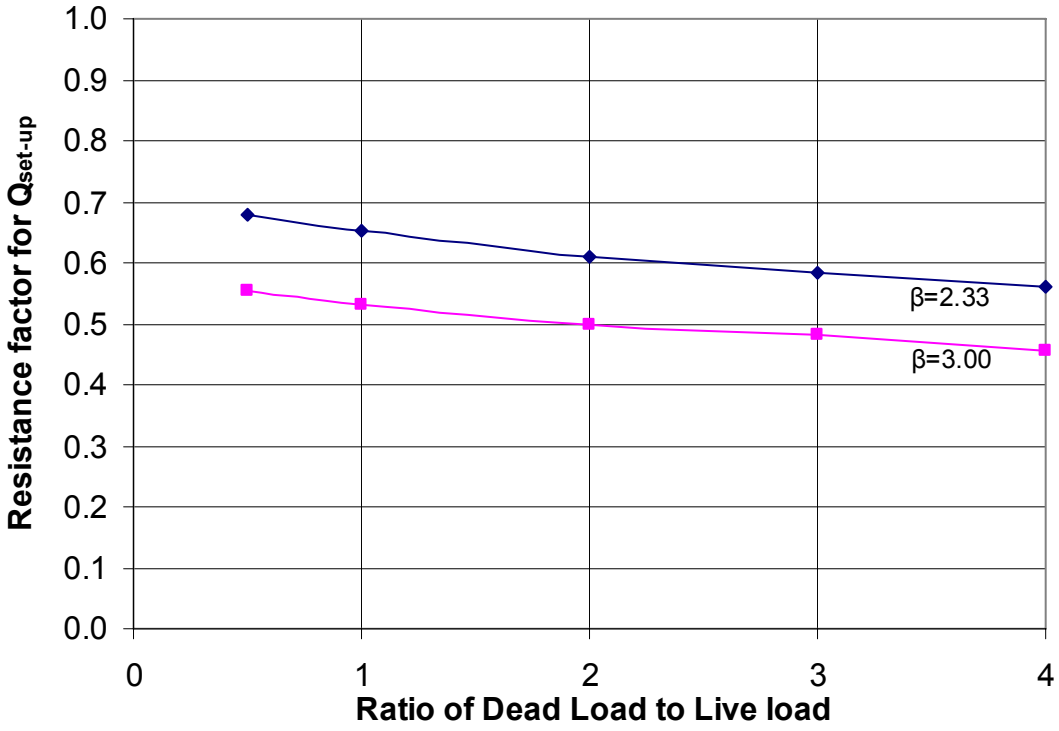

Figure 5-7 Variation of Resistance Factor for $Q_{set\text{-}up}$ in Sand versus the Ratio of Dead Load to Live Load

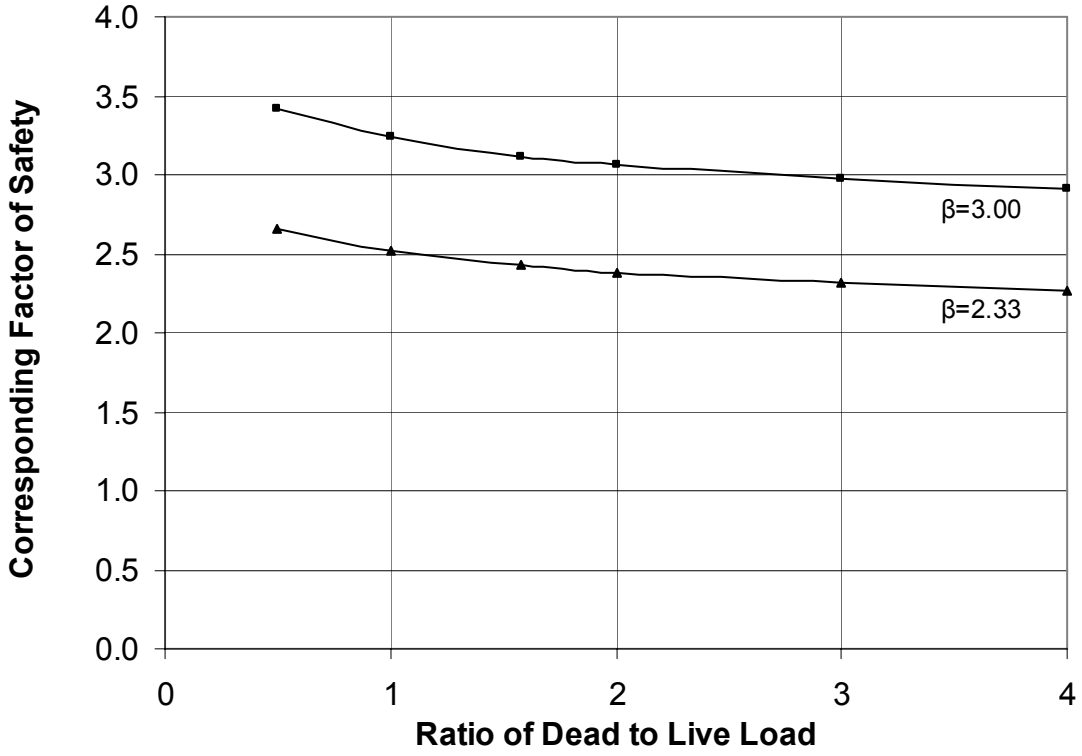

Figure 5-8 Variation of the F.S versus the Ratio of Dead Load to Live Load for Piles Driven into Sand

CHAPTER VI

BAYESIAN BASED FORMALISM FOR UPDATING LRFD RESISTANCE FACTORS FOR DRIVEN PILES

6.1 Introduction

Beginning in 2007, AASHTO (American Association of State Highway and Transportation Officials) requires that the Load and Resistance Factor Design (LRFD) method be used for foundation design. Whereas Allowable Stress Design (ASD) in prior AASHTO Guide lumps all uncertainties in the applied load and ultimate geotechnical or structural capacity into a single value of factor of safety (FS), LRFD accounts for the variability of loads and resistances by respective load and resistance factors. The resistance factors for various design methods are recommended in 2006 AASHTO LRFD specifications (AASHTO 2006). The preliminary design of foundation piles is usually performed with static analytical calculations using the soil parameters from geotechnical site investigations and the accompanied laboratory test results. In current LRFD method (AASHTO 2006), the uncertainties with respect to the prediction method, the errors of calculation model, and the spatial variability of soil parameters, are incorporated in a single resistance factor for a particular design method, regardless of individual site-specific situation. For each construction site, soil profiles, soil types, pile driving equipment, and hammer performance, may be different. Therefore, it may

be desirable to develop a strategy for site-specific calibration of the resistance factor to improve foundation design.

Currently, dynamic pile tests are carried out to verify the pile capacity during pile driving and to monitor the installation process for avoiding pile damage due to hammer impact. The pile length estimated using a static analysis method requires verification by dynamic pile tests during pile installation. Recognizing that either static pile load test or dynamic pile test may be performed for most pile driving projects, Vrouwenvelder (1992) presented an approach for incorporating either the static or dynamic test results to update FS in the ASD design of driven piles. Recently, Zhang et al. (2002) demonstrated that the results from static pile load tests could be incorporated into pile design using Bayesian theory by updating the resistance factor in LRFD. Dynamic pile testing, however, has become a commonly used method. Accordingly, a methodology needs to be developed for improving static pile capacity calculation by updating the corresponding resistance factor using Bayesian theory and the dynamic pile test results.

This chapter presents a methodology for static method based pile design by combining the static calculation with dynamic pile testing data. Bayesian theory is employed to combine the two methods in the framework of LRFD approach. The First Order Reliability Method (FORM) is used to derive the updated resistance factor. Specifically, the results from dynamic pile tests are incorporated to reduce the uncertainties associated with static analysis methods via updating of the corresponding resistance factor. It is shown that by a combination of two methods, one can improve accuracy and

confidence level on predicting pile capacity. Two case studies are presented to illustrate the proposed methodology and its applicability.

6.2 Characteristics of LRFD Method

The LRFD criterion for substructure is stated as follows (AASHTO, 2006):

$$\sum \eta_i \gamma_i Q_i \le \phi R_n \tag{6-1}$$

where R_n= nominal resistance, ϕ= resistance factor, Q_i=load effect, γ_i=load factor, and η_i= load modifier to account for the effects of ductility, redundancy and operational importance.

In AASHTO (2003), the recommended resistance factors of various static analysis methods for axially loaded driven piles include a parameter, λ_v, to account for the effect of quality control procedure during pile driving. For example, if α method is used to predict the pile's friction resistance in clay, a resistance factor of 0.7 is recommended. If, an ENR (Engineering News-Record) driving formula is used to verify the pile capacity, a λ_v factor of 0.8 is recommended. Therefore, the resistance factor to be used in the above scenario is 0.56 (i.e. 0.7×0.8). The concept of incorporating the parameter, λ_v, to static analysis is attractive; nevertheless, a single value of λ_v for each quality control method appears to be less desirable.

6.3 First Order Reliability Method (FORM)

Barker et al. (1991) and Withiam et al. (1998) described a first-order second-moment (FOSM) method for developing the resistance factors based on load tests in a large

number of sites. However, LRFD for structural design has evolved beyond FOSM to the more invariant FORM approach. Paikowsky, et al. (2004) suggested that the use of FOSM method might result in the resistance factors that could be approximately 10% lower than those obtained by FORM. In order to be consistent with the current structural code, Phoon et al. (2003a and 2003b), Ayyub and McCuen (2003), Paikowsky et al. (2004), and Allen et al. (2005) have proposed the application of FORM approach to calibrate resistance factors for deep foundations. Ang and Tang (1984) provide detailed descriptions about the procedure of using FORM to calibrate LRFD partial safety factors. FORM can be used to assess the reliability of a pile with respect to specified limit states as well as to calculate partial safety factors ϕ_i and γ_i for resistances and loads, respectively, for a chosen target reliability index β.

6.4 Uncertainty of Static Analysis Methods

The sources of error in predicting axial driven pile capacity via static analysis methods can be enumerated as follows (Withiam et al. 1998):

1. Model error that relates to an overall bias of the prediction method;
2. Systematic error that can be divided into systematic error in the trend and bias in the procedures;
3. Inherent spatial variability – only a limited number of soil borings and samplings at a site to characterize the subsurface condition for a large volume of soil and rock;
4. Random testing error and statistical uncertainty due to insufficient number of tests;

5. Error in measuring actual pile capacities in static load tests that are used as baseline to judge accuracy of the prediction method.

It is important to bear in mind that different error sources may exert different degrees of effect on the reliability analysis (Christian 2004). For example, the contributions of soil shear strength are generally summed along the shaft length of driven piles in which the value of soil shear strength is estimated from soil boring samples. The contribution of the scatter in the shear strength to the uncertainty in the predicted axial driven pile capacity may be reduced greatly by increasing the numbers of soil borings. On the other hand, the model error and systematic error propagate throughout the analysis.

The lognormal function was generally used for describing the variable λ_R, defined as the ratio of the measured pile capacity from the static load test, R_s, to the capacity predicted with a static analysis method, R_p (Withiam et al. 1998).

$$\lambda_R = \frac{R_S}{R_P} \tag{6-2}$$

6.5 Uncertainty of Dynamic Pile Testing Methods

Compared to the static analysis methods, the dynamic pile testing methods also have model and systematic errors. For example, the errors associated with the energy methods (Paikowsky et al. 1994, Liang and Zhou 1997) are the errors of energy input in the prediction equation. The wave equation based methods, such as CAse Pile Wave Analysis Program (CAPWAP) and Case Method (Rausche et al. 1972, 1985), improved

on energy methods by partially eliminating the errors of energy input; nevertheless, they simultaneously introduced other uncertainties, such as the errors of signal recording of the transducers as well as the assumed damping models.

The correction factor, *K*, of the dynamic pile testing method is introduced as the ratio of the pile capacity determined from the static load test, R_S, divided by the pile capacity determined from the dynamic pile testing method, R_D:

$$R_S = KR_D \tag{6-3}$$

McVay et al. (2000) and Paikowsky et al. (2004) showed that the lognormal distribution could be used to describe the distribution function of K.

6.6 Improving Static Method with Dynamic Test Results

The uncertainty of a static analysis method can be reduced if the available dynamic pile test results are incorporated in an updating process. Supposing that a number of dynamic pile tests are conducted at a given site, the dynamic pile test results consist of a set of n dynamic pile capacities R_{D1}, R_{D2}, …, R_{Dn}. For simplicity, assuming that the static load test results involve negligible uncertainty, then the following expressions can be obtained,

$$\lambda_R = \frac{R_S}{R_P} = K\frac{R_D}{R_P} = K(RDS) \tag{6-4}$$

$$\overline{\lambda_R} = \mu_k \frac{R_D}{R_p} \tag{6-5}$$

$$\sigma_{\lambda_R} = \sigma_k \frac{R_D}{R_p} \tag{6-6}$$

where R_P = pile capacity predicted by a static method, RDS = ratio of the dynamic prediction capacity over the static prediction capacity, $\overline{\lambda_R}$ = mean value of RDS; μ_k = mean value of K; σ_{λ_R} = standard deviation of RDS; σ_k = standard deviation of K.

Bayesian sampling theory can be expressed as:

$$f''(\theta) = \frac{P(\varepsilon/\theta) f'(\theta)}{\int_{-\infty}^{+\infty} P(\varepsilon/\theta) f'(\theta) d\theta} \tag{6-7}$$

where $f'(\theta)$ and $f''(\theta)$ are the prior and the posterior density functions of the parameter θ, respectively. The term $P(\varepsilon/\theta)$ is the conditional probability or likelihood of observing the experimental outcome ε, assuming that the value of the parameter is θ. In the present analysis, the dynamic pile test results are treated as the experimental outcome ε assuming that the pile capacity computed by a static analysis method is θ. Therefore, the posterior distribution parameters (updated) of the variable λ_R is expressed as

$$\psi'' = \frac{\psi'(\zeta_K{}^2/n) + \zeta'^2 \overline{\ln x}}{\zeta_K{}^2/n + \zeta'^2} \tag{6-8}$$

$$\zeta'' = \sqrt{\frac{\zeta'^2(\zeta_K{}^2/n)}{\zeta'^2 + \zeta_K{}^2/n}} \tag{6-9}$$

Then, based on FORM analysis, the updated resistance factors can be recalculated using the obtained posterior statistical parameters of the variable λ_R.

6.7 Combination of Static Analysis and Dynamic Pile Testing Methods

For illustration purpose, the statistics of loads is taken from the LRFD Bridge Design Specifications (AASHTO, 2006). They are as follows: bias factor for dead load λ_{QD} = 1.05, bias factor for live load λ_{QL} = 1.15, load factor for dead load γ_D=1.25, load factor for live load γ_L = 1.75, COV value of dead load COV_{QD} = 0.1, and COV value of live load COV_{QL} = 0.2, ratio of dead load to live load Q_D/Q_L = 1.58 corresponding to the bridge span length of 27 m. A target reliability index of β = 2.33, corresponding to the probability of failure P_f = 1%, is used as an illustration to determine the resistance factors for the driven piles.

A study of the statistics of various design methods for driven piles was summarized by Paikowsky, et al. (2004) and reproduced in Table 6-1. As can be seen, α –API method exhibits the best accuracy among the static analysis methods. Among different dynamic methods, CAPWAP BOR (Beginning of Restrike) provides more accurate prediction than CAPWAP EOD (End of Driving) and EA (Energy Approach, Paikowsky et al. 1994).

To investigate the potential benefits of combining two methods, Fig. 6-1 is presented to show the effect of combining CAPWAP BOR with several different static analysis methods. After updating, the most accurate static analysis method in prior prediction, α–API, still provides the smallest COV for posterior distribution. The dynamic pile testing methods provides less benefit in updating the high-accuracy static analysis methods, particularly when the prior static analysis method possesses higher accuracy than the

dynamic pile testing method chosen for the updating purpose. Fig. 6-2 shows the effect of using different dynamic pile testing methods on the updated λ-method distributions. The incorporation of CAPWAP BOR, which exhibits higher accuracy than the other dynamic methods, yields the smallest COV of the updated distribution of λ-method. This demonstrates that, when the static analysis and dynamic pile testing methods are combined to obtain the posterior distribution, combination of two accurate design methods generate more reliable updating of posterior distributions.

The effect of RDS on updating is illustrated in Fig. 6-3, where CAPWAP BOR is used to update the λ-method. When the value of RDS increases, the mean of the posterior distribution increases and the COV remains the same. It shows that the latter is not related to the value of RDS, but a function of the standard deviations of prior static analysis method and dynamic pile testing method as well as the number of dynamic tests. Fig. 6-4 shows the effect of the number of dynamic tests on the updated distributions. One can see that COV decreases with an increase in the number of dynamic pile tests. Thus, the posterior prediction of pile capacity becomes more reliable, as the number of dynamic pile tests incorporated in updating increases.

6.8 Updated Resistance Factors versus RDS and Number of Dynamic Pile Tests

After obtaining the statistical parameters of the posterior distribution, the resistance factors can be recalculated using FORM. Fig. 6-5 shows the variation of the updated resistance factors with RDS. The updated resistance factors are approximately proportional to RDS for all the combinations examined. The slope in Fig. 6-5 represents

the effect of RDS on the updated resistance factors for various combinations. For the combination of β-method and CAPWAP BOR, RDS exerts the largest influences on the updated resistance factors for the posterior static analysis method. The least effect of RDS on the updated resistance factor is observed in the combination of α-API and CAPWAP EOD. This demonstrates that the use of more reliable dynamic pile testing method (e.g., CAPWAP BOR) can provide better beneficial updating on the resistance factors for the static analysis methods. On the other hand, the resistance factors for more accurate static analysis method (e.g., α-API method) is generally not affected by using dynamic pile test for updating.

The resistance factors can be significantly increased not only by using dynamic method that yields favorable RDS, but also by incorporating a larger number of dynamic pile testing results. Fig. 6-6 shows the relationship between the updated resistance factors and the number of dynamic pile tests used in different combinations of dynamic pile testing methods and static analysis methods. For all the combinations considered, the resistance factor increases as the number of the dynamic pile tests incorporated in updating increases. The static analysis methods with higher accuracy, such as α-API and λ-method, are less affected by the number of dynamic pile tests on the updated resistance factors. The first two dynamic pile tests give more contribution to the increase of the resistance factors for the α-API and λ-method. The use of dynamic pile tests of more than two can only result in a small improvement of the reliability of the static methods. It suggests that two dynamic tests could be considered sufficient to update the high accuracy static analysis methods. However, for the static methods with

low accuracy (e.g., α-Tomlinson and β-method), the effect of the number of dynamic pile tests used to update resistance factor is very pronounced. The updated resistance factors are remarkably increased by the first four dynamic tests. Therefore, the number of dynamic tests to be conducted to update the static calculation depends largely on the static methods used.

6.9 Case Study I

Test piles #2 at Newbury site is selected from the Appendix D of NCHRP Report 507 (Paikowsky et al. 2004) as a case study. Test pile #2 is a closed-end steel pipe pile, with O.D. = 324 mm (12.76 in), thickness = 12.7 mm (0.5 in), and penetration depth = 24.4m (80 ft). The soil profile at the Newbury site is shown in Fig. 6-7. The ground soil primarily consists of the normally consolidated clay with interbedded silty sand. The water level is at the depth of 1.5 m (4.9 ft).

The α-API/Nordlund/Thurman method and the β/Thurman method are used to predict the pile capacities as shown in Table 6-2. Applying the resistance factor (NCHRP Report 507), the factored capacities are 376 kN (84.5 kip) and 310 kN (69.7 kip) for the α-API/Nordlund/Thurman method and β/Thurman method, respectively.

The predicted ultimate capacity from the dynamic pile testing methods are 418 kN (94.0 kip), 1112 kN (250.0 kip), and 792 kN (178.0 kip) using CAPWAP EOD, CAPWAP BOR, and EA EOD, respectively. The factored capacities are 268 kN (60.2 kip), 723 kN

(162.5 kip), and 420 kN (94.4 kip) based on CAPWAP EOD, CAPWAP BOR, and EA EOD, respectively.

Table 6-3 provides a summary of the capacities from the prior static analysis, the dynamic testing method, and the posterior static analysis methods, in comparison to the actual static load test results. It can be seen that the updated resistance factors using CAPWAP BOR for updating are highest for both static analysis methods.

Fig. 6-8 shows the effect of combining two methods. It can be seen that, for β /Thurman method, the ratio of static load test capacity to factored prediction capacity varies from prior 2.16 to posterior 1.64, 1.06, and 1.40 after updating using CAPWAP EOD, CAPWAP BOR, and EA EOD, respectively. The pile capacity prediction using α-API/Nordlund/Thurman method is also improved when updating the resistance factors by incorporating the results of dynamic pile tests.

6.10 Case Study II

Test piles #3 at Newbury site from the Appendix D of NCHRP Report 507 (Paikowsky et al. 2004) is a square (356 mm by 356 mm) precast, prestressed concrete (PPC) pile with penetration depth of 24.4 m in the same soil condition as that in case study I.

The details of calculation using α-API/Nordlund/Thurman and β/Thurman methods are summarized in Table 6-4. The pile capacities from the dynamic pile testing methods based on CAPWAP EOD, CAPWAP BOR, and EA EOD are given in Table 6-5 as well.

The prior resistance factors in the table are taken from NCHRP Report 507 (Paikowsky et al. 2004).

Table 6-5 shows the comparison between the predicted capacities from the prior static analysis, the dynamic testing, and the posterior static analysis methods, and the actual static load test results. In this case, the updated resistance factors by the three dynamic testing methods are very close to each other. It could be due to an accurate prediction of pile capacities by the original static analysis methods. Thus, if the static analysis methods provide relatively accurate prediction of pile capacity, the improvement on the updated resistance factors in predicting pile capacity using dynamic testing results may be negligible.

Fig. 6-9 shows the comparisons of the factored pile capacities based on different combinations of two methods. It can be seen that, combining β/Thurman method with CAPWAP EOD, CAPWAP BOR, and EA EOD, the ratio of static load test capacity to posterior factored prediction capacity ranges from 1.08, 1.00, and 1.03, respectively. The predictions of pile capacities by combining α-API/Nordlund/Thurman method with different dynamic pile testing method are also shown in Fig. 6-9. Although the combining of two methods did not significantly alter the predicted pile capacity, but did result in more consistent comparisons with the static load test results, the important point is that combining two methods adds confidence to the predicted pile capacities.

The two case studies demonstrate the benefit of combining two methods to improve pile capacity prediction as opposed to using only one method. The improvement is mainly due to reduction of uncertainties associated with one method. By combining more accurate static and dynamic methods, one can predict the updated, factored pile capacity to be more consistent with the static load test result.

6.11 Conclusions

One of the benefits of LRFD approach is its suitability for applying reliability analysis to quantify uncertainties associated with various methods for estimating loads and resistances, respectively. With the reliability theory, Bayesian approach is employed to combine different analysis methods to improve accuracy and confidence level of predicted factored pile capacity as opposed to the case where a single analysis method is employed. The main benefit of combining two different methods is the reduction of uncertainties associated with each method itself.

The example analyses presented in this chapter for steel pipe piles and PPC piles in mixed soil profiles have demonstrated the applicability and reasonableness of the proposed approach. The updated, factored pile capacities are closer to the static load test results than the originally predicted factored capacities by the two methods used in a stand-alone analysis.

Specific conclusions drawn from this study can be enumerated as follows:

- When the static analysis and dynamic pile testing methods are combined to obtain the posterior distribution, combination of two accurate design methods generate more reliable updating of posterior distributions.
- The dynamic pile testing methods provides less benefit in updating the high-accuracy static analysis methods, particularly when the prior static analysis method possesses higher accuracy than the dynamic pile testing method chosen for the updating purpose.
- The posterior prediction of pile capacity becomes more reliable, as the number of dynamic pile tests incorporated in updating increases.
- Two dynamic tests could be considered sufficient to update the high accuracy static analysis methods. For the static methods with low accuracy, the updated resistance factors are remarkably increased by the first four dynamic tests.

Table 6-1 Statistical Parameters and Resistance Factors for Driven Piles from NCHRP Report 507 (β = 2.33) (Paikowsky et al. 2004)

Method category	Prediction method	Number of cases	Bias factor λ_R or Correction factor K	Coefficient of variation	Resistance factor, Φ
Static analysis methods (Concrete piles in Clay)	λ- Method	18	0.76	0.29	0.48
	α –API	17	0.81	0.26	0.54
	β – Method	8	0.81	0.51	0.32
	α –Tomlinson	18	0.87	0.48	0.36
Dynamic methods with measurements	CAPWAP EOD	125	1.63	0.49	0.64
	CAPWAP BOR	162	1.16	0.34	0.65
	EA EOD	128	1.08	0.40	0.53

Table 6-2 Summary of Calculated Capacities from Static Analysis Method for Test Pile #2

Layer #	Layer Thickness (m)	α-API/Nordlund		β- Method	
		Unit Skin Friction (kPa)	Friction Capacity (kN)	Unit Skin Friction (kPa)	Friction Capacity (kN)
1	2.5	41.8	104	71.2	180
2	6.1	26.6	162	26.6	162
3	4.9	26.6	130	39.4	193
4	7.9	43.7	345	68.4	540
Tip Resistance (kN) –Thurman Method			309		309
Total resistance (kN)			1050		1384

Layer #	Layer Thickness (ft)	α-API/Nordlund		β- Method	
		Unit Skin Friction (psf)	Friction Capacity (kip)	Unit Skin Friction (psf)	Friction Capacity (kip)
1	8.2	873	23.4	1487	40.5
2	20.0	556	36.4	556	36.4
3	16.1	556	29.2	823	43.4
4	25.9	913	77.6	1429	121.4
Tip Resistance (kip) –Thurman Method			69.5		69.5
Total resistance (kip)			236		311.1

Table 6-3 Pile Capacities of Prior Static Analysis, Dynamic Testing, Posterior Static Analysis, and Static Load Test (Test Pile #2 in Newbury)

Prior static analysis method				Dynamic pile testing method				Posterior static analysis method			Static load test (kN)
Static design method	Pile capacity (kN)	Prior resistance factor, Φ	Factored capacity (kN)	Dynamic Design Method	Pile capacity (kN)	Resistance factor, Φ	Factored capacity (kN)	Pile capacity (kN)	Posterior resistance factor, Φ	Factored capacity (kN)	
α-API/ Nordlund/ Thurman	1050	0.36	378	CAPWAP EOD	418	0.64	268	1050	0.40	420	658
				CAPWAP BOR	1112	0.65	723		0.62	651	
				EA EOD	792	0.53	420		0.46	483	
β / Thurman	1384	0.22	304	CAPWAP EOD	418	0.64	268	1384	0.29	401	
				CAPWAP BOR	1112	0.65	723		0.45	623	
				EA EOD	792	0.53	420		0.34	471	

Table 6-4 Summary of Calculated Capacities from Static Analysis Method for Test Pile #3

Layer #	Layer Thickness (m)	α-API/Nordlund		β- Method	
		Unit Skin Friction (kPa)	Friction Capacity (kN)	Unit Skin Friction (kPa)	Friction Capacity (kN)
1	2.5	41.8	146	71.2	249
2	6.1	26.6	227	26.6	227
3	4.9	26.6	182	39.4	270
4	7.9	93.1	1030	68.4	756
Tip Resistance (kN) –Thurman Method			473		473
Total resistance (kN)			2058		1975

Table 6-5 Pile Capacities of Prior Static Analysis, Dynamic Testing, Posterior Static Analysis, and Static Load Test (Test Pile #3 in Newbury)

Prior static analysis method				Dynamic pile testing method				Posterior static analysis method			Static load test (kN)
Static design method	Pile capacity (kN)	Prior resistance factor, Φ	Factored capacity (kN)	Dynamic Design Method	Pile capacity (kN)	Resistance factor, Φ	Factored capacity (kN)	Pile capacity (kN)	Posterior resistance factor, Φ	Factored capacity (kN)	
α-API/ Nordlund/ Thurman	2058	0.36	741	CAPWAP EOD	738	0.64	472	2058	0.37	761	872
				CAPWAP BOR	1228	0.65	798		0.42	864	
				EA EOD	1228	0.53	651		0.40	823	
β / Thurman	1975	0.42	830	CAPWAP EOD	738	0.64	472	1975	0.41	810	
				CAPWAP BOR	1228	0.65	798		0.44	869	
				EA EOD	1228	0.53	651		0.43	849	

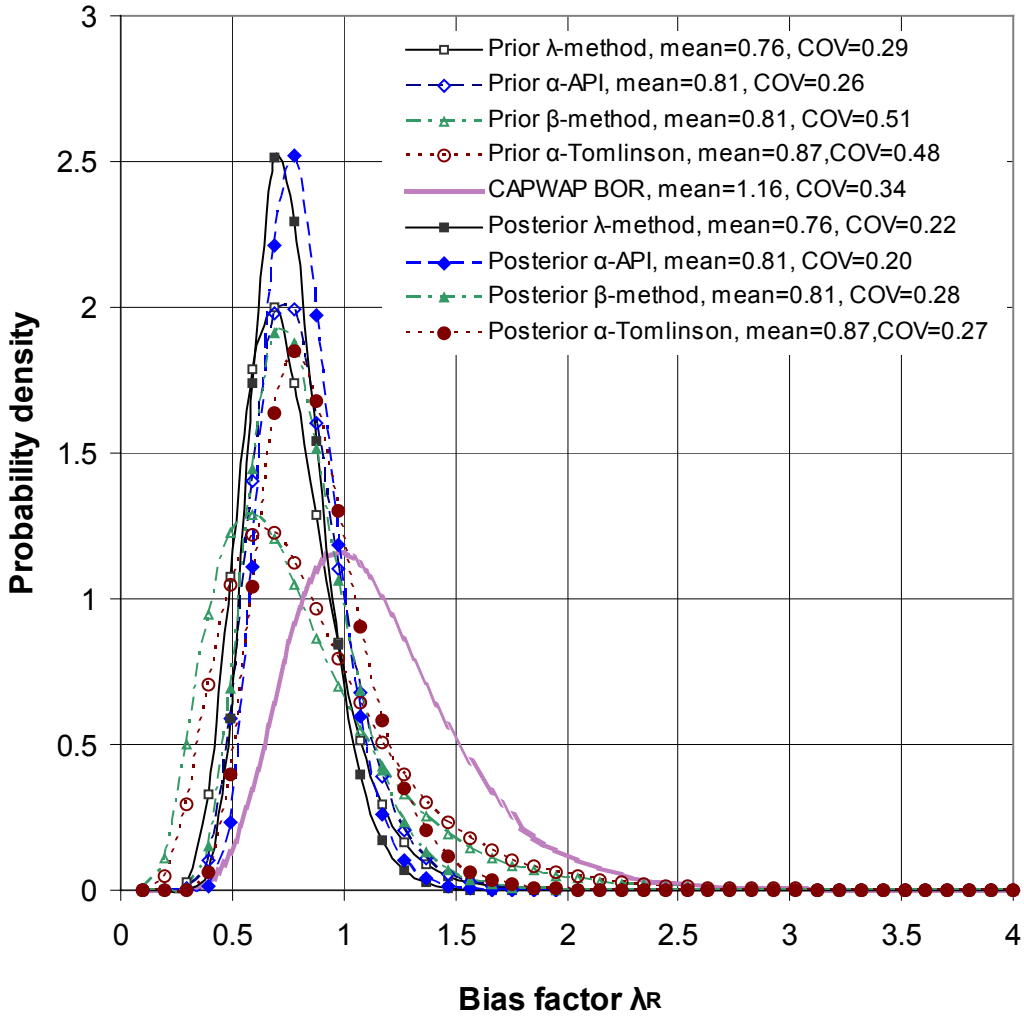

Figure 6-1 Prior and Posterior Distribution of Different Static Design Methods When CAPWAP BOR Is Used for Updating

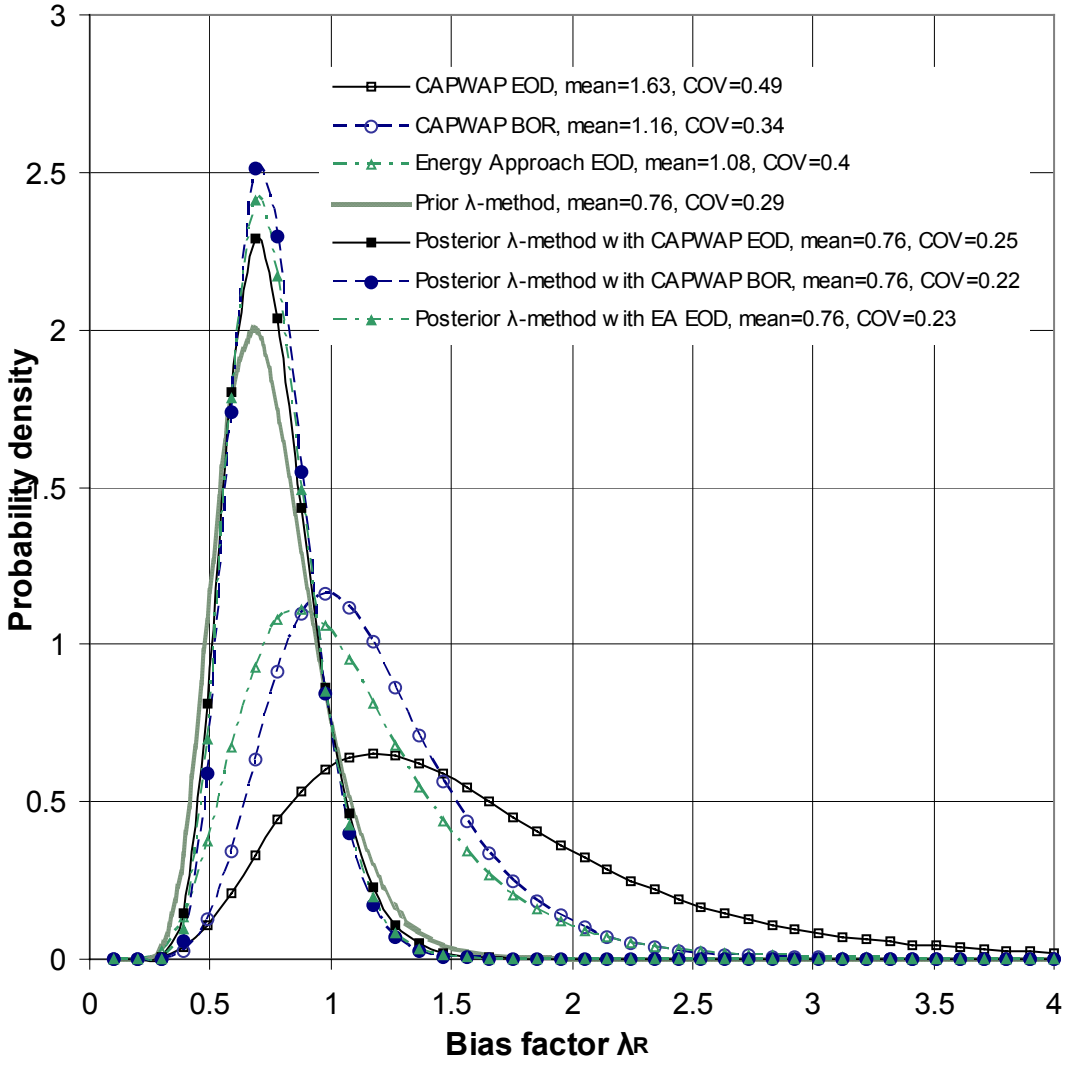

Figure 6-2 Prior and Posterior Distribution of Static λ-Method when Different Dynamic Pile Tests Are Used for Updating

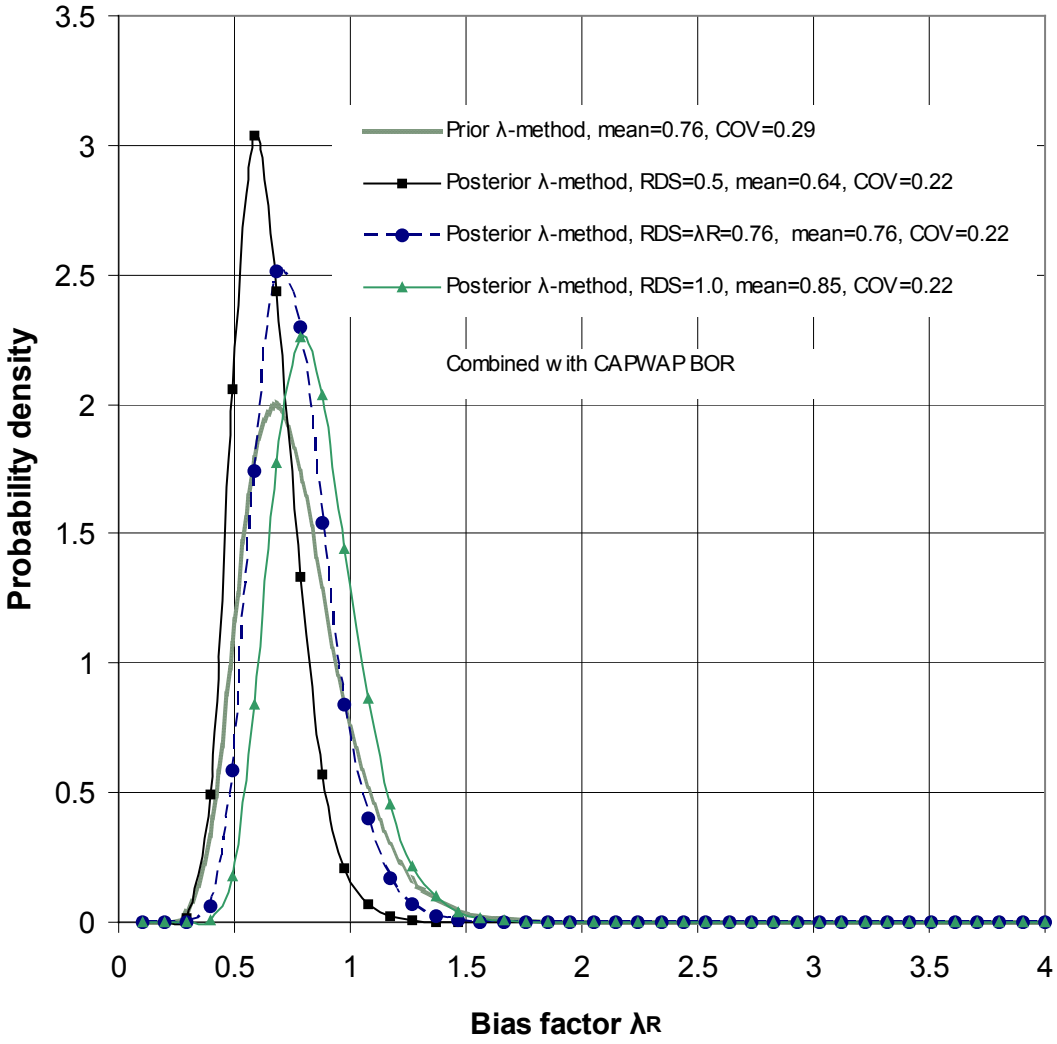

Figure 6-3 Prior and Updated Distribution of Static λ-Method with Different RDS

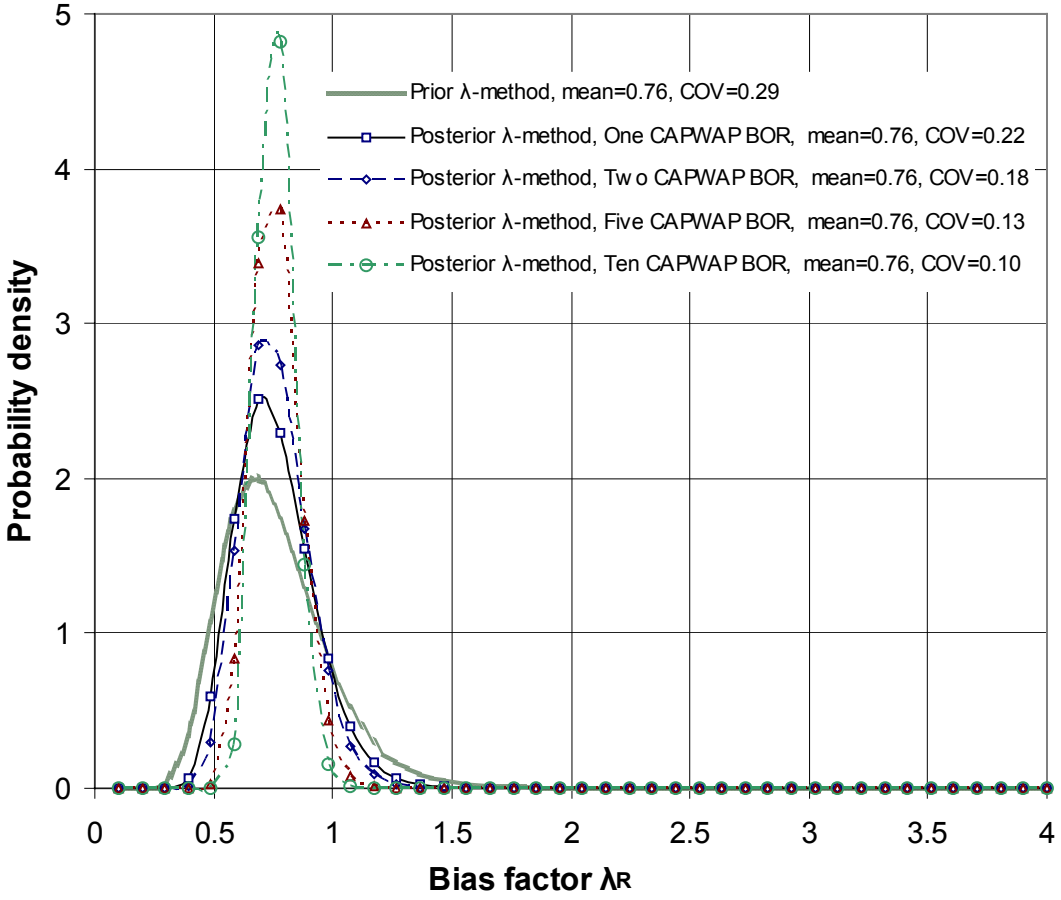

Figure 6-4 Prior and Updated Distribution of Static λ-Method with Different Numbers of Dynamic Tests

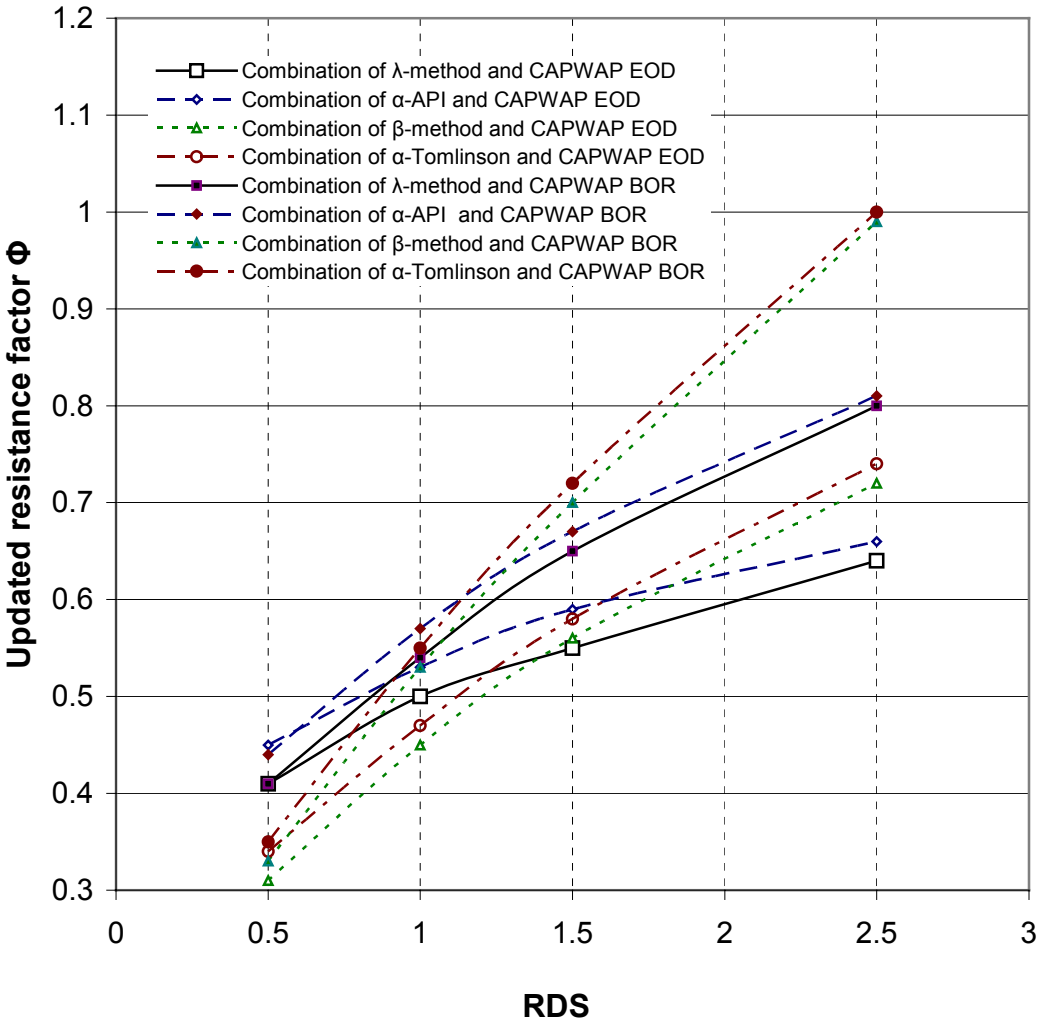

Figure 6-5 Variation of Updated Resistance Factors with RDS

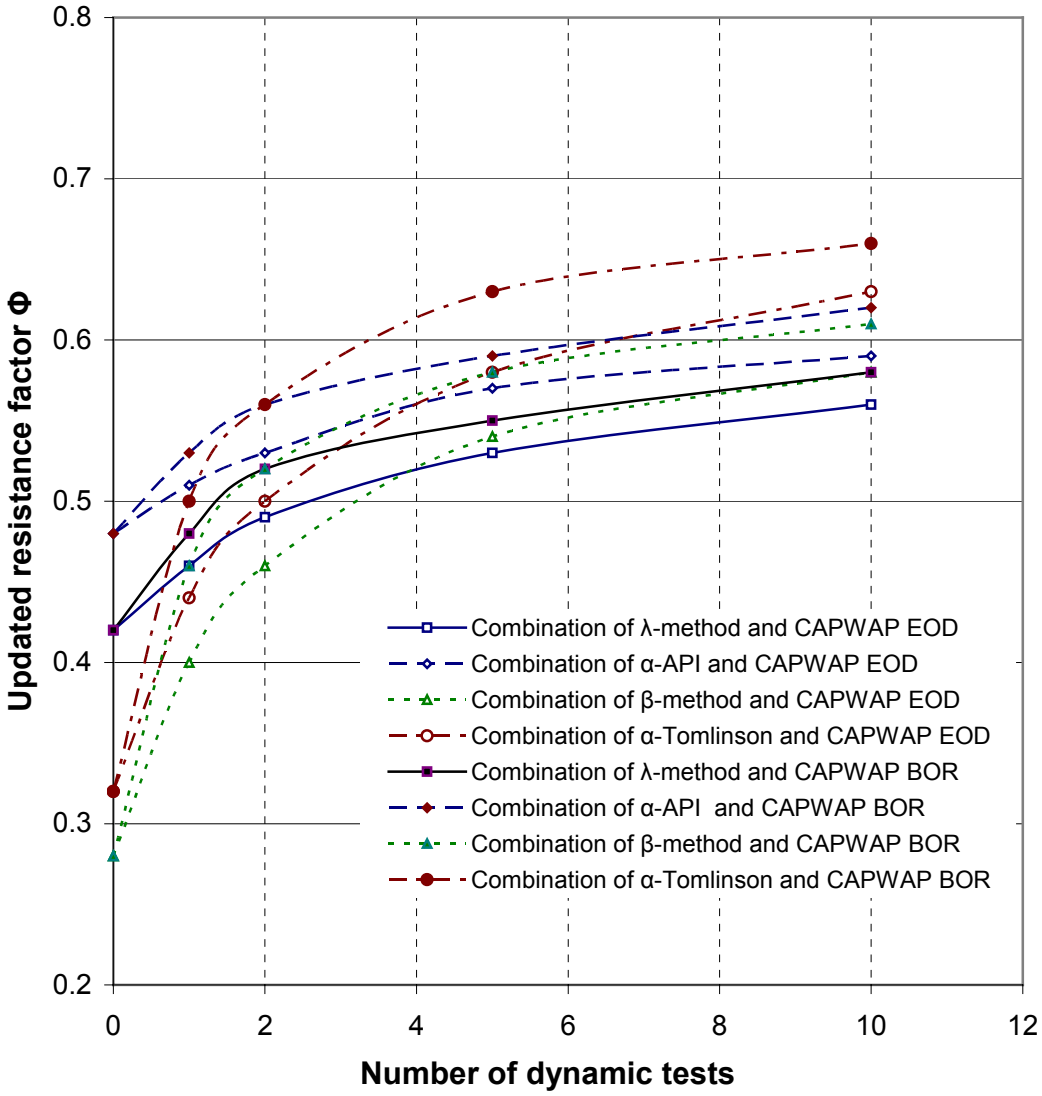

Figure 6-6 Variation of Updated Resistance Factors with Number of Dynamic Tests

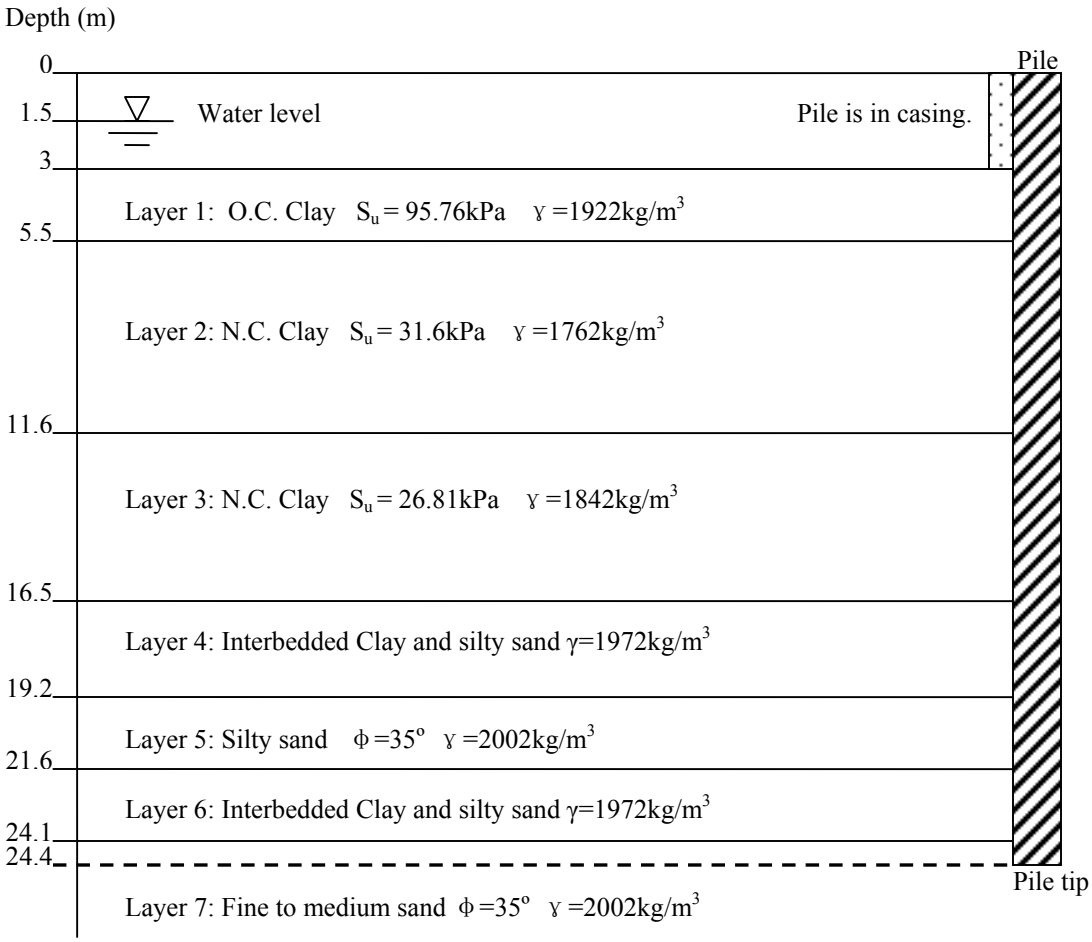

Figure 6-7 Soil Profile in Newbury Site

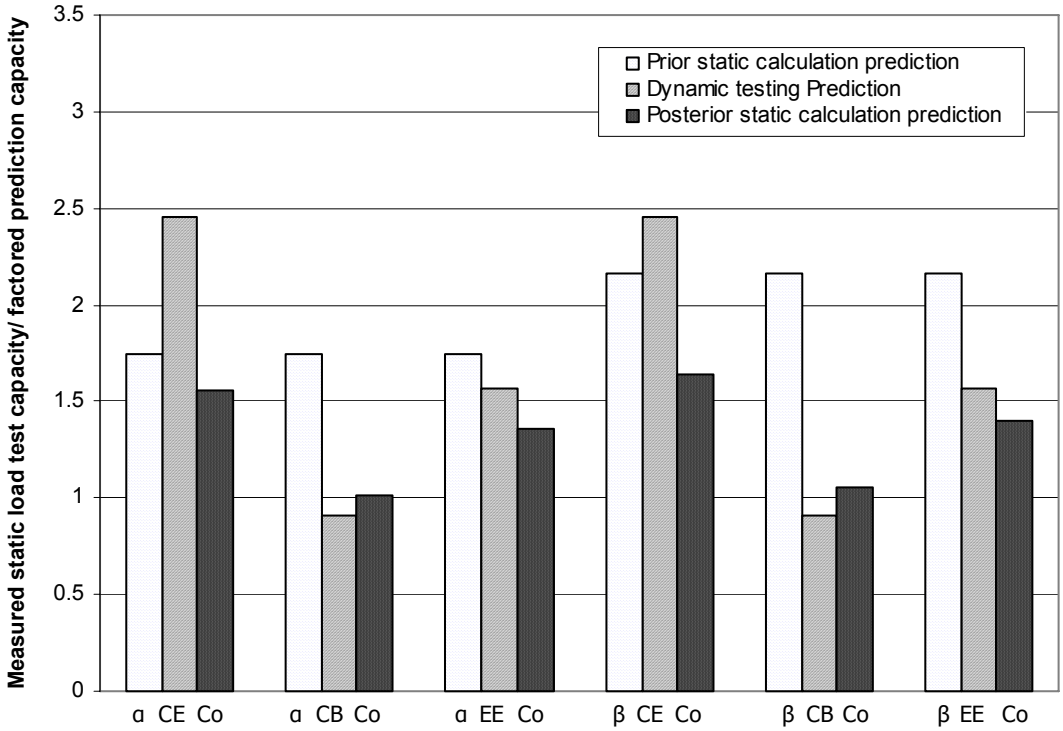

Figure 6-8 Comparison of Ratio of Static Load Test Capacity to Factored Prediction Capacity for Test Pile #2

α =α-Tomlinson/ Nordlund/ Thurman; β=β-Method/ Thurman; CE=CAPWAP EOD; CB=CAPWAP BOR; EE=EA EOD; Co=Combination of two design methods.

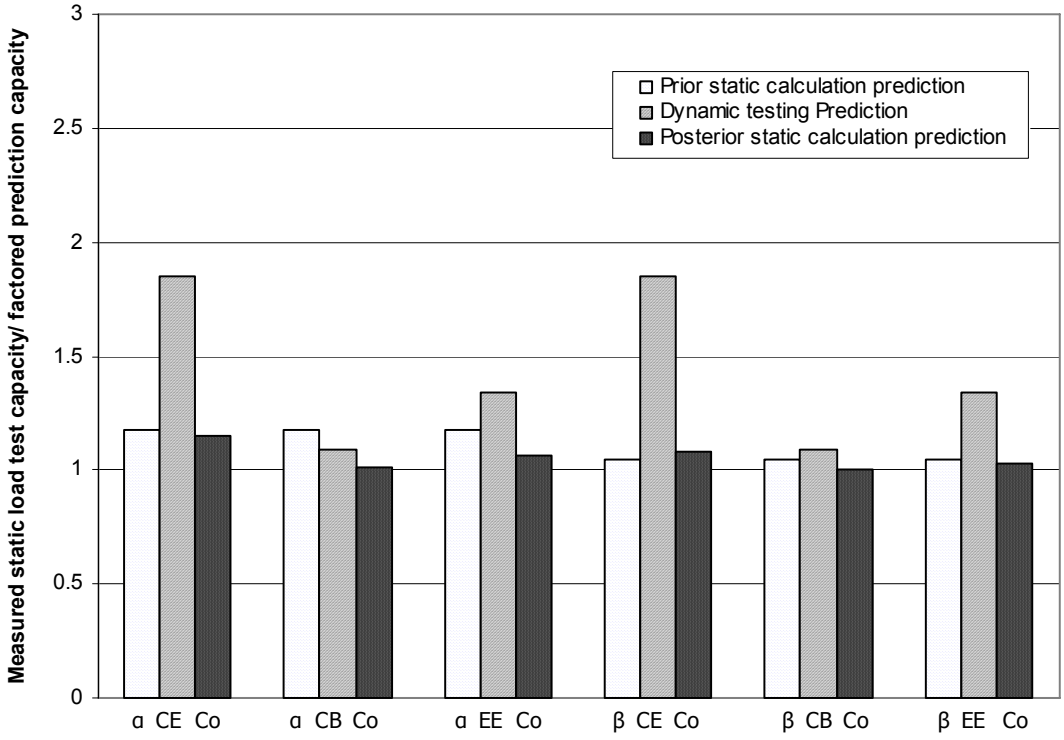

Figure 6-9 Comparison of Ratio of Static Load Test Capacity to Factored Prediction Capacity for Test Pile #3

α =α-Tomlinson/ Nordlund/ Thurman; β=β-Method/ Thurman; CE=CAPWAP EOD; CB=CAPWAP BOR; EE=EA EOD; Co=Combination of two design methods.

CHAPTER VII

WAVE EQUATION TECHNIQUE FOR ESTIMATING DRIVEN PILE CAPACITY

7.1 Introduction

Dynamic pile testing has been widely used in estimating the pile capacity and deciding the driving criteria during pile driving. During dynamic pile testing, the strain gages and accelerometers are usually attached near the pile head to record the waveforms. The measured strains are converted into axial forces and the measured accelerations are integrated over time to obtain velocity, both as a function of real time. Both the measured force and the product of measured velocity and pile impendence are usually proportional during the initial rising period at each hammer blow, then separated from each other once the shaft and toe resistance are reflected upward to the pile head. Some researchers such as Rausche et al. (1972, 1985), Hirsch et al. (1976), Liang and Zhou (1996), and Liang (2003) have proposed various approaches to interpret the measured force and velocity histories on determining the pile capacity.

With the development and acceptance of PDA (Pile Driving Analyzer), the Case method (Rausche et al. 1985), utilizing the measured force and velocity histories in approximate simple algebraic equations, has become one of the widely used methods to evaluate the pile capacities. However, the static soil resistances determined by the Case

method are very sensitive to the assumed Case damping factor, and the shaft and the toe resistance cannot be separated by the Case method. In an effort to overcome some of the shortcomings of the Case method, an alternative procedure, known as the CAPWAP (Goble Rausche Likins and Associates, Inc., 1996), was developed by Rausche et al. (1972, 1985). The CAPWAP approach is based on the one-dimensional wave propagation model suggested by Smith (1960). In CAPWAP analysis, one of the two HST data (either force or velocity) is used as input to generate simulation results to match closely with the other HST data by adjusting Smith model parameters. Once the acceptable match is achieved, then the pile capacities and the Smith model parameters can be determined. However, the requirement of experienced program operator and substantial time-consuming computation hinders the further application of CAPWAP procedure.

In this chapter, a one-dimensional wave equation based algorithm to interpret the HST data for estimation of the shaft and toe resistance of driven piles is introduced. Both the force and velocity time histories measured at the pile head are used as input boundary conditions in the new algorithm. The Smith damping factor and the static soil resistance can be directly determined based on the closed form solution of the one-dimensional wave equation, which is computationally efficient compared to the existing numerical procedure. Furthermore, the shaft resistance and the toe resistance could be successfully separated by the proposed wave equation method as well. Numerical examples are presented to illustrate the methodology and applicability of the proposed analysis approach.

7.2 Soil-Pile Interaction Model

The soil-pile interaction model is shown in Fig. 7-1 where the following assumptions are made: 1) the pile is represented by a linear elastic bar with Young's modulus E, total length L, cross-section area A, and mass density ρ; 2) the soil around the pile is a homogenized isotropic medium; 3) the resistance along pile shaft is a function of the displacement and velocity related to the depth and time.

The general equation of motion for the soil-pile interaction model can be formulated as follows:

$$A\frac{\partial \sigma}{\partial x}dx - \frac{\partial^2 u(x,t)}{\partial t^2}dm - dF = 0 \tag{7-1}$$

$$\sigma = E\varepsilon = E\frac{\partial u(x,t)}{\partial x} \tag{7-2}$$

$$dm = \rho A dx \tag{7-3}$$

$$dF = R(x,t)dx \tag{7-4}$$

where

σ = stress of unit pile cross-sectional area;

ε = strain of unit pile length;

m = mass of unit volume of pile body;

R(x,t) = soil resistance along pile shaft, as a function of time and depth.

A general expression of the soil resistance along pile shaft can be written as follows:

$$R(x,t) = c_1 f_1(u(x,t)) + c_2 f_2(v(x,t)) \tag{7-5}$$

where c_1 and c_2 are the coefficients of stiffness and viscous damping,

$$c_1 = K_S, \quad f_1(u(x,t)) = \begin{cases} u(x,t), & u(x,t) < Q_s, \\ Q_s, & u(x,t) \geq Q_s \end{cases} \tag{7-6}$$

$$c_2 = c_1 J_s f_1(u(x,t)) \ , \qquad f_2(v(x,t)) = v(x,t) \tag{7-7}$$

where K_s is soil stiffness, Q_s is shaft quake, and J_s is shaft damping factor.

In most cases, the displacement of pile particles along the shaft is greater than the recoverable soil deformation (i.e. the soil quake). Therefore, it is reasonable to assume that the static shaft resistance be totally mobilized during pile driving. The pile shaft resistance can be expressed as follows

$$R(x,t) = K_s Q_s (1 + J_s v(x,t)) = R_s^S (1 + J_s \frac{\partial u(x,t)}{\partial t}) \tag{7-8}$$

where $R_s^S (= K_s Q_s)$ is the static pile shaft resistance per unit embedded pile length.

7.3 Identification of Shaft Parameters

In Eq. (7-1), the analytical model only considers the soil resistance along the pile shaft that is expressed in Eq. (7-8) as a function of static pile shaft resistance, R_s^S, shaft damping factor, Js, and the displacement of pile particles along the pile shaft. In the following section, the unknown parameters, R_s^S and Js, along the pile shaft will be identified based on the solution of the proposed analytical model.

Substituting Eqs. (7-2) ~ (7-8) into Eq. (7-1), the original equation for soil-pile interaction can be written as follows:

$$\rho A\frac{\partial^2 u(x,t)}{\partial t^2}+R_s^S(1+J_s\frac{\partial u(x,t)}{\partial t})-EA\frac{\partial^2 u(x,t)}{\partial x^2}=0 \tag{7-9}$$

or

$$\frac{\partial^2 u(x,t)}{\partial t^2}+\frac{R_s^S}{\rho A}(1+J_s\frac{\partial u(x,t)}{\partial t})-c^2\frac{\partial^2 u(x,t)}{\partial x^2}=0 \tag{7-10}$$

where, $c=\sqrt{E/\rho}$ is the longitudinal wave velocity in the pile.

The initial conditions are:

$$\begin{cases} u(x,0)=0 \\ \dot{u}(x,0)=0 \end{cases} \tag{7-11}$$

where the dot $\bullet$ represents the time derivative.

The boundary conditions at the pile head are given by the measured force, $F_m(t)$, and the measured velocity, $V_m(t)$, as follows:

$$\begin{cases} \dfrac{\partial u(0,t)}{\partial x}=-\dfrac{F_m(t)}{EA} \\ \dfrac{\partial u(0,t)}{\partial t}=V_m(t) \end{cases} \tag{7-12}$$

Let

$$u(x,t)=e^{-\mu t}w(x,t) \tag{7-13}$$

where

$$\mu = \frac{R_s^S J_s}{2\rho A} \tag{7-14}$$

Eq. (7-10) becomes:

$$w_{tt}(x,t) - \mu^2 w(x,t) + \frac{R_s^S}{\rho A} e^{\mu t} - c^2 w_{xx}(x,t) = 0 \tag{7-15}$$

The Laplace's transform (Thomson 1950) of Eq. (7-15) gives:

$$c^2 w_{xx}(x,s) - (s^2 - \mu^2) w(x,s) = \frac{R_s^S}{\rho A} \frac{1}{s-\mu} \tag{7-16}$$

The general solutions of the above equation are:

$$w(x,s) = A_1 e^{\frac{x\sqrt{s^2-\mu^2}}{c}} + A_2 e^{-\frac{x\sqrt{s^2-\mu^2}}{c}} - \frac{R_s^S}{\rho A (s+\mu)(s-\mu)^2} \tag{7-17}$$

The Laplace's transform of the boundary conditions can be expressed as:

$$\begin{cases} \dfrac{\partial w(0,s)}{\partial x} = -\dfrac{F_m(s-\mu)}{EA} \\ w(0,s) = \dfrac{V_m(s-\mu)}{s-\mu} \end{cases} \tag{7-18}$$

Hence, the coefficients A_1 and A_2 can be solved as follows:

$$\begin{cases} A_1 = -\dfrac{c}{2EA} \dfrac{F_m(s-\mu)}{\sqrt{s^2-\mu^2}} + \dfrac{R_s^S}{\rho A} \dfrac{1}{2(s+\mu)(s-\mu)^2} + \dfrac{V_m(s-\mu)}{2(s-\mu)} \\ A_2 = \dfrac{c}{2EA} \dfrac{F_m(s-\mu)}{\sqrt{s^2-\mu^2}} + \dfrac{R_s^S}{\rho A} \dfrac{1}{2(s+\mu)(s-\mu)^2} + \dfrac{V_m(s-\mu)}{2(s-\mu)} \end{cases} \tag{7-19}$$

Then, w(x,s) can be determined as:

$$w(x,s) = (-\frac{c}{2EA}\frac{F_m(s-\mu)}{\sqrt{s^2-\mu^2}} + \frac{R_s^S}{\rho A}\frac{1}{2(s+\mu)(s-\mu)^2} + \frac{V_m(s-\mu)}{2(s-\mu)})e^{\frac{x\sqrt{s^2-\mu^2}}{c}} +$$
$$(\frac{c}{2EA}\frac{F_m(s-\mu)}{\sqrt{s^2-\mu^2}} + \frac{R_s^S}{\rho A}\frac{1}{2(s+\mu)(s-\mu)^2} + \frac{V_m(s-\mu)}{2(s-\mu)})e^{-\frac{x\sqrt{s^2-\mu^2}}{c}} + \frac{R_s^S}{\rho A(s+\mu)(s-\mu)^2} \quad (7\text{-}20)$$

Taylor's series expansion theory is applied to simplify the above equation:

$$\begin{cases} \frac{1}{2}(e^{\frac{x\sqrt{s^2-\mu^2}}{c}} + e^{-\frac{x\sqrt{s^2-\mu^2}}{c}}) \approx 1 + \frac{1}{2!}\frac{x^2(s^2-\mu^2)}{c^2} \\ \frac{1}{2}(e^{\frac{x\sqrt{s^2-\mu^2}}{c}} - e^{-\frac{x\sqrt{s^2-\mu^2}}{c}}) \approx \frac{x\sqrt{s^2-\mu^2}}{c} + \frac{1}{3!}(\frac{x\sqrt{s^2-\mu^2}}{c})^3 \end{cases} \quad (7\text{-}21)$$

Thus, w(x,s) becomes

$$w(x,s) = -\frac{x}{EA}F_m(s-\mu) - \frac{1}{6}\frac{c}{EA}(\frac{x}{c})^3 F_m(s-\mu)((s-\mu)^2 + 2\mu(s-\mu)) + \frac{2R_s^S}{\rho A(s+\mu)(s-\mu)^2}$$
$$+\frac{x^2}{2c^2}\frac{R_s^S}{\rho A}\frac{1}{s-\mu} + \frac{V_m(s-\mu)}{s-\mu} + \frac{V_m(s-\mu)}{2}\frac{x^2}{c^2}((s-\mu)+2\mu) \quad (7\text{-}22)$$

Neglecting the high order of (s-μ) and performing the inverse Laplace's transform of w(x,s), w(x,t) can be obtained as follows:

$$w(x,t) = L^{-1}(w(x,s))$$
$$= -e^{\mu t}\frac{x}{EA}F_m(t) - \frac{c}{3EA}(\frac{x}{c})^3 \mu e^{\mu t}F_m^{'}(t) + \frac{R_s^S}{\rho A}\frac{x^2}{2c^2}e^{\mu t} + e^{\mu t}\int_0^t V_m(\tau)d\tau + \frac{x^2}{2c^2}e^{\mu t}[2\mu V_m(t) + V_m^{'}(t)] \quad (7\text{-}23)$$

Then,

$$u(x,t) = e^{-\mu t}w(x,t)$$
$$= -\frac{x}{EA}F_m(t) - \frac{c}{6EA}(\frac{x}{c})^3 2\mu F_m^{'}(t) + \frac{R_s^S}{\rho A}\frac{x^2}{2c^2} + \int_0^t V_m(\tau)d\tau + \frac{x^2}{2c^2}[V_m^{'}(t) + 2\mu V_m(t)] \quad (7\text{-}24)$$

The boundary condition at the pile toe is considered to be motionless before the downward wave reaches the toe. It means, for $t < L/c$, the displacement at the pile toe is considered to be zero.

$$u(L,t) = -\frac{L}{EA}F_m(t) - \frac{c}{6EA}(\frac{L}{c})^3 2\mu F_m^{'}(t) + \frac{R_s^S}{\rho A}\frac{L^2}{2c^2} + \int_0^t V_m(\tau)d\tau + \frac{L^2}{2c^2}[V_m^{'}(t) + 2\mu V_m(t)] = 0 \quad (7\text{-}25)$$

Eq. (7-25) can be used to determine the representative parameters, R_s^S and J_s, for the time period before the stress wave introduced at the pile head reaches the pile toe. Since $F_m(t)$ and $V_m(t)$ measured at the pile head are used in Eq. (7-25) as input, the motion at the pile toe is not recorded by the pile head transducers during the time period $0<t<2L/c$. By adjusting these two parameters, R_s^S and J_s, Eq. (7-25) can be satisfied within the specific tolerance for this time period.

7.4 Identification of Pile Capacity at the Pile Toe

After the expression of displacement u(x,t) has been obtained without unknown parameters, the force at the pile toe, for $t \geq L/c$, can be expressed as follows:

$$\begin{aligned} R_t(L,t) &= EA\frac{\partial u(x,t)}{\partial x}\Big|_{x=L} \\ &= -F_m(t) - \frac{L^2}{2c^2}2\mu F_m^{'}(t) - R_s^S L + EA\frac{L}{c^2}(V_m^{'}(t) + 2\mu V_m(t)] \end{aligned} \tag{7-26}$$

The velocity at the pile toe can be expressed as follows:

$$v(L,t) = \frac{\partial u(x,t)}{\partial t}\Big|_{x=L} = -\frac{L}{EA}F_m^{'}(t) - \frac{L^3}{6EAc^2}2\mu F_m^{''}(t) + V_m(t) + \frac{L^2}{2c^2}\{V_m^{''}(t) + 2\mu V_m^{'}(t)] \tag{7-27}$$

The soil resistance at the pile toe, similar to that along the pile shaft, can also be expressed as follows:

$$R(L,t) = c_3 f_3(u(L,t)) + c_4 f_4(v(L,t)) \tag{7-28}$$

where c_3 and c_4 are coefficients of stiffness and viscous damping at the pile toe, respectively.

$$c_3 = K_t, \quad f_3(u(L,t)) = \begin{cases} u(L,t), & u(L,t) < Q_t, \\ Q_t, & u(L,t) \geq Q_t \end{cases} \tag{7-29}$$

$$c_4 = c_3 J_t f_3(u(L,t)), \qquad f_4(v(L,t)) = v(L,t) \tag{7-30}$$

where K_t is soil stiffness at the pile toe, Q_t is toe quake, and J_t is toe damping factor.

When the pile toe resistance is totally mobilized, the force at the pile toe can be expressed as follows:

$$R(L,t) = K_t Q_t (1 + J_t v(L,t)) = R_t^S (1 + J_t v(L,t)) \tag{7-31}$$

where R_t^S is the static resistance at the pile toe.

For the case in which the pile toe resistance is totally mobilized, Eq. (7-31) can be used to determine the static resistance, R_t^S, and damping factor, J_t, at the pile toe, when making the calculated force match the calculated velocity within the specific tolerance.

Sometimes, the pile toe resistance, however, is not totally mobilized, that is, the displacement at the pile toe does not reach the elastic deformation limit (i.e., the toe quake, Q_t). The following equation, in lieu of Eq. (7-31) can be employed to describe the relationship for this case:

$$R(L,t) = K_t u(L,t)(1 + J_t v(L,t)) \tag{7-32}$$

The coefficient of stiffness, K_t, and the damping factor, J_t, at the pile toe can be determined by making the calculated pile toe forces match with the calculated pile toe displacement and velocity within the specific tolerance. The static resistance at the pile toe can be obtained by multiplying the calculated K_t with the maximum calculated displacement at the pile toe.

7.5 Case Study

A steel pipe pile was driven about 15.6 m below the ground surface. The soils along the pile shaft and under the pile toe are clay. The Young's modulus of the pile E = 210,000,000 Pa; the cross-section area A = 48.5 cm^2; the mass density ρ = 7850 kg/m^3. The measured HST data are shown in Fig. 7-2.

By extracting the force and velocity time histories before the downward wave reaches the pile toe, two unknown parameters, R_s and J_s, can be determined when satisfying Eq. (7-25) within the specified tolerance. The static resistance and damping factor along the pile shaft are 59.2 KN and 3.882 s/m, respectively. After R_s and J_s are determined, R_t and J_t can be further calculated as 568.1 KN and 0.558 s/m, respectively. The calculated results from the proposed method are summarized in Table 7-1 with the CAPWAP analysis results and static load test results. It can be seen that the total resistance calculated from the proposed method shows good match with the results from static load test and CAWAP analysis. The distribution of pile resistance and Smith damping factor from the proposed approach do not match CAPWAP results very well. The sources of inconsistency may be identified as follows: 1) CAPWAP results may not be correct; 2) the assumption of homogeneous soil condition along the pile deviates from the actual conditions; 3) the model of soil-pile interaction needs to be further improved.

7.6 Comparisons

The performance of the proposed method is evaluated by the comparisons with the CAPWAP approach which is widely accepted as one of the most accurate procedure of

dynamic pile testing. An index, denoted as K, is used to define the ratio of the CAPWAP capacity to the predicted capacity from the proposed method. A total of 26 pile testing cases were used in this comparison study. The scattergram of the CAPWAP results versus the predicted capacities from the proposed method is shown in Fig. 7-3. It can be seen that the K values for most of pile cases fall in the range 0.7~1.5, which means that the capacities calculated from the proposed method match well with the CAPWAP results. The mean value, standard deviation, and COV value of index K are 1.167, 0.498, and 0.427, respectively. It should be pointed out that the high COV value is not unusual for the pile-foundation engineering. On the other hand, the computational efficiency and the close-form solution of one-dimensional wave equation make the proposed method attractive.

7.7 Conclusions

A wave equation-based algorithm has been developed in this chapter to estimate the driven pile capacity based on the High Strain Testing (HST) data. The Smith model is employed to illustrate the soil-pile interaction effect in the one-dimensional wave equation. The static shaft resistance is reasonably assumed to be totally mobilized during pile driving at the most cases. The pile static resistances and Smith model parameters can be directly determined in an analytical solution of one-dimensional wave equation. The proposed wave equation method may also separate the pile shaft and toe resistances. The numerical example is presented to illustrate the application of the proposed wave equation method. The predicted capacities from proposed method exhibit a favorable comparison when compared with the CAPWAP analysis results.

Table 7-1 Comparison of Results from Different Methods

Methods	Shaft resistance (KN)	Shaft damping factor J_s (s/m)	Toe resistance (KN)	Toe damping factor J_t (s/m)	Total resistance (KN)
Proposed method	59.2	3.882	568.1	0.558	627.3
CAPWAP method	361.2	0.561	211.7	0.108	572.9
Static load test					516.2

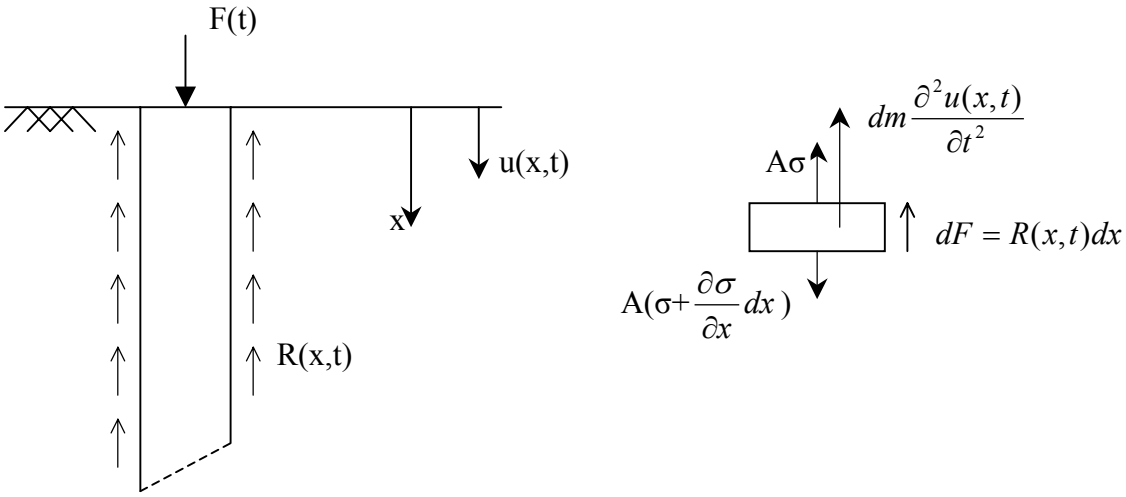

Figure 7-1 Soil-Pile Interaction Model

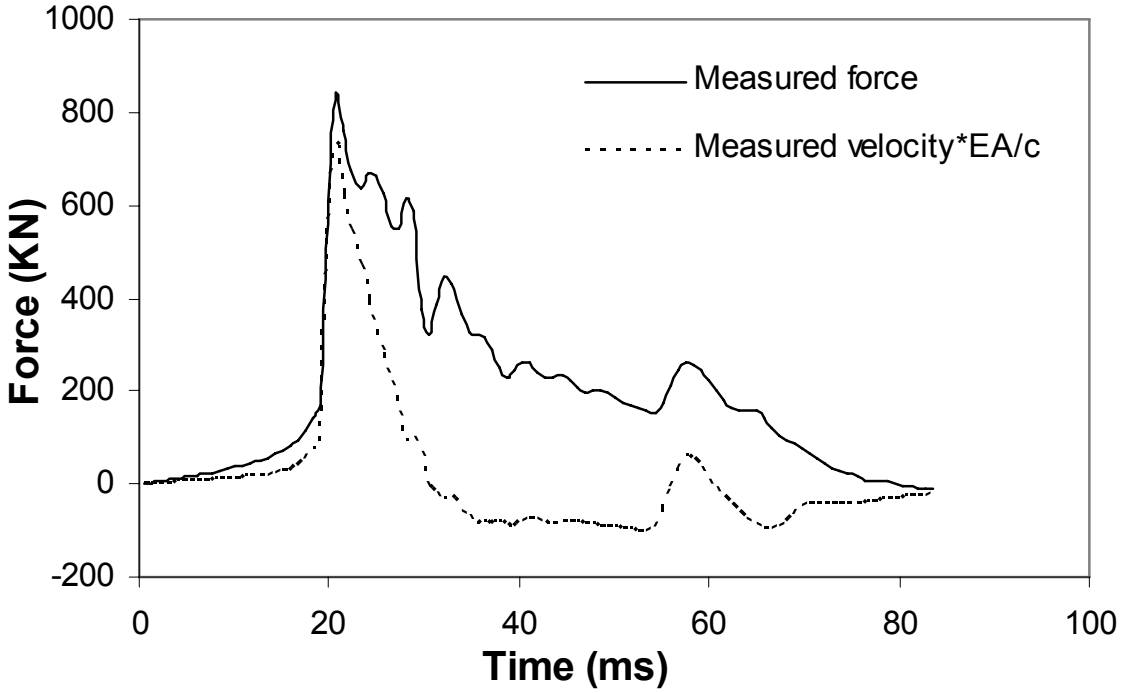

Figure 7-2 Measured Force and Velocity at the Pile Head

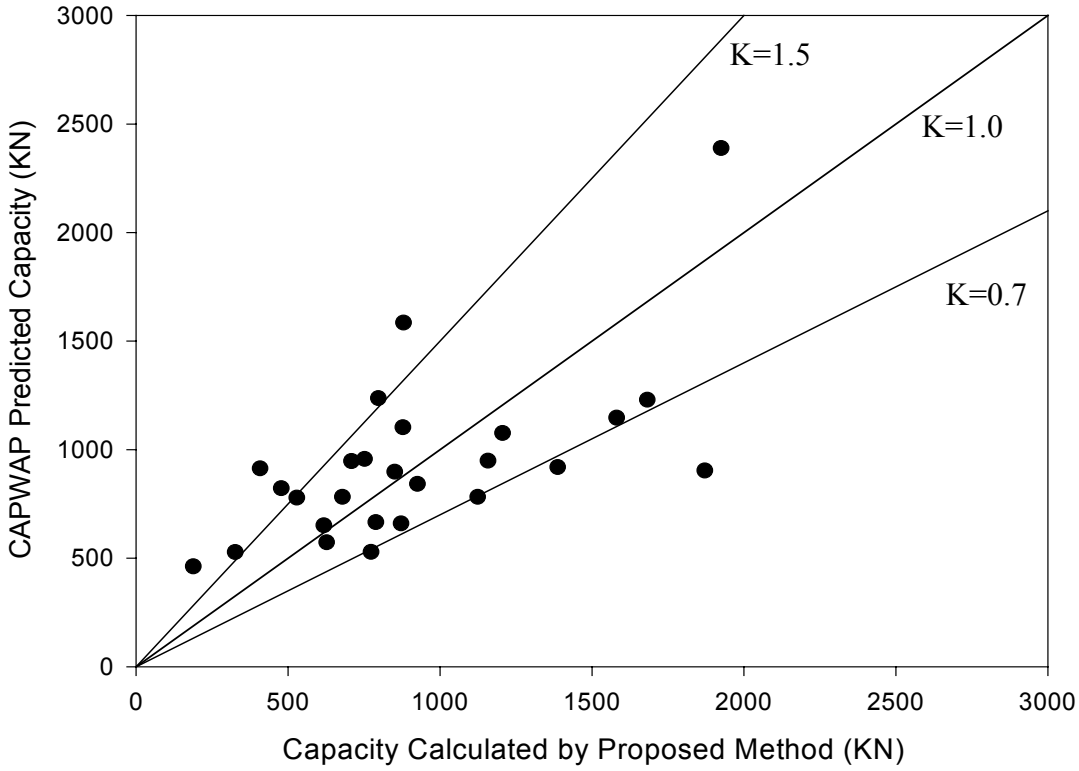

Figure 7-3 CAPWAP Results vs. the Results Calculated from the Proposed Method

CHAPTER VIII

NEW MEASUREMENT AND REMOTE SENSING TECHNOLOGY

8.1 Introduction

The NetDaq system is designed to acquire data remotely through wireless network. It is intend for the application where real time data monitor is necessary, but the location is hard to reach or human being cannot stay at the site because of safety or other reasons. The system consists of two major components: Stationary PC (Laptop or Desktop PC) and Remote Data Acquisition Unit.

The stationary PC has the application program allowing for user's interaction with system for data acquisition, data display and data process on real time basis. The developed system provides four channels of data flow plus the channel monitoring the remote system power supply.

The Remote Data Acquisition Unit will take the commands from stationary PC. Then it will command the data acquisition card to get data. Finally, it will send the data back to the stationary PC.

8.2 Hardware

Fig. 8-1 shows the developed wireless dynamic pile testing equipment. The new system consists of sensors and wireless communication for remote data acquisition and management. Accordingly, hanging cables from the sensor location to the data acquisition unit are no longer needed, so that dynamic pile testing can be conducted in a safer environment. The system is physically divided into two modules. The first module is the remote data acquisition unit. The second module is the stationary PC for the data processing.

Remote Data Acquisition Unit gathers seven components as follows:

- MicroSys SBC 1586 single board computer With PCMCIA adapter and network card adapter. OS: Microsoft Windows 2000.
- National Instrument data acquisition card: DaqCard AI-16XE-50.
- National Instrument Signal conditioner: SCC 2341 (for strain gauge), SCC-XXX (for Accelerator gauge).
- Strain gauge sensors and Accelerator gauges (same as PDI's sensors)
- Wireless Network: D-Link wireless bridge, Model DWL-810+.
- Customized signal conditioner module (Compact version for the NI SCC 2345 module)
- Power: 10 NiMH Batteries (12 V 4000mAh)

Stationary PC includes two components as follows:

- Laptop PC: Dell model Inspiron 700M operated with Microsoft Windows XP
- Remote wireless Presentation pointer: Kensington Model 33062

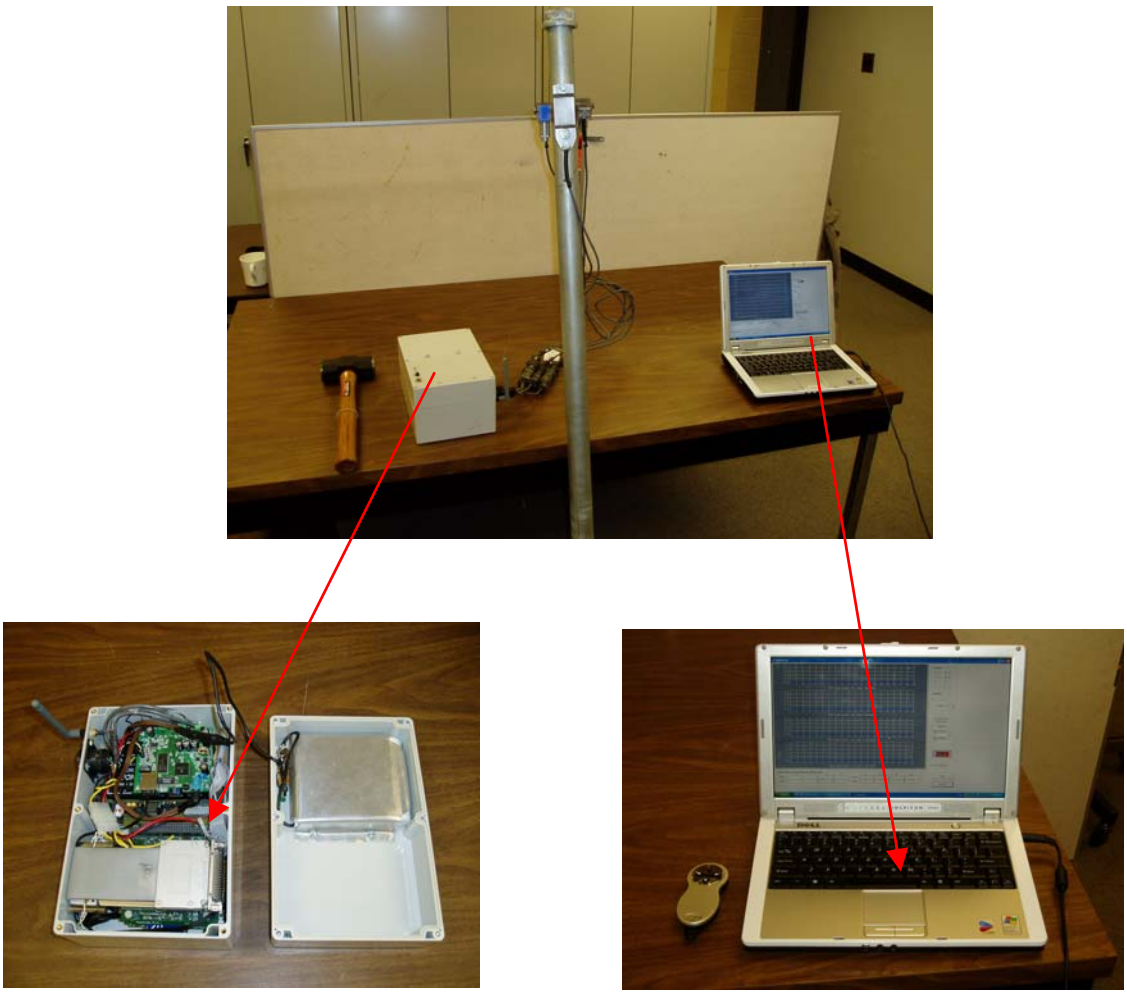

a) Remote Data Acquisition Unit b) Stationary PC

Figure 8-1 New wireless dynamic pile testing system

The block diagram of wireless data acquisition system is shown in Fig. 8-2.

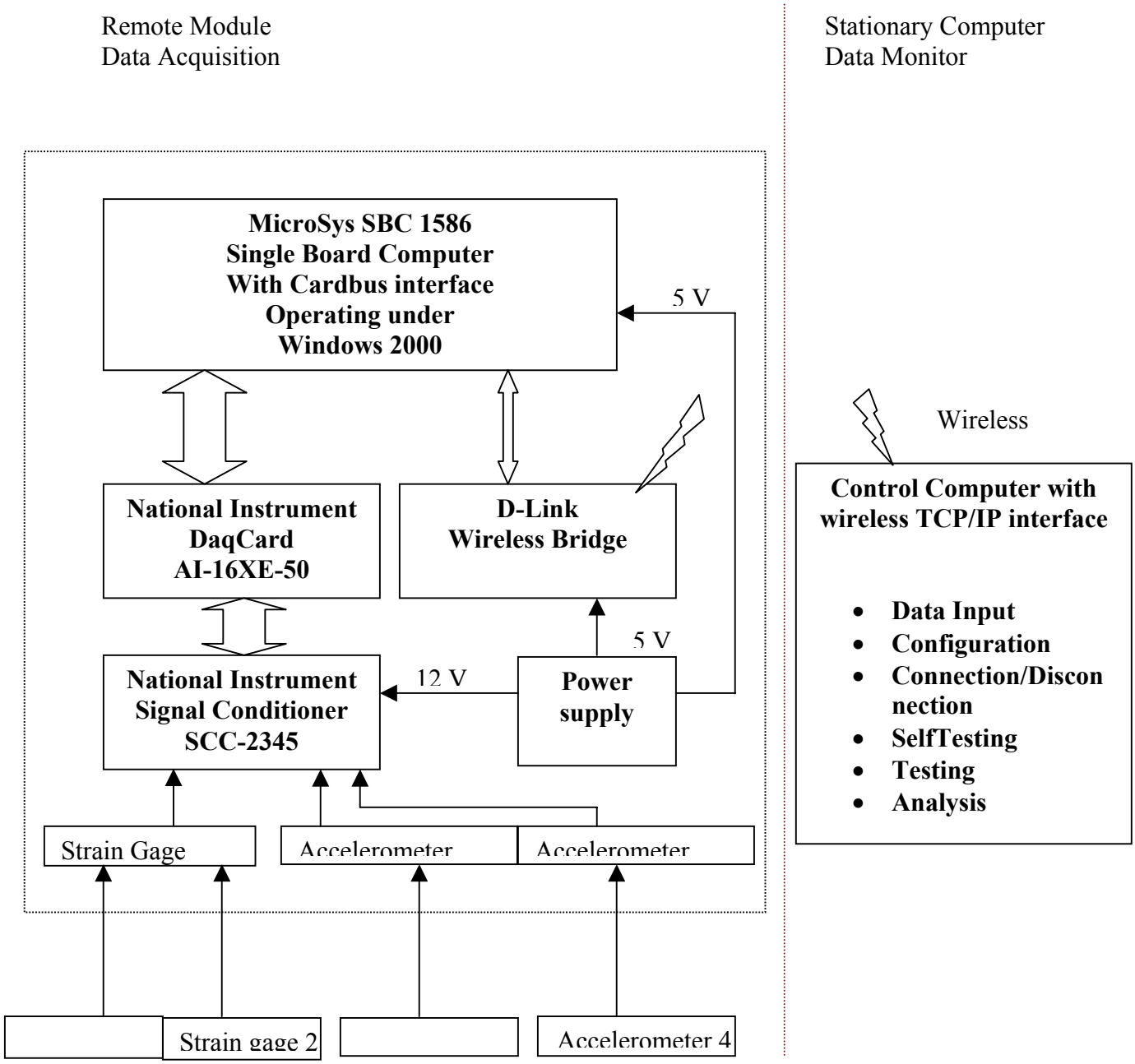

Figure 8-2 Block Diagram of Wireless Data Acquisition System

i) Hardware Function of Remote Data Acquisition Unit

SBC 1586 is a core part for the remote unit. It commands the DaqCard to obtain data and establish the network connection. The signal from sensors is first processed by the

signal conditioner to reduce noise and spike. Then it feeds into the DaqCard. DaqCard AI-16XE-50, connected to the PCMCIA interface of SBC1586, converts analog signal into digital data. Finally, the digital data is transmitted to the stationary PC through wireless bridge. The wireless network is also used to communicate with the PC to take commands from stationary PC and send the status of remote unit to stationary PC.

ii) Hardware Function of Stationary PC

The stationary PC is major platform for the data acquisition. It interacts with the user to get user's command. It also displays graphs of raw data and processed data. The wireless presentation remote is used to increase the depth value remotely during the data acquisition process.

8.3 Software

i) Software programs on Remote Data Acquisition Unit

- Microsoft Windows 2000
- Symantec pcAnywhere server version 11.0
- National Instruments Measurement & Automation application package
- NetDaq server application
- Other software tools and components: Daq controls, Winsock, compression tools etc.

ii) Software programs on Stationary PC

- Microsoft Windows XP
- Symantec pcAnywhere client (version 11.0).
- PileTest application program
- NetDaq client application
- Other software tools and components: Graph server, DAQ controls, etc.

iii) Function of software programs on Remote Data Acquisition Unit

The Windows 2000 is the foundation of the remote unit. It communicates with DaqCard through national instrument driver software. Windows also sets up the communication with network. NetDaq server communicates with NetDaq client through wireless network to receive commands and parameters from the DaqCard and send data from DaqCard to NetDaq client.

Symantec pcAnywhere is the tool for remote control of the Remote unit, including configuration and Parameters settings.

iv) Function of software programs on Stationary PC

The software for data processing on the stationary PC was called PDC and coded with Visual Basic, C language, and a real time graphic display facility. The software of PDC includes three capacity-decision methods: UA energy method, Case Method, and UA wave equation method.

a) UA Energy Method

$$R^S = -\frac{(S+\frac{1}{2}Q_s)}{2\beta(1+j_sV)} + \frac{\sqrt{(S+\frac{1}{2}Q_s)^2+4E_{in}\beta}}{2\beta(1+j_sV)} \quad (8\text{-}1)$$

where:

E_{in} = energy transferred to pile during hammer impact;

V = the maximum velocity at the pile head;

R^S = static pile capacity;

j_s = shaft damping;

Q_s = shaft quake;

S = the permanent set per hammer blow;

$\beta = \frac{L}{10EA}$ for triangular shaft resistance distribution, typical for sand;

$\beta = \frac{L}{6EA}$ for rectangular shaft resistance distribution, typical for clay;

in which L = embedded pile length; E = Young's modulus of the pile; A = cross section area of the pile.

b) Case Methods (Rausche et al. 1985)

1) Total resistance, RTL

$$RTL=[FT1+FT2]/2+[(VT1-VT2)*EA/c]/2 \quad (8\text{-}2)$$

where T1=TP+DELAY and TP is the time of the first relative maximum velocity peak and DELAY is a time required in uneven impacts or in soils capable of large deformation before achieving full resistance.

2) Damping Factor Method, RSP

$$RSP=RTL-Jc*(VT1*EA/c+FT1-RTL) \quad (8\text{-}3)$$

where J_c is case damping constant.

c) UA Wave Equation Method

UA wave equation method can be used to determine the pile capacity in the post analysis. The Kelvin model is employed to represent the soil-pile interaction. The two unknown model parameters are spring constant K, and the damping coefficient C. By matching the calculated displacement with the measured displacement at the pile head, the two unknown parameters can be determined. The identified soil-pile interaction parameters can be used in the forward calculation scheme to predict the pile shaft and toe capacities using the measured force and velocity histories.

The PDC software also includes probability analysis and Bayesian updating approach. The detailed description of the above methods and approaches can be found in the report FHWA/OH-99/008 (Liang, 1999).

8.4 System Installation and Configuration

The SBC 1586 of the remote data acquisition unit is a compact, embedded computer. The installation of Windows 2000 is much different with regular PC. Special procedures have to be followed properly to install Windows 2000. The Stationary PC communicates with the Remote wireless data acquisition unit through peer-to-peer network, and there is

no router or access point between computers. Proper configuration is necessary to establish the connection.

i) Remote Unit

a) Windows installation on SBC 1586

The SBC 1586 core is Pentium 586 processor. The Windows 2000 system can be installed on it. But it can not be directly loaded to the Compact Flash (CF) card because it considers the CF card as removable storage. So the Windows and other software components have to be installed on a hard drive first. Then, this hard drive image could be transferred to the CF card. After this transfer, the SBC 1586 becomes fully functional Windows computer system. The processes are described below:

1. Set up the SBC 1586 like regular PC by connect keyboard, mouse, monitor, hard driver, CD ROM and others.
2. Install Windows 2000 professional, NI measurement & automation, Symantec pcAnywhere on the hard drive.
3. Configure the network for the TCP/IP connection, pcAnywhere, and DaqCard driver. And test them separately.
4. Shut down the machine, insert the CF card, and restart the SBC 1586.
5. Run the image transfer utility (provide name) to transfer image of hard drive to CF card.
6. Shut down the machine, disconnect the hard drive, and restart machine. The system should run on the Windows on the CF card

Now the SBC 1586 becomes a compact fully functional system. All of the controls can be done through pcAnywhere.

b) Other software installation on SBC 1586

The NetDaq can be installed on the SBC 1586 using the following procedure:

1. Copy the NetDaq folder of the developer machine to the SBC 1586.
2. Register the Winsock, Compress, and other components (list all details).
3. Setup the NetDaq server to be run at windows startup by dragging the NetDaqServer.exe to Startup program item.

c) Network connection configuration on SBC 1586

Computer Name:	SBC1586
Work Group:	Workgroup
IP address:	192.168.0.10

d) Wireless configuration of D-Link 810+

Operating Mode:	Ad-hoc (peer to peer)
SSID:	NetDaq
Channel:	6
WEP:	Enabled
WEP Encryption:	64Bit
WEP Mode:	HEX
Key1:	0000000000

Key2: 0000000000

The above parameters can be set through Configuration utility at: http://192.168.0.30/ .

Login: Admin with blank password

e) Symantec pcAnywhere server configuration

Start Symantec pcAnywhere by click Start -> Symantec pcAnywhere to launch the Symantec pcAnywhere. At the host window, right click on the "Network,Cable,DSL" item, then property. At the property window, the parameter can be changed to receive the connection from Symantec pcAnywhere client.

f) DaqCard configuration

Click Start -> Programs -> National Instruments -> Measurement & Automation to launch the Measurement & Automation Explore. On the left panel of the Measurement & Automation Explore, expand the Device and Interface; the DaqCard AI-16XE-50 should be listed. Right click on the DaqCard Item, then go to and left click properties. The Configuring Device 1:… window should appear. From this window, the basic parameters for the DaqCard can be changed.

ii) Stationary PC

Follow the standard installation instructions to install Windows on the stationary PC (Laptop PC) if necessary.

a) Network connection configuration on Laptop PC

Computer Name: SD-Notebook1

Work Group: Workgroup

IP address: 192.168.0.110

b) Wireless configuration

Operating Mode: Ad-hoc (Computer to computer)

SSID: NetDaq

Channel: 6

WEP: Enabled

WEP Encryption: 64Bit

WEP Mode: HEX

Key1: 0000000000

Key2: 0000000000

Configuration Parameter: http://192.168.0.30/ Login: Admin with blank password

c) Symantec pcAnywhere client configuration

Start Symantec pcAnywhere by click Start -> Symantec pcAnywhere to launch the Symantec pcAnywhere. At the Remotes window, right click on blank space, then new to create new TCP/IP connection. Rename it properly, and right click on this new item, then click on properties to start the connection configuration screen. To connect with the remote unit, the IP address of remote unit has to be used. The login name and password have to be matched with the one assigned on the server or host of pcAnywhere.

8.5 NetDaq Client/Server Architecture

The NetDaq client and server are the same as typical client/server application. The server runs on server machines to serve the request from client. The client makes request to server to get data.

When the server started, it starts listening to the network for connection. If it gets connected to client, it changes itself to stand by mode waiting for command. During this process, a timer is used to periodically check the status of connection. If it finds the client disconnected, it automatically changes to listening mode, waiting another client to connect.

i) Server

When the server started, it tries to listen to the connections from client. If it detects the client is connecting, it will respond and establish connection. Now the client can send requests to ask server to do the tasks. After client finishes the job, it will disconnect from the network. Then the server will detect this action and change to the "listen" status waiting for another client to make call.

Functions of server application components:

FrmNetDAQServer: It holds the CWAI, WinSock, and Timer controls. Through Winsock control, the server application communicates with client

application to get and send commands and data. CWAI control is used to configure DaqCard and acquire data from DaqCard.

ModMain: Having the basic functions for server application.

ClsDaqCard: Processing commands for DaqCard from client

ModZip: It will compress the data before sending to network for large amount of data.

ii) Client

When client needs to request some information from server, it will start by connecting with server. If a connection is made successfully, it can send command to server to request data or other action.

Function of client application components:

UcNetDAQ: User control which holds Winsock and Timer control communicates with server application.

ModMain: Having the basic functions for client application.

ClsDB: It processes server's data and saves it to MS Access database for further process.

ModZip: It will compress the data before sending to network for large amount of data.

iii) Command Format

The client and server communicate with each other in the predefined command protocol. The format of these commands is pipe delimited string commands with

parameters, such as Data|…, Command|Start, ScanClock|Period|5. The first string before the first pipe is the top level command, the second string between first pipe and second pipe is second level command, and so on. After commands for each level, it should follow by the parameters, each separated by pipe, if the parameters are required. Taking the ScanClock|Period|5 as example, the "ScanClock" is the top level command; the "Period" is the second level command, and the "5" is the parameter. In this case, it only requires one parameter.

Table 8-1 List of commands from Client

Top level command	Second level command	Parameter 1 (example)	Parameter 2 (example)	***Note***
Command	Start			Command to DaqCard
	Configure			
	Reset			
	Stop			
	NScans			
	Device			
Channel	RemoveAll			DaqCard channel setup
	Add			
	ChannelString	"0,1,2,8"		
	Coupling	1		
	Gain	0		
	LowerLimit	2		
	Polarity	1		
	Range	0		
	InputMode	1		
	ScaleMultiplier	2		
	ScaleOffset	1		
	UpperLimit	10		
ScanClock	ActualFrequency			DaqCard scan parameters
	ActualPeriod			
	ActualTimebaseDivisor			

	ClockSourceSignal			
	ClockSourceType			
	Frequency			
	InternalClockMode			
	Period			
	TimebaseDivisor			
	TimebaseSignal			
	TimebaseSource			
StartCondition	ActualHysteresis			DaqCard start condition
	ActualLevel			
	Hysteresis			
	Level			
	Mode			
	PreTriggerScans			
	SkipCount			
	Source			
	Type			
StopCondition	ActualHysteresis			DaqCard stop condition
	ActualLevel			
	Level			
	Mode			
	PreTriggerScans			
	SkipCount			
	Source			
	Type			
DataFormat				Format of returned data
DataFilter				Data space
Close Connection				Close network connection
Battery		1 or 2		Get the battery voltages for 5 or 12 volts supplies
ResetTrigger				Reset trigger level

Table 8-2 List of commands from Server:

Top level command	Parameter 1 (example)	Parameter 2 (example)	***Note***
DATA	1.0|2.3|3|…		Acquired data from DaqCard
MSG	Connected		Server message
ERROR	Divided by 0		Server error message
Battery	1.2		Battery volts

8.6 Trouble Shooting

i) Remote Unit

1. Make sure that the batteries are fully charged. It takes about 15 hours to have the batteries fully changed, therefore, it has to be done early.
2. Install the remote unit and attach the remote unit to its holder.
3. Turn on the switch on the remote unit. The power indicator should light up.
4. After finished, turn off the system by switching it to “off”.

The NetDaq server should be running on the remote unit silently. The user interface of the server is basically for tracking the error and checking the status of the application. Fig. 8-3 shows the user interface of the server.

Inside the window, just below the blue title area, the top line displays the network information of local unit: name, IP address, and port.

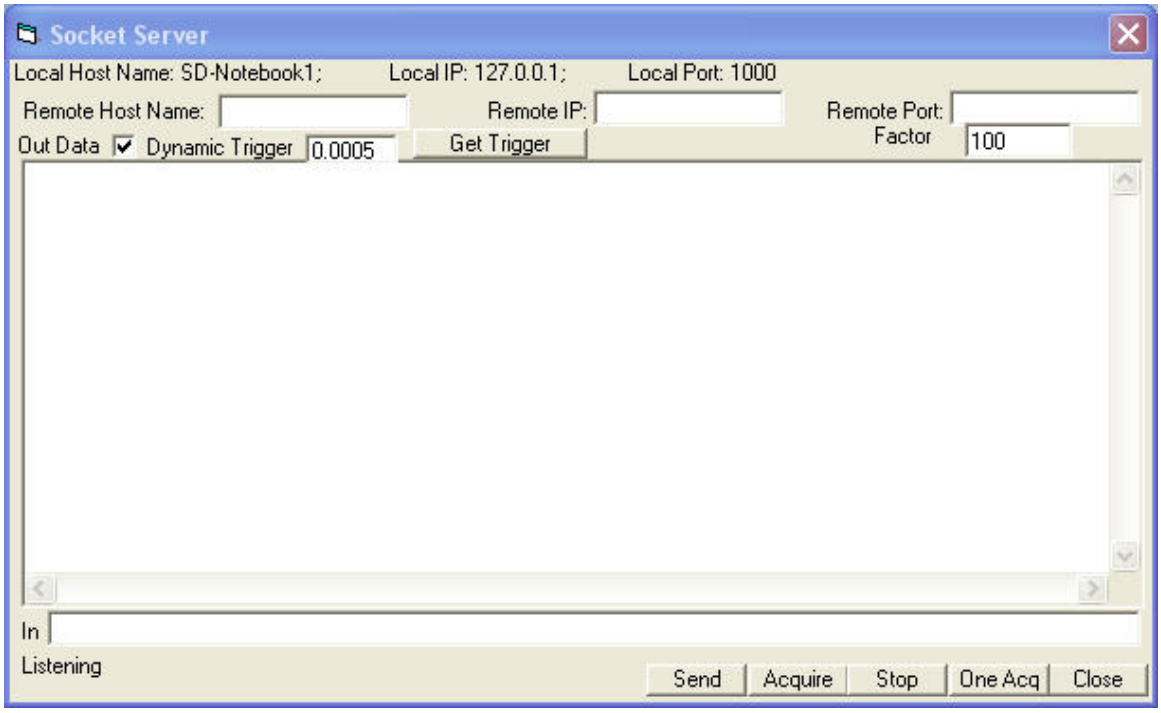

Figure 8-3 User interface of the server

The second line displays the information about remote machine if it is connected. The third line displays trigger information of sensors. The main text box below holds all of the text sent out to the client PC (Stationary PC). It is refreshed every time when the server sends something to client. The little text below, captioned with "In" is used to display the information receive from Stationary PC. Below the "In" box, on the left side, is the area to show the network connection status, e.g., closed, connected, listening. On the right side, below the "in" box, there are several buttons.

"Send"-- will send whatever in the main text box to client.

"Acquire" -- will start data acquisition on the DaqCard continually

"Stop" -- to stop the data acquisition process started by 'Acquire"

"One Acq" -- will run the data acquisition one time only.

"Close" -- exit the server application.

ii) Stationary PC

Start up:

1. Turn on the PC and login
2. Click the PileTest icon on the desktop to start data acquisition.
3. After data acquisition, shut down the remote unit first, then shut down the stationary PC.

Check network:

1. On the laptop PC, click start -> Run…
2. At the open box of the run window, type ping <IP address>, then ok.

   Example: ping 192.168.0.10
3. A DOS window will show up with the results. If the network connection is established, one can see the message on this DOS window.
4. If the network connection can not be established, please refer to the troubleshooting part to correct the problem.

Remote control of remote unit by pcAnywhere:

1. Start up the Symantec pcAnywhere by click its icon on the desktop, or click Start -> programs -> Symantec pcAnywhere. The pcAnywhere window will be displayed.

2. On the left side, there is pcAnywhere manager panel. If the item “remotes” is not highlight, click on it to highlight. Now the right panel should have caption “remotes” with different remote location items.
3. Double click the item “SBC 1586” to start connecting to remote unit.
4. After a while, the pcAnywhere connecting window will appear. Then the Symantec pcAnywhere Remote windows will display the desktop windows of remote unit.
5. Check and configure remote unit as necessary.
6. Close the pcAnywhere client application by click the x on the top right corner or exit on the file submenu.

Description of the user interfaces of NetDaq Client:

The NetDaq client is component referred by PileTest application on stationary PC. The user interface of the NetDaq client sits behind the regular PileTest window. On both selftest and Test window, there is check box on the left side of big command button like Start (see Fig. 4). When the check box is checked, the user interface of NetDaq client will show up in the place where the parameters are shown before.

Figure 8-4 Control of user interface of NetDaq client

The items on the part of UI are shown in Fig. 8-5. The top two rows are the network information of local and remote computers. The two “out” and “in” text boxes are used to display the message send to server (out) and come from server (in). The two buttons “Connect” and “Disconnect” are used to connect and disconnect to server. If the “Save Data” check box is checked, the data from server will be saved to the MS Access database in the application’s database folder of NetDaq client. Periodically, the NetDaq client will send command to server to retrieve battery voltage. If the battery voltage drop to certain voltage, the speaker will sound a beep to warn user that the battery is running low. This period is defined by the text box right after the in text message box(in minute). The “Reset Trigger” button will force the NetDaq server to acquire the current value of the trigger channel so the new trigger value can be obtained.

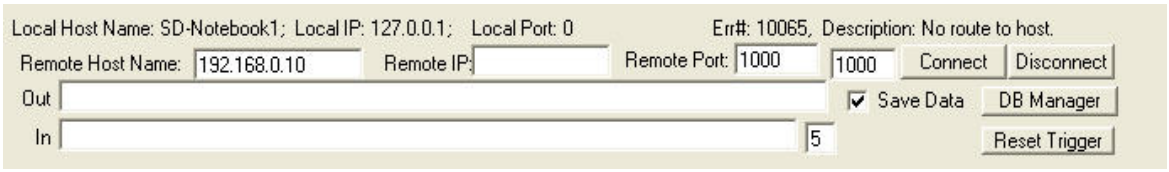

Figure 8-5 User interface of NetDaq client

8.7 Other errors

Sometime, the stationary PC can not connect to the remote unit. There are several items that could cause this problem.

First use ping to check the connection and to see whether the user can not ping to the remote unit (192.168.0.10). If it works the problem should be in the NetDAQ server. Use the pcAnywhere to connect to the remote unit to check the server is running or not.

If you cannot ping to the (192.168.0.10), try to ping the wireless adapter at (192.168.0.30). If it works, the remote SBC1586 may not start yet. Wait for 3-5 minutes to retry. If it cannot ping to the (192.168.0.30), the wireless network cannot communicate with each other. Try to start Internet Explore and go to the wireless configuration site at 192.168.0.30. If it still does not work, the setup parameter on the wireless box must be wrong. Then, open the remote unit box; unplug the network cable and plug the one from your local computer; use the Internet Explorer and go to the 192.168.0.30; go to the wireless tab to reconfigure the wireless connection; restart the remote unit.

8.8 Laboratory Testing of the System

Laboratory testing of the whole system has been performed. The results are positive.

The two strain gauges and two accelerometers are mounted on an iron tube with a diameter of 1 inch and 5 foot long. A cap to avoid the damage of the tube and to distribute the force of the hammer protects both ends of the tube.

The two strain gauges are mounted on the opposite sides of the tube, about 10 inches below the top of the tube. The two accelerometers are installed about the same height, but perpendicular to the two strain gauges. See Fig. 8-6 for the details.

Figure 8-6 Installation of strain gages and accelerometers

One problem we find during lab test is trigger level. The system was designed to use one of the strain gauge signals as trigger signal. Every time there is force applied on the strain gauge, the signal of the strain gauge will increase. At certain predefined level, the

data acquisition card will be triggered to start collecting data. These data plus the data collected by pre-trig will be constructed as a whole trace of the data points.

When the system was in test, initially certain predetermined trigger level had been used. This trigger level is just above the level when the strain gages are in a total released state. After the strain gauge is mounted, every hammer hit will create stress on the strain gauge. This stress will take much longer time to release because the strain gauge is bounded onto the pole. This time interval is usually much longer than that of a hammer hit. Therefore, the signal level of strain gauge, when the second hammer hit, will be different because of this stress. It reflects that signal level some time is high and some time is low. This will lead to the system sometime not responding to the hammer hit after first hammer hit and data is lost.

To solve the problem, a dynamic trig level mechanism is introduced. For every hammer hit, the last certain data points are collected and averaged to form the base signal of the trigger level for next hammer hit. This signal level of last hammer hit adds a small increment will be the trigger level for the next hammer hit. This will guarantee that the signal of next hammer hit will be acquired at appropriate time. All of this mechanism now has been built into the application program of a remote unit.

Another problem we found during lab test is data transmission speed from remote unit to the base computer. Initially the system is using the sequential method mechanism and data compression for the data transmission from remote unit to base computer

wirelessly. This will give about 4 seconds for the system to acquire data, to transfer data to base computer, and to display and to store data in the base computer. This speed is too slow in practice because the hammer should hit the pole about 1~2 second interval. After checking the software carefully, it turns out that the bottleneck is at the remote unit. Because the remote unit is the embedded computer, the CPU has much lower speed than the regular desktop or laptop computer. The data compression process will take about 1 second to be finished. Data compression truly gives much faster data transmission speed wirelessly. Since the data transmission speed on the wireless network is very fast (11 Mb per second), it really does not have to compress the data. After the data compression on the remote unit is taken out, the system response time was reduced less than one second. Now most of time used in the system is to display the data points on the base computer. It takes about 0.5 second to show the trace. This also can be solved by multiple threading and/or show the traces selectively (show one trace for two or three data acquisition).

The detailed operation instruction on the program of Pile Driving Controller in the stationary PC can be found in the section VI.3 of the report FHWA/OH-99/008 (Liang, 1999).

8.9 Conclusions

Evolving from the operating risk encountered in the current dynamic testing technology, a set of new wireless dynamic testing equipment has been successfully developed. This new technology utilizes remote data acquisition and management unit to build the wireless connection between the sensors and the monitoring PC. The new

measurement technology is also provided with a user-friendly operational software package, supplemented with a computer graphical interface that allows continuous monitoring and detection during pile driving or testing. The laboratory testing has been performed to validate the applicability of hardware and software of the wireless dynamic pile testing equipment and to verify the accuracy of signal recordings by comparing the laboratory testing results from the developed wireless equipment with those from the PDA testing equipment. The new wireless dynamic testing equipment is anticipated to be successfully applied in the field testing that will advance pile driving control and monitoring to a more secure environment.

CHAPTER IX

SUMMARIES AND CONCLUSIONS

9.1 Summaries and Conclusions

Driven piles, as an important type of deep foundations, have been commonly used for the buildings, bridges, towers, and dams. In AASHTO, the design of driven piles has been moving from the traditional ASD method to the more formal and rational LRFD method. The reliability analyses in LRFD allow the evaluation of the relative contributions of uncertainties of load and resistance components to the design of driven piles in the framework of probability theory. The application of reliability analyses has dramatically motivated the evolution and the improvement on the design and quality control of driven piles. However, the reliability analyses on driven piles needs to be further developed in order to make the LRFD method more understandable and applicable by designers. Towards the objective of improving the design and quality control of driven piles, a series of research works on the reliability-based analyses have been carried out in this research.

In Chapter III, based on the acceptance-sampling analysis, the reliability-based quality control criteria on driven piles were developed for both static and dynamic test methods. The lognormal distribution function was used to characterize the statistical

characteristics of the methods. The relationship between the number of load tests and the criterion on acceptance of the measured capacity was elucidated. It was shown that the measured capacity required to assure adequate quality control decreases with an increase in the number of load tests performed. Either the number of load tests or the target measured capacity or both needs to be increased in order to obtain a higher target reliability index. An optimum approach was developed for the selection of the number of load tests and the required measured capacities for quality control using various types of load test methods of driven piles.

In Chapter IV, a statistical database was compiled to describe the increase of axial pile capacity with time, known as set-up, when piles were driven into clay. Based on the collected pile testing data, pile set-up is significant and continues to develop for a long time after pile installation. The statistical parameters for set-up effect combined with the previously documented statistics of the loads and the resistances were systematically accounted for in the framework of reliability-based analysis using First Order Reliability Method (FORM). Separate resistance factors in Load and Resistance Factor Design (LRFD) were obtained to account for different degrees of uncertainties associated with the measured short-term capacity and the predicted set-up capacity at various reliability levels. The design procedure to incorporate the set-up into the LRFD of driven piles in clay was proposed. The incorporation of set-up effect in LRFD could improve the prediction of design capacity of driven piles. Thus, pile length or numbers of pile could be reduced and economical design of driven piles could be achieved.

In Chapter V, a statistical database was developed to describe the set-up when piles driven into sand. Based on the compiled database of driven piles in sand, the various prediction methods for the development of the set-up of driven piles in sand were evaluated. The same reliability-based analysis approach as proposed for driven piles in clay was employed to develop the separate resistance factors for the measured short-term capacity and the predicted set-up capacity for driven piles in sand. The design procedure was also proposed for incorporating the set-up into LRFD of driven piles in sand.

In Chapter VI, a mathematic algorithm based on Bayesian theory was developed to allow for updating the resistance factors for the driven piles when static analysis methods are combined with dynamic pile testing in a given project site. The results of dynamic pile tests could be incorporated to minimize the uncertainties of static design methods by updating the resistance factors in LRFD. The main benefit of combining the two methods was the added confidence and accuracy on the predicted pile capacity, thus allowing for the adoption of a more reasonable resistance factor as opposed to the case in which only one analysis method is used for design. The example analyses have demonstrated that the combination of two methods would make the predictions of driven pile capacity more consistent with the static load test results.

In Chapter VII, a new one-dimensional wave equation based algorithm for estimation of shaft and toe resistance of driven piles using High Strain Testing (HST) data was presented. The pile was represented by a uniform elastic bar, while the soil around the

pile was assumed as a homogenized isotropic medium, and Smith model was adopted to represent soil-pile interaction in the wave equation analysis. The static shaft resistance was reasonably assumed to be totally mobilized during pile driving. Smith damping factor was used to account for the combined dynamic and rate effect. Force and velocity time histories measured at the pile head were used as input boundary conditions in an analytical solution of the one-dimensional wave equation. Two unknown parameters, static shaft resistance and Smith damping factor, were incorporated into the one-dimensional wave equation and determined analytically for the time duration prior to the first downward wave reaching the pile toe. Once these two shaft parameters are determined, the soil resistance and Smith damping factor at pile toe can be determined. Numerical examples were presented to demonstrate the validity of the proposed method on the determination of the static resistances.

In Chapter VIII, a set of new wireless dynamic testing device for dynamic pile testing was successfully developed. This new technology utilizes remote data acquisition and management unit to build the wireless connection between the sensors and the monitoring PC. The laboratory testing has been performed to validate the applicability of hardware and software of the wireless dynamic pile testing equipment. The application of this new technology to dynamic pile testing should significantly improve the operating safety and advance pile driving control and monitoring to a more secure environment.

9.2 Recommendations for Implementations

Three new methodologies and one new product have been developed through the efforts of this research and they are recommended for adoption by Ohio DOT.

1) New Wireless Dynamic Pile Testing Equipment

The newly developed wireless dynamic pile testing equipment incorporates the innovative application of wireless communication technology that is outlined in detail in Chapter VIII. The application of this new technology to dynamic pile testing should significantly improve the operating safety. The elimination of the need for long cables should also help speed up the testing process. It is recommended that ODOT adopt and promote the new wireless dynamic pile testing equipment in the field.

2) New Quality Control Method on Driven Piles

The developed quality control method systematically account for the statistical characteristics of various pile testing method. In the framework of reliability-based analysis with consideration of finite population, the number of testing piles and the required measured capacity are derived for a target reliability index. The recommended quality control criteria can be adopted by ODOT in Bridge Design Manual.

3) Incorporating Set-up into Design of Driven Piles

The separate resistance factors for the measured CAPWAP capacity and the predicted set-up capacity have been developed based on the reliability-based FORM in Chapters IV and V for driven piles in sand and in clay, respectively. The step-by-step procedure has

been recommended for the incorporation of the set-up into LRFD of driven pile. The incorporation of the set-up into design of driven piles will generally reduce the required pile length or number of piles. The recommended resistance factor, along with the set-up prediction method, can be incorporated in ODOT Bridge Design Manual.

4) Bayesian Based Formalism for Updating LRFD Resistance Factors for Driven Piles

The Bayesian based formalism to combine dynamic testing and static calculation results for LRFD of driven piles has been developed. The current design practices of driven piles treat the static calculation and dynamic testing independently, resulting in a large variability in the estimated pile capacities. The combination of various design methods could improve accuracy and confidence level on predicting pile capacity as opposed to the case of using only one design method. Furthermore, the uncertainties on the estimation of pile capacity can be effectively reduced so that shorter pile length or less pile number can be used.

9.3 Recommendations for Future Research

Areas for future studies are identified in the following:

1) LRFD Resistance Factor Calibration for Deep Foundations in Ohio

In 2006, ODOT will supersede the traditional ASD with the new LRFD. The resistance factors for deep foundations recommended by AASHTO are calibrated based on the compiled database with a wide range of soil conditions, soil testing techniques, analysis and design procedures, foundation types, and foundation construction procedures.

Therefore, there is a need for ODOT to establish the resistance factors which are appropriate for Ohio soil conditions and ODOT foundation practice.

In order to calibrate the resistance factors for ODOT practice, comprehensive databases for driven piles and drilled shafts should be respectively compiled based on the testing data in Ohio. The pile or shaft testing data should be categorized based on soil conditions, pile driving time, pile or shaft sizes, and pile or shaft types. The restrike testing should be separately performed for the driven piles at 1 day after EOD and longer time after EOD so that the development of set-up can be evaluated for the Ohio soil conditions.

Based on the compiled databases, the recommended quality control method can be validated for the ODOT foundation practice. The separate resistance factors for the measured CAPWAP capacity and predicted set-up capacity can be further calibrated for the appropriate application in Ohio. With the availability of more driven pile data on static analysis results, dynamic testing results, and static load test results, the Bayesian-based formalism can be further improved and validated.

2) Validation and Implementation of Wireless Dynamic Pile Testing Equipment

The newly developed wireless dynamic pile testing equipment utilizes wireless data communication technology to eliminate the need for hanging cables from the sensor locations to the data acquisition unit. As a result, dynamic pile testing can be conducted more efficiently in safer environment. The new measurement device also provides a user-

friendly operational software package, supplemented with a computer graphical interface, that allows continuous monitoring and detection during pile driving. Due to its safety and cost-saving features, the new equipment is particularly suited for ODOT implementation. This new wireless dynamic pile testing equipment was developed based on the laboratory testing and calibration; therefore there is a need to validate the applicability of the new technology for field applications.

3) Reliability-Based Analysis of the Effect of Pile Group on Calibration of Resistance Factors in LRFD of Drive Piles

It is generally accepted that a pile group system can be more robust than a single pile due to a combination of three key factors: a) redundancy (indeterminacy, extra load carrying paths); b) ductility (ability to tolerate and absorb large inelastic deformations and shift excess loadings to other piles); and c) excess capacity (piles all driven to the same penetration as the maximum loaded pile, thus having the ability to carry overloads and displacements). Without the recognition of robustness of a pile group system, the economical design of driven piles may not be realized.

In AASHTO code, a target reliability β of 2.3 was used for the calibrations of resistance factors of deep foundation elements, taking into account that piles are almost always driven in groups, resulting in additional redundancy in the foundation. However, the pile group effect on the calibrated resistance factors is dependent on the design methods and types of structures. A single target reliability β of 2.3 set for all structures

and prediction methods would be too generic. Therefore, there is a need to exam more thoroughly the resistance factors or various prediction methods of driven piles in a pile group.

REFERENCES

1. AASHTO, (1997). Standard Specifications for Highway Bridges: 16th Edition (1996 with 1997 interims). AASHTO, Washington, DC.

2. AASHTO, (2003). LRFD Bridge Design Specifications. Second Edition, 1998 with 2003 interim. AASHTO, Washington, DC.

3. AASHTO (2006). LRFD Bridge Design Specifications Section 10: Foundations. Interim, AASHTO, Washington, DC.

4. Allen, T. M., Nowak, A. S., and Bathurst, R.J. (2005). "Calibration to Determine Load and Resistance Factors for Geotechnical and Structural Design." Transportation Research Circular. No. E-C079.

5. Ang, A. H-S. and Tang, W. H. (1975). Probability Concepts in Engineering Planning and Design. Vol. 1, Basic Principles. John Wiley & Sons, New York.

6. Ang, A. H-S., and Tang, W. H. (1984). Probability Concepts in Engineering Planning and Design. Volume II. John Wiley & Sons, New York.

7. Astedt, B., Weiner, L., and Holm, G. (1992). “Increase in Bearing Capacity with Time of Friction Piles in Sand.” Proceedings of Nordic Geotechnical Meeting, pp. 411-416.

8. Attwooll, W. J., Holloway, D. M., Rollins, K. M., Esrig, M. I., Sakhai, S., and Hemenway, D. (1999). “Measured Pile Set-up during Load Testing and Production Piling – I-15 Corridor Reconstruction Project in Salt Lake City, Utah.” Transportation Research Record 1663, Paper No. 99-1140, pp. 1-7.

9. Axelsson, G. (1998). “Long-Term Set-Up of Driven Piles in Non-Cohesive Soils Evaluated from Dynamic Tests on Penetration Rods.” Proceedings of the First International Conference on Site Characterization, Vol. 2, pp. 895-900.

10. Axelsson G. (2002). “A Conceptual of Pile Set-up for Driven Piles in Non-cohesive Soils.” Conference Proceedings, Deep Foundations 2002, ASCE GSP No. 116, pp. 64-79.

11. Ayyub, B. M., and McCuen, R. H. (2003). Probability, Statistics, and Reliability for Engineers and Scientists. Second Edition, Published by Chapman & Hall, ISBN 1-58488-286-7.

12. Barker, R. M., Duncan, J. M., Jojiani, K. B., Ooi, P. S. K., Tan, C. K., and Kim, S. G. (1991). "Manuals for the Design of Bridge Foundations." NCHRP Report 343, Transportation Research Board, National Research Council, Washington, DC.

13. Bjerrum, L., Hansen, and Sevaldson (1958). "Geotechnical Investigations for A Quay Structure in Ilorton." Norwegian Geotech. Publ. No. 28, Oslo.

14. Bogard, J. D., and Matlock, H. (1990). "Application of Model Pile Tests to Axial Pile Design." Proceedings, 22nd Annual Offshore Technology Conference, Houston, Texas, Vol. 3, pp. 271-278.

15. Bullock, P. J. (1999). Pile Friction Freeze: A Field and Laboratory Study, Volume 1, Ph.D. Dissertation, University of Florida, USA.

16. Bullock, P. J., Schmertmann, J. H., McVay, M. C., and Townsend, F. C. (2005a). "Side Shear Setup. I: Test Piles Driven in Florida." Journal of Geotechnical and Geoenvironmental Engineering, ASCE, Vol. 131, No. 3, pp. 292-300.

17. Bullock, P. J., Schmertmann, J. H., McVay, M. C., and Townsend, F. C. (2005b). "Side Shear Setup. II: Results from Florida Test Piles." Journal of Geotechnical and Geoenvironmental Engineering, ASCE, Vol. 131, No. 3, pp. 301-310.

18. Camp, W. M., and Parmar, H.S. (1999). “Characterization of Pile Capacity with Time in the Cooper Marl – Study of Application of A Past Approach to Predict Long-Tern Pile Capacity.” Journal of the Transportation Research Board, No. 1663, Washington, DC, pp. 16-24.

19. Chow, F. C. (1997). Investigations into Displacement Pile Behaviour for Offshore Foundations. Ph.D Thesis, University of London (Imperial College).

20. Chow, F. C., Jardine, R. J., Brucy, F., and Nauroy, J. F. (1998). “Effects of Time on Capacity of Pipe Piles in Dense Marine Sand.” Journal of Geotechnical and Geoenvironmental Engineering, Vol. 124, No. 3, ASCE, pp. 254-264.

21. Christian, J. T. (2004), “Geotechnical Engineering Reliability: How Well Do We Know What We Are Doing?” Journal of Geotechnical and Geoenvironmental Engineering, ASCE, Vol. 130, No. 10, pp. 985-1003.

22. Davisson, M. T. (1972). “High Capacity Piles.” Proceedings of Lecture Series on Innovations in Foundation Construction, ASCE, Illinois Section, Chicago, pp. 81-112.

23. DeBeer, E. E. (1968). “Proefondervindlijke bijdrage tot de studie van het grensdraag vermogen van zand onder funderingen op staal.” Tijdshift der Openbar Verken van Belgie, No. 6, 1967 and No. 4, 5, and 6, 1968.

24. Decourt, L. (1999) "Behavior of Foundations under Working Load Conditions." Proceedings of the 11th Pan-American Conference on Soil Mechanics and Geotechnical Engineering, Foz DoIguassu, Brazil, Vol. 4, pp. 453-488.

25. Esrig, M. I., and Kirby, R. C. (1979). "Soil Capacity for Supporting Deep Foundation Members in Clay." ASTM STP. No. 670, pp. 27-63.

26. Evangelista, A., Pellegrino, A., and Viggiani, C. (1977). "Variability among Piles of the Same Foundation." Proc. 9th ICSMFE, Tokyo, pp. 493-500.

27. Finno, R. J., Achille, J., Chen, H. Cosmao, T., Park, J. B., Picard, J., Smith, D. L., and Williams, G. P. (1989). "Summary of Pile Capacity Predictions and Comparison with Observed Behavior." Predicted and Observed Axial Behavior of Piles, Geotechnical Special Publication, No. 23, ASCE, pp. 356-385.

28. Gates, M. (1957). "Empirical Formula for Predicting Pile Bearing Capacity." Civil Engineering, Vol. 27, No. 3, pp. 65-66.

29. Goble Rausche Likins and Associates, Inc. (1996). CAPWAP Introduction to Dynamic Pile Testing Methods, Cleveland, OH, USA.

30. Hannigan, P.J., Goble, G. G., Thendean, G., Likins, G. E., and Rausche, F. (1998). Design and Construction of Driven Pile Foundations, Workshop Manual. Vol. 2, Publication No. FHWA-HI-97-014, Federal Highway Administration, Washington, DC.

31. Hansen, J. B. (1963). "Discussion on Hyperbolic Stress-Strain Response. Cohesive Soils." Journal for Soil Mechanics and Foundation Engineering, ASCE, Vol. 89, SM4, pp. 241-242.

32. Hirsch, T. J., Carr, L., and Lowery, L. L. (1976). Pile Driving Analysis—Wave Equation Users Manual, Vol. 1: Background, Texas Transportation Institute, College Station, Texas A&M, USA.

33. Holloway, D. M., and Beddard, D. L. (1995). 'Dynamic Testing Results, Indicator Pile Test Program – I-880, Oakland, California." Deep Foundations Institute 20th Annual Members Conference and meeting, pp. 105-126.

34. Huang, S. (1988). "Application of Dynamic Measurement on Long H-Pile Driven into Soft Ground in Shanghai." In Proceedings of 3rd International Conference on the Application of Stress-Wave Theory to Piles, Bi-Tech Publishers, Ottawa, Ontario, Canada, pp. 635-643.

35. Komurka, V. E., Wanger, A. B., and Tuncer, B. E. (2003). "Estimating Soil/Pile Set-up." Final Report, Wisconsin Highway Research Program #0092-0014, Prepared for The Wisconsin Department of Transportation.

36. Komurka, V. E., Winter, C. J., and Maxwell, S. (2005). "Applying Separate Safety Factors to End-of-Drive and Set-up Components of Driven Pile Capacity."

Proceedings of the 13th Great Lakes Geotechnical and Geoenvironmental Conference, Milwaukee, Wisconsin, USA, pp. 65-80.

37. Kulhawy, F. H., and Phoon, K. K. (1996). "Engineering Judgment in the Evolution from Deterministic to Reliability-Based Foundation Design." Uncertainty in the Geologic Environment; from Theory to Practice; Proceedings of Uncertainty '96, C. D. Shackelford, P. P. Nelson, and M. J. S. Roth eds., Madison, WI, July 31-Augest 3, ASCE, New York, pp. 29-48.

38. Lacasse, S., Guttormsen, T. R., and Goulois, A. (1989). "Bayesian Updating of Axial Capacity of Single Pile." Proc., 5th International Conference on Structural Safety and Reliability, ASCE, New York, pp. 287-290.

39. Lai, P., and Kuo, C. L. (1994). "Validity of Predicting Pile Capacity by Pile Driving Analyzer." Proceedings of International Conference on Design and Construction of Deep Foundations, Florida, USA, Dec., 1095-1102.

40. Liang, R. Y. (1999). "Development and Implementation of New Driven Pile Technology." Report FHWA/OH-99/008, Ohio Department of Transportation.

41. Liang, R. (2003). "New Wave Equation Technique for High Strain Impact Testing of Driven Piles," Geotechnical Testing Journal, ASTM, Vol. 26, No. 1, pp. 1-7.

42. Liang, R. and Husein, A. I. (1993). "Simplified Dynamic Method for Pile-Driving Control." Journal of Geotechnical Engineering, ASCE, Vol. 119, No. 4, pp. 694-713.

43. Liang, R. and Zhou, J. (1996). "Pile Capacity Estimation Using New HST Interpretation Method," In Proceedings of 5rd International Conference on the Application of Stress-Wave Theory to Piles, Orlando, Florida, USA, pp. 367-381.

44. Liang, R. and Zhou, J. (1997). "Probability Method Applied to Dynamic Pile-Driving Control." Journal of Geotechnical and Geoenvironmental Engineering, ASCE, Vol. 123, No. 2, pp. 137-144.

45. Long, J. H., Kerrigan, J. A., and Wysockey, M. H. (1999). "Measured Time Effects for Axial Capacity of Driven Piles." Journal of the Transportation Research Board, No. 1663, Washington, DC, pp. 8-15.

46. McVay, M. C., Alvarez, V., Zhang, L., Perez, A., and Gibsen, A. (2002). "Estimating Driven Pile Capacities during Construction." Research Report WPI 0510852, Florida Department of Transportation.

47. McVay, M. C., Biergisson, B., Zhang, L. M., Perez, A., and Putcha, S. (2000). "Load and Resistance Factor Design (LRFD) for Driven Piles Using Dynamic Methods-A Florida Perspective." Geotechnical Testing Journal, ASTM, 23 (1), pp. 55-66.

48. McVay, M. C., Schmertmann, J., Townsend, F., and Bullock, P. J. (1999). "Pile Friction Freeze: A Field and Laboratory Study." Research Report WPI 0510632, Florida Department of Transportation.

49. Meyerhof, G. (1976). "Bearing Capacity and Settlement of Pile Foundations." Journal of the Geotechnical Engineering Division, ASCE, Vol. 102, No. 3, pp.195-228.

50. Nordlund, R. L. (1963). "Bearing Capacity of Piles in Cohesionless Soils." Journal of Soil Mechanics and Foundation Engineering, JSMFE, Vol. 89, SM 3, pp. 1-36.

51. Nottingham, L., and Schmertmann, J. (1975). "An Investigation of Pile Capacity Design Procedures." Final Report D629 to Florida Department of Transportation, Department of Civil Engineering, University of Florida.

52. Nowak, A. (1999). "Calibration of LRFD Bridge Design Code." National Cooperative Highway Research Program Report 368, Transportation Research Board, National Research Council, Washington, D.C.

53. Paikowsky, S. G., Birgisson, B., McVay, M., Nguyen, T., Kuo, C., Beacher, G., Ayyub, B., Stenersen, K., O'Malley, K., Chernauskas, L., and O'Neill, M. (2004). "Load and Resistance Factor Design (LRFD) for Deep Foundations." NCHRP Report 507. Transportation Research Board, Washington, D. C.

54. Paikowsky, S. G., Regan, J. E., and MaDonnell, J. J. (1994). "A Simplified Field Method for Capacity Evaluation of Driven Piles." Publication FHWA-RD-94-042, U.S. Department of Transportation and Federal Highway Administration.

55. Paikowsky, S. G., and Stenerson K. (2000). "The Performance of the Dynamic Methods, Their Controlling Parameters and Deep Foundation Specifications." Keynote Lecture in the Proceeding of the Sixth International Conference on the Application of Stress-Wave Theory to Piles, Niyama S. and Beim J. edt., September 11-13, Sao Paulo, Brazil, Balkema, pp.281-304.

56. Parsons, J. D. (1966). "Piling Difficulties in the New York Area." Journal of the Soil Mechanics and Foundations Division, ASCE, Vol. 92, No. 1, pp. 43-64.

57. Pestana, J. M., Hunt, C. E., and Bray, J. D. (2002). "Soil Deformation and Excess Pore Pressure Field around A Closed-Ended Pile." Journal of Geotechnical and Geoenvironmental Engineering, ASCE, Vol. 128, No. 1, pp. 1-12.

58. Phoon, K. K., and Kulhawy, F. H. (1996). "On Qualifying Inherent Soil Variability." Uncertainty in the Geologic Environment; from Theory to Practice; Proceedings of Uncertainty '96, C. D. Shackelford, P. P. Nelson, and M. J. S. Roth eds., Madison, WI, July 31-Augest 3, ASCE, New York, pp. 326-340.

59. Phoon, K. K., and Kulhawy, F. H. (1999a). “Characterization of Geotechnical Variability.” Canadian Geotechnical Journal, 36(4), 612-624.

60. Phoon, K. K., and Kulhawy, F. H. (1999b). “Evaluation of Geotechnical Property Variability.” Canadian Geotechnical Journal, 36(4), 625-639.

61. Phoon K. K., and Kulhawy, F. H. (2005). “Characterization of Model Uncertainties for Laterally Loaded Rigid Drilled Shafts”, Geotechnique, 55(1), 45-54.

62. Phoon, K. K., Kulhawy, F. H., and Grigoriu, M. D. (2003a). “Development of A Reliability-Based Design Framework for Transmission Line Structure Foundations.” Journal of Geotechnical and Geoenvironmental Engineering, ASCE, Vol. 129, No. 9, pp. 798 - 806.

63. Phoon, K. K., Kulhawy, F. H., and Grigoriu, M. D. (2003b). “Multiple Resistance Factor Design (MRFD) for Shallow Transmission Line Structure Foundations.” Journal of Geotechnical and Geoenvironmental Engineering, ASCE, Vol. 129, No. 9, pp. 807 - 818.

64. Preim, M. J., March, R., and Hussein, M. (1989). “Bearing Capacity of Piles in Soils with Time Dependent Characteristics.” Piling and Deep Foundations, Vol. 1, pp. 363-370.

65. Rausche F., Goble, G., and Likins, G. (1985). “Dynamic Determination of Pile Capacity.” Journal of Geotechnical Engineering, ASCE, Vol. 113, No. 3, pp. 367-383.

66. Rausche, F., Moses, F., and Goble, G. G., (1972) “Soil Resistance Predictions from Pile Dynamics,” Journal of the Soil Mechanics and Foundations Division, ASCE, Vol. 98, No. SM9, pp. 917-937.

67. Samson, L. and Authier, J. (1986). “Change in Pile Capacity with Time: Case Histories.” Canadian Geotechnical Journal, 23(1), pp. 174-180.

68. Seidel, J. P., Haustorfer, I. J., and Plesiotis, S. (1988). “Comparison of Static and Dynamic Testing for Piles Founded into Limestone.” Proceedings of 3rd International Conference on the Application of Stress-Wave Theory to Piles, Bi-Tech Publishers, Ottawa, Ontario, Canada, pp. 717-723.

69. Skov, R., and Denver, H. (1988). “Time Dependence of Bearing Capacity of Piles.” In Proceedings of 3rd International Conference on the Application of Stress-Wave Theory to Piles, Bi-Tech Publishers, Ottawa, Ontario, Canada, pp. 879-888.

70. Smith, E. A. L. (1960). “Pile Driving Analysis by the Wave Equation,” Journal of Soil Mechanics and Foundation Division, ASCE, Vol. 86, No. SM4, pp. 35-61.

71. Soderberg, L. O. (1961), "Consolidation Theory Applied to Foundation Pile Time Effects." Geotechnique, London, Vol. 11, No. 3, pp. 217-225.

72. Svinkin, M. R. (2002). "Engineering Judgment in Determination of Pile Capacity by Dynamic Methods." Deep Foundations Congress, Geotechnical Special Publication, No. 116, Vol. 2, ASCE, pp. 898-914.

73. Svinkin, M.R., Morgano, C. M., and Morvant, M. (1994). "Pile Capacity as A Function of Time in Clayey and Sandy Soils." In Proceedings of 5th International Conference and Exhibition on Piling and Deep Foundations, Belgium, pp. 1.11.1-1.11.8.

74. Svinkin, M. R., and Skov, R. (2000). "Set-up Effect of Cohesive Soils in Pile Capacity." Proceedings of 6th International Conference On Application of Stress Waves to Piles, Sao Paulo, Brazil, pp. 107-111.

75. Tan, S. L., Cuthbertson, J., and Kimmerling, R. E. (2004). "Prediction of Pile Set-up in Non-cohesive Soils." Current Practices and Future Trends in Deep Foundations, Geotechnical Special Publication No. 125, pp. 50-65.

76. Tavenas, F. and Audy, R. 1972. "Limitation of the Driving Formulas for Predicting the Bearing Capacities of Piles in Sand." Canadian Geotechnical Journal, 9(1), pp. 47-62.

77. Titi, H. H. and Wathugala, G. W. (1999). "Numerical Procedure for Predicting Pile Capacity – Setup/Freeze." Transportation Research Record 1663, Paper No. 99-0942, pp. 25-32.

78. Thomson, W. T., (1950). Laplace Transformation, Prentice Hall, Inc., New York, NY, USA.

79. Tomlinson, M. J. (1986). Foundation Design and Construction. Longman Scientific and Technical, Essex, England.

80. Vijayvergiya, V. N., and Focht Jr., J. A. (1972). "A New Way to Predict Capacity of Piles in Clay." Proceedings of the 4th Annual Offshore Technology Conference, Texas, Vol. 2, pp. 856-874.

81. Vrouwenvelder, A. (1992). "Effects of inspection on the reliability of foundation piles." 4th International Conference on Application of Stress-Wave Theory to Piles, Balkema, Rotterdam, pp.657-663.

82. Walton, P. A., and Borg, S. L. (1998). "Dynamic Pile Testing to Evaluate Quality and Verify Capacity of Driven Piles." Transportation Research Board, pp. 1-7.

83. Wang, S., and Reese, L. C. (1989). "Predictions of Response of Piles to Axial Loading." Predicted and Observed Axial Behavior of Piles, Geotechnical Special Publication No. 23, ASCE, pp. 173-187.

84. Wellington, A. (1892). "Discussion of 'The Iron Wharf at Fort Monroe, Va. By J. B. Cuncklee." Transactions, ASCE Vol. 27, Paper No. 543, Aug. 1982, pp. 129-137.

85. Withiam, J. L., Voytko, E. P., Barker, R. M., Duncan, J. M., Kelly, B. C., Musser, S. C., and Elias V. (2001). "Load and Resistance Factor Design (LRFD) for Highway Bridge Substructures." FHWA HI-98-032, National Highway Institute.

86. Yang, N. (1956). "Redriving Characteristics of Piles." Journal of the Soil Mechanics and Foundations Division, Vol. 82, Paper 1026, SM 3, July, ASCE.

87. Yang, N. (1970). "Relaxation of Piles in Sand and Inorganic Silt." Journal of the Soil Mechanics and Foundations Division, ASCE, Vol. 96, SM2, pp. 395-409.

88. York, D. L., Brusey, W. G., Clemente, F., M., and Law, S. K. (1994). "Set-up and Relaxation in Glacial Sand." Journal of Geotechnical Engineering, ASCE, Vol. 120, No. 9, pp. 1498-1513.

89. Zai, J. (1988). "Pile Dynamic Testing Experience in Shanghai." Proceedings of 3rd International Conference on the Application of Stress-Wave Theory to Piles, Bi-Tech Publishers, Ottawa, Ontario, Canada, pp. 781-792.

90. Zhang, L. M. (2004). "Reliability Verification Using Proof Pile Load Tests." Journal of Geotechnical and Geoenvironmental Engineering, Vol. 130, No. 11, pp. 1203-1213.

91. Zhang, L. M. and Tang, W. H. (2002). "Use of Load Tests for Reducing Pile Length." Geotechnical Special Publication No. 116, Deep Foundation 2002 – An International Perspective on Theory, Design, Construction, and Performance, Vol. 2, pp. 993-1005.

92. Zhu, G. (1988). "Wave Equation Applications for Piles in Soft Ground." Proceedings of 3rd International Conference on the Application of Stress-Wave Theory to Piles, Ottawa, Ontario, Canada, pp. 831-836.